

ROBUSTLY ESTIMATING HETEROGENEITY IN FACTORIAL DATA USING RASHOMON PARTITIONS

APARAJITHAN VENKATESWARAN[§], ANIRUDH SANKAR[‡], ARUN G. CHANDRASEKHAR^{‡,*},
AND TYLER H. MCCORMICK^{§,¶}

ABSTRACT. Many statistical analyses, in both observational data and randomized control trials, ask: how does the outcome of interest vary with combinations of observable covariates? For example, how do various drug combinations affect health outcomes, or how does technology adoption depend on incentives and demographics? Our goal is to partition this factorial space into “pools” of covariate combinations where the outcome differs across the pools (but not within a pool). Existing approaches for identifying such partitions either (i) search for a single “optimal” partition under some assumptions about the association between covariates or (ii) attempt to *sample* from the *entire* set of possible partitions. Both these approaches ignore the reality that, especially with correlation structure in covariates, many ways to partition the covariate space may be indistinguishable from a statistical perspective, despite very different implications for policy or science. We develop an alternative perspective, called *Rashomon Partition Sets* (RPSs). Each item in the RPS partitions the factorial space of covariates using a tree-like geometry. RPSs incorporate *all* partitions that have posterior values near that of the *maximum a posteriori* partition, even if they offer substantively very different explanations, and do so using a prior that makes no assumptions about the associations between covariates. This prior is the ℓ_0 prior, which we show is minimax optimal. Given the RPS we can calculate the posterior of *any* measurable function of the vector of feature combination effects on outcomes, conditional on being in the RPS. We also characterize approximation error relative to the entire posterior and provide bounds on the size of the RPS. Simulation experiments demonstrate the usefulness of this framework and that it allows for robust conclusions relative to conventional regularization techniques. We apply our method to three empirical settings: price effects on charitable giving, heterogeneity in chromosomal structure (telomere length), and the introduction of microfinance. We highlight robust conclusions, including affirmations and reversals of extant literature’s findings, in each setting.

We gratefully acknowledge Abhijit Banerjee, Emily Breza, Kevin Chen, Paul Goldsmith-Pinkham, Rachel Heath, Muriel Niederle, Cynthia Rudin, and Bo Zhang for their helpful discussions. We thank Garrett Allen and Jessica Kunke for their feedback on earlier versions of our paper. We thank Brian Xu for exceptional research assistance.

[§]Department of Statistics, University of Washington.

[‡]Department of Economics, Stanford University.

*J-PAL, NBER.

[¶]Department of Sociology, University of Washington.

1. INTRODUCTION

“You didn’t come here to make the choice, you’ve already made it. You’re here to try to understand why you made it. I thought you’d have figured that out by now.”

— The Oracle, *The Matrix Reloaded*

Researchers and policymakers often study settings where an outcome of interest varies with combinations of features or covariates (e.g., characteristics, treatment assignments) of a given unit. Examples include (1) learning what combination of drugs, at what frequency and dosages, and for what sub-groups in the population reduce a given illness (e.g., in the cases of HIV and non-small cell lung cancer, [Hammer et al. \(1997\)](#); [Cascorbi \(2012\)](#); [Nair et al. \(2023\)](#)); (2) studying how an individual’s wage is associated with combinations of age, education, parental wealth, race/ethnicity, and gender ([Mincer, 1958](#); [Aakvik et al., 2010](#); [Forster et al., 2021](#)); (3) analyzing vaccination campaigns that leverage incentives, reminders, network strategies across the wealth distribution ([Chernozhukov et al., 2018](#); [Banerjee et al., 2021](#)), and; (4) determining when and why microfinance is more effective for certain classes of sub-populations and markets ([Banerjee et al., 2019](#)).

Fundamentally, the researcher wants to learn a response function that describes how the outcome changes (or doesn’t) when moving between levels of a feature. If the outcome is very sensitive to certain changes in feature combinations, the response function needs to be very local, meaning in practice that the researcher needs to test between many similar feature combinations. In contrast, a simpler response function means that several combinations can effectively be thought of as the same, which can also be useful for theorizing about mechanisms and policy. For example, will anyone who has previous entrepreneurial experience and has had an active savings account put a micro-loan to business use? Will the effectiveness of drug combinations follow the same pattern across the patient weight distribution? Intuitively, if a patient is on a drug cocktail with drugs A and B and the marginal effect of incrementally increasing the dosing of A from 1 to 2 is zero (holding fixed the dosing of B and the patient’s weight), then one can think of combining, or pooling, treatments with 1 and 2 units of drug A (holding fixed B and the patient’s weight). This teaches us the local shape of the treatment effect function, which is interesting in its own right, but also increases the effective amount of data to estimate this pooled average treatment effect.

Of course, the researcher doesn’t know the local complexity of the response function *a priori* and needs to learn it while also estimating the effect of specific feature combinations. This problem has a “factorial” structure, though: even with 3 values per feature and 3 features, there are 27 distinct combinations. This can put pressure on the effective number of observations per parameter, meaning that the analysis can be potentially very noisy. Additionally, due to interdependence, decisions about

pooling some feature combinations impact others. Finally, so many feature combinations could in principle be pooled with each other that feasibility and multiple hypothesis concerns quickly arise; the number of possible partitions is given by Bell’s number $B_n = \mathcal{O}((n/\log(n+1))^n)$, so in our example $B_{27} > 10^{20}$.

The enormous space of feature combinations and interdependence make the process of producing a model for heterogeneity fragile. Different pooling models can both (a) explain the data nearly equally well and yet (b) correspond to very different shapes of treatment effect functions. The latter may also correspond to different interpretations as the differing models may treat different combinations as poolable or not. As there will be distinct models of heterogeneity that nearly equally well explain a given data set, it is entirely possible that the different pooling models can lead to very distinct scientific interpretations, counterfactuals, and policy decisions.

Existing approaches to this problem either (i) search for a single “optimal” model under some assumptions about the association between covariates (e.g., Lasso) or (ii) attempt to sample from the *entire* set of possible models (e.g., Bayesian Model Averaging, BMA). Our approach offers a new alternative using the idea of *Rashomon Effect* from Breiman (2001)’s “Two Cultures” paper (and the highly related *Occam’s Window* approach from Madigan and Raftery (1994)’s seminal paper on model uncertainty in graphical models using BMA) to enumerate and explore a small number of high (posterior) probability models, which we call the *Rashomon Partition Set (RPS)* because each item in the RPS partitions the factorial space of covariates using a tree-like geometry.

We show a number of results that give this seemingly simple idea profound implications. In a Bayesian framework, we propose a set of novel priors over explanations for heterogeneity and then show that the RPS is enumerable. We bound the difference between posterior quantities computed using the entire posterior and using only the RPS. The result is that conclusions using RPS are robust since it incorporates all partitions that are near the *maximum a posteriori*, even if they offer substantively very different explanations. When constructing this posterior, we take the view that marginal effects in a factorial setting are complex to uniformly model and use a prior that makes no assumptions about the associations between covariates: the ℓ_0 prior, which we show is minimax optimal. In that sense, the RPS is robust because it uses a robust prior *and* it enumerates every high posterior model. For experiments, policymakers can then weigh additional considerations (e.g., cost, equity, privacy) in choosing which policies from the RPS to implement. RPSs also yield insights to generate new scientific theories. Looking across models in the RPS, one can build an archetype of feature combinations that appear consistently and have consistent effects on the outcome, regardless of the structure imposed on other covariates by other high posterior partitions.

In the remainder of this section, we first provide a detailed example to illustrate the environment and fix ideas. Then, with this environment in mind, we preview the results and direction for the remainder of the paper. To begin with the example, suppose that researchers are interested in the health outcome of a possible drug combination on individuals. The two drugs in question are A and B and each can take on three values: 0 (not taken), 1 (low dosage), and 2 (high dosage). Drug effects can vary by weight – for the sake of discussion, say weights are low, medium, or high. Thus, there are 27 distinct bundles of heterogeneity and it’s conceivable that for each different weight, a different drug cocktail (or equivalence class thereof) is most effective.¹ Let M be the number of features (here 3) and R the number of values per feature (here 3). There are $K := R^M$ unique feature combinations. Let $w \in \{\text{low, medium, high}\}$ be weight, $(a, b) \in \{0, 1, 2\}^2$ be the dosages of A and B, and $Y_i(a, b, w)$ be the health potential outcome for individual i , with $\mathbb{E}[Y_i(0, 0, w)] = 0$ for all w as a normalization. The sample consists of n individuals, the n -vector of outcomes \mathbf{y} , the matrix of features $\mathbf{X}_{1:n, 1:M}$, the matrix $\mathbf{D} = \mathbf{D}(\mathbf{X})$ with entries $D_{ik} = 1$ if i has unique feature combination $k = (a_i, b_i, w_i)$. The dataset is $\mathbf{Z} := (\mathbf{y}, \mathbf{X})$. So, the researcher studies

$$(1) \quad \mathbf{y} = \mathbf{D}\boldsymbol{\beta} + \boldsymbol{\epsilon},$$

where $\beta_k = \mathbb{E}[Y_i \mid D_{ik} = 1]$ is the expected outcome in the population given the feature combination and ϵ_i is some idiosyncratic mean-zero residual.²

In this illustration, let us make three assumptions as to how drugs may operate in the population. First, suppose that low and medium weight people face the same effects across all drug combinations, and only at the highest weight do the effects behave differently. This means that

- (1) $\mathbb{E}[Y_i(a, b, \text{low})] = \mathbb{E}[Y_i(a, b, \text{medium})]$ for every (a, b) , and
- (2) $\mathbb{E}[Y_i(a, b, \text{low})] \neq \mathbb{E}[Y_i(a, b, \text{high})]$ for some (a, b) .

¹We will use this example to build intuition, but the applications are well beyond health. For instance, we could imagine an application to the study of microfinance. A microcredit organization enters markets and randomly varies interest rates with baseline, low discount, and high discount levels (Karlan and Zinman, 2010) to understand demand. The markets it enters may have zero, low, or high amounts of pre-existing debt. Credit-eligible individuals may have no, low, or high levels of previous entrepreneurship. These potential future borrowers of the microcredit loans may themselves vary in their education levels. Learning whether previous entrepreneurial experience, in thick versus thin credit markets, for adversely versus not selected agents gives insights into the fundamental economic mechanics. One of our three empirical examples in Section 7 concerns microfinance.

²This representation was developed in prior work in Banerjee et al. (2021) (Chandrasekhar and Sankar are co-authors) in the context of factorial randomized controlled trials. Our work in the present paper – a setting of general heterogeneity (not only cross-randomized trials), the study of robustness, development of the RPS, usage of robust priors, and tree-based estimations circumventing correlation restrictions – is all entirely novel to the literature and faces new technical challenges.

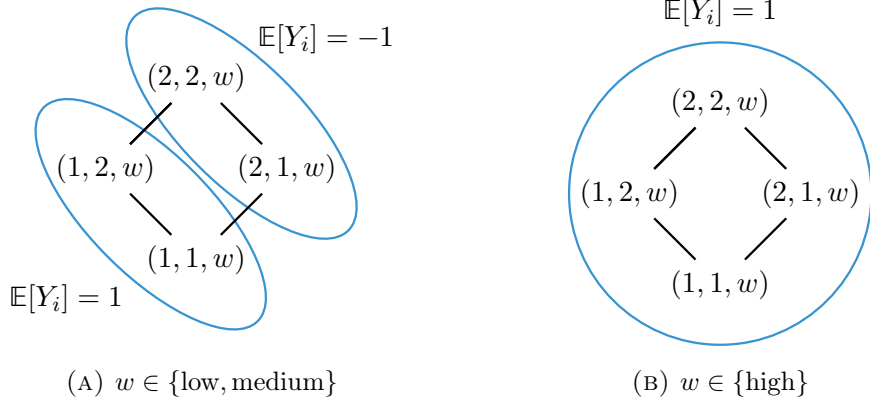


FIGURE 1. Hasse diagram representing the partition Π^* for the drug-weight interaction example.

Second, suppose that at the low and medium weight levels, the best outcome is delivered by a cocktail of low doses of drug A, but overdosing is possible at these lesser weights: the maximal dosings of drug A are too strong per pound and interaction effects can be quite severe. For instance,

- (1) $\mathbb{E}[Y_i(1, b, w)] = 1$ for $b \in \{1, 2\}$, $w \in \{\text{low, medium}\}$, and
- (2) $\mathbb{E}[Y_i(2, b, w)] = -1$ (i.e., worse than control) for $b \in \{1, 2\}$, $w \in \{\text{low, medium}\}$, and
- (3) $\mathbb{E}[Y_i(a, b, w)] = 0$ for $(a, b) \in \{(0, 1), (1, 0), (0, 2), (2, 0)\}$ and $w \in \{\text{low, medium}\}$, so single drug treatments are ineffective.

Third, for the highest weight individuals, suppose that there is no overdosing in the dosage levels in the support of the study (1 or 2 for each drug and combinations therein): beyond the minimum therapeutic doses, all combination cocktails are equally effective. So $\mathbb{E}[Y_i(a, b, \text{high})] = 1$ for $(a, b) \in \{(1, 1), (1, 2), (2, 1), (2, 2)\}$. All single-drug therapies are ineffective. These assumptions present a sketch of drug interaction patterns across weight classes. In practice, we would not know these three rules *a priori*. Testing all possible factorial combinations could reveal these patterns with enough data, but even in this small example, there are 27 scenarios so statistical power will reduce quickly.

Instead, we would like to pool together data to aggregate information and more efficiently estimate marginal effects. A *partition* Π , in the space of all partitioning models, \mathcal{P} , is a model of heterogeneity wherein every feature combination is assigned to a pool $\pi \in \Pi$, possibly a singleton, where $\beta_k = \beta_{k'}$ if $k, k' \in \pi$. These pools are referred to as leaves in the regression tree literature. In our example, there is a single (maximal) pooling scheme, which we can call Π^* . In Π^* , all single-dose therapies are pooled with control because they are not effective. Low and medium weight individuals are fully pooled, but the drug combinations themselves are not, with $\{(1, 1), (1, 2)\}$ being effective and

the others being detrimental. High weight individuals are split from the lower weight groups, and all combination therapies are pooled. We visualize this in Figure 1. If we knew this, we could double the data per cell in the low and medium weight samples and then quadruple the data in the high weight sample between all cocktail treatments $\{(1, 1), (1, 2), (2, 1), (2, 2)\}$. Further, Π^* has direct scientific value teaching us about the underlying scientific mechanisms. However, obviously, we know none of this *ex-ante*.

In principle, *any* estimation strategy corresponds to some partition. A “saturated regression,” treating all 27 cells as independent, corresponds to the most granular pooling (which is degenerate as no cells are pooled), where there is no information across cells to be gleaned – $\hat{\Pi}$ such that every pool $\pi \in \hat{\Pi}$ consists of a unique feature combination: $\pi = \{(a, b, w)\}$. Conducting a “short” regression of outcomes on level of drug A and level of drug B in a linear regression can be thought of as a pooling corresponding to additive separability with no interaction effects. Here $\tilde{\Pi}$ is such that each $\pi \in \tilde{\Pi}$ consists of $\pi = \{(a, b, \cdot)\}$.³ One could also use machine learning to regularize and select the best pooling structure, leading to $\check{\Pi}$ (Banerjee et al., 2021). The important point is that the specific approaches to handling data necessarily correspond to implicit partitions, e.g., $\hat{\Pi}$, $\tilde{\Pi}$, and $\check{\Pi}$ here. The implicit partitions assumed can very much drive results and, therefore, policy, counterfactuals, and interpretation of mechanisms and development of theory.

Returning to our Bayesian framework, we study the posterior given the data \mathbf{Z} , $\mathbb{P}(\Pi \mid \mathbf{Z})$, and then the posterior distribution over β that follows. We want to use a robust prior: one that does not impose false independence or unwarranted assumptions on correlations on the relationship between the β_k ’s. Given the complexity, it is unclear and perhaps unlikely that a medical researcher can neatly describe their prior on the joint distribution of marginal effects of the 27 feature combinations in our drug cocktail and weight example. Thus, we use a prior that is robust to any correlational structure. In Theorem 2, we prove that this corresponds to a prior over the number of unique feature combinations that have distinct effects on the outcome, which is an ℓ_0 penalty. Stated differently, $\mathbb{P}(\Pi) \propto \mathbb{P}(H(\Pi))$ where H counts the number of distinct feature combinations after all poolings i.e., the number of pools in the partition Π . This prior places no structure on the independence (e.g., ℓ_1) or correlation structure (e.g., Gaussian processes with structured sparsity) within the partitioning, and it is not obvious that doing so would be reasonable from a scientific perspective. For instance, drugs may need to be combined in certain ratios to be optimally effective, or economic production functions may exhibit strong complementarities in inputs. Our key motivation is those cases where at the time of research the structure of these dependencies is not yet discovered, motivating the

³In fact, even an additive specification of levels of drugs A, B, and weight falls into this trap in our generalization in Section 8. It pools cells implicitly using common slopes.

study in the first place.⁴ This also imposes no specific distributional structure on β , in contrast with other methods.⁵

We next represent our problem using a specific type of tree known as a Hasse diagram (see Figure 1). Several of the present paper’s authors first developed this representation in Banerjee et al. (2021), which we extend considerably here in a different statistical context. This geometry naturally handles partially ordered sets, unlike typical regression trees that impose a false hierarchy between variables. We use these Hasse diagrams to construct partitions. After restricting ourselves to a subset that meets our admissibility criteria, which we denote $\mathcal{P}^* \subset \mathcal{P}$, we enumerate all partitions that have a posterior probability above some threshold θ of our choosing. To see the value of this tree-based geometry, consider two feature combination variants, $k = (a, b, w)$ and $k' = (a + 1, b, w)$ in our drug-by-weight example. We calculate the incremental change in our loss function (or equivalently, the posterior) if we were to assume the two features had the same expected outcome. The lower the posterior that k and k' belong in the same pool, the larger the loss. Further, with the ℓ_0 prior, the posterior for a tree of pooling decisions is lower when more splitting is done: the only assumption is that there are not too many sources of meaningful heterogeneity, though one is silent on their correlations.

With this statistical and geometric setup in place, we have the language to define the RPS.

Definition 1 (Rashomon Partition Set (RPS)). *For some posterior probability threshold θ , we define the Rashomon Partition Set \mathcal{P}_θ as,*

$$(2) \quad \mathcal{P}_\theta = \{\Pi \in \mathcal{P}^* : \mathbb{P}(\Pi \mid \mathbf{Z}) \geq \theta\}.$$

Further, given a posterior over the partition models – and in practice one that only specifies a prior over how many effectively distinct feature combinations there are (or equivalently the number of pools) – we can easily develop a posterior over the effects of various feature combinations, possibly pooled, on the outcome of interest conditional on the partition models in this set. So

$$(3) \quad P(\beta \mid \mathbf{Z}, \mathcal{P}_\theta) = \sum_{\Pi \in \mathcal{P}_\theta} P(\beta \mid \mathbf{Z}, \Pi) \mathbb{P}(\Pi \mid \mathbf{Z}, \mathcal{P}_\theta),$$

⁴Of course, if the researcher had strong prior knowledge, one could freely incorporate this for a specific application. However this prior knowledge would be tailored for the application, and there is not a one-size-fits-all parameterization for all conceptual restrictions in all domains.

⁵E.g., ℓ_1 implies independent Laplace random variables and Gaussian processes are intrinsically parametric.

and analogously for measurable functions of β . Using Hasse diagrams avoids imposing an artificial hierarchy on the partially ordered set of covariates, which allows us to interpret the partitions in the RPS.⁶

The posterior for β restricted to the RPS, Equation (3), is, of course not the same as the distribution over all possible partitions, $P_{\beta|\mathbf{z}}(\beta)$. Computing $P_{\beta|\mathbf{z}}(\beta)$ requires sampling from the distribution of admissible Hasse diagrams, which is computationally taxing and inefficient, since evaluating the posterior at a partition with very low posterior probability requires just as much effort as one with very high probability. Depending on the structure of the posterior and the θ of the RPS, the posterior within the RPS may come close to capturing the entire mass of the posterior, making the approximation using Equation (3) a reasonably proxy for using the full posterior.

This intuition brings us to the first of three main results in the remainder of the paper. First, Theorem 1, characterizes the uniform approximation error of the posterior distribution of β , and measurable functions of it, restricting to the RPS. Second, in Section 4, we show that the ℓ_0 prior is minimax optimal (Theorem 2). This prior is robust to any potential correlation structure between covariates and assumes only sparsity in heterogeneity, without making statements about correlation (or independence). This prior allows us to calculate bounds on the size of the RPS in Theorem 3. We characterize its size and its relationship to (a) the number of features, (b) the number of values per feature, (c) the prior over H , the number of distinct pools in the partition, and (d) the minimum posterior value θ . The main idea is that given θ , the prior dictates some threshold level $H(\theta)$ with $H(\theta) = \max_{\Pi \in \mathcal{P}_\theta} H(\Pi)$. If there were more pools than this, then the prior would be so low that the partition would not make it into the RPS. So we can characterize the bound on the size of \mathcal{P}_θ and, further, clearly study how this varies with the prior (and therefore the bound $H(\theta)$). Third, in Section 5, we show that one can enumerate the entirety of \mathcal{P}_θ . In Algorithm 1, we develop a search process that enumerates the full RPS (Theorem 6). At any point in the search, if one has a posterior about a potential partition that is sufficiently low such that no amount of perfect matching down the road could make the posterior high enough to exceed θ , then one should discard the entire collection of partitions that use this unlikely initial structure. This approach is inspired by [Xin et al. \(2022\)](#).

To construct the RPS, it is useful to start with a reference partition model. This is some reference model that we can estimate by a machine learning algorithm that we deem sensible. This is useful because θ of the RPS is the posterior of the reference model (which should already be high). The RPS then enumerates all models with posteriors at least as high as this reference. By definition, this

⁶We discuss this distinction in more detail in Section E in the context of frequentist tree-based methods that use the same geometry.

will include the *maximum a posteriori* (MAP) partition. Given this set, one has a list of models that can be ordered by relative posterior value from the MAP downwards and one can take any decisions querying this list. It is also helpful to note the computational and philosophical distinctions here. Like in the [Xin et al. \(2022\)](#) approach, the reference model allows us to sidestep a computational difficulty with the normalizing constant. But unlike [Xin et al. \(2022\)](#), in a Bayesian framework, there is a natural interpretation and we know the MAP. Using the MAP as the reference, we can interpret the size of the RPS as our tolerance for deviance from the MAP partition. The larger the RPS, the more we're willing to entertain high posterior probability models that are not the MAP. Smaller RPSs hone in on explanations that are very similar, in terms of posterior probability, to the MAP.

Along with these theoretical results, we also provide several empirical examples. Section 6 reports two simulation studies, the first a case where there is interdependence between feature combinations and the second illustrating the Rashomon Effect. We show results using three datasets in Section 7. These examples highlight the interpretability of RPSs while also demonstrating how RPS generate new scientific hypotheses. Looking for commonalities across partitions within the RPS provides evidence for the robustness of conclusions across high posterior probability partitions. We also demonstrate how RPSs can provide a pathway for robustly avoiding adverse events in experiments by ensuring they are not present in the RPS.

We conclude the paper by discussing two generalizations to our work and then situating our work with a discussion of related literature. Section 8 speaks to two possible extensions to our work, one that allows for a broad class of heterogeneous effects functions (e.g. checking if there is a linear increase in outcome with increasing a feature level) and the other that pools on the space of covariances rather than on coefficients themselves. Given that this work is related to several active areas of research, we have dedicated a section, Section 9, to contextualizing our work. Section 10 concludes and offers areas for future work. All of our code is available at <https://github.com/AparaV/rashomon-tva>.

2. ENVIRONMENT

Suppose that there are n units (or individuals) and each has M features with the feature matrix given by \mathbf{X} . Every feature has R possible values, partially ordered. Let \mathcal{K} be the set of all $K = R^M$ unique feature combinations. Each feature combination $k \in \mathcal{K}$ can be represented in a dummy matrix \mathbf{D} with entries $D_{ik} = 1$ if observation i has feature combination k . Depending on the context, we let k denote the vector of feature values or its index in \mathcal{K} . Owing to the partial ordering of the feature values, we can define a partial ordering on the feature combinations themselves. We

say $k \geq k'$ if and only if $k_m \geq k'_m$ for all $m = 1, \dots, M$. We say $k > k'$ if $k \geq k'$ but $k \neq k'$, and say that k and k' are incomparable if there are two features m_1 and m_2 such that $k_{m_1} > k'_{m_1}$ and $k_{m_2} < k'_{m_2}$. We denote incomparability by $k \not\leq k'$. We denote the expected outcome of feature combination k by β_k .

We will restrict attention to a subset of partitions that is scientifically coherent (admissible). Most obviously, partitions should pool only those feature combinations with identical expected outcomes. Recalling the Hasse diagrams representing the partial ordering of features, admissibility will restrict the geometry of the partitions that appear on these diagrams. First, a pool of feature combinations will be considered inadmissible when these feature combinations are only in unrelated Hasse diagrams. Second, a pool should have an interpretation as capturing (the lack of) marginal changes climbing up or down the ordering. Finally, admissible partitions should be robust so that it doesn't rely on measure zero events on these climbs. We now explore these ideas in detail.

Definition 2 (Pool). *Given M features taking on R partially ordered values each, a pool π is any set of feature combinations having identical expected outcomes.*

For a given pool π , two feature combinations $k_1, k_2 \in \pi$ only if $\beta_{k_1} = \beta_{k_2}$. Note that the converse is not true. That is, we could have $k_1 \in \pi_1$ and $k_2 \in \pi_2$ for $\pi_1 \neq \pi_2$ even though $\beta_{k_1} = \beta_{k_2}$.

Definition 3 (Partition). *Given M features taking on R partially ordered values each, a partition Π is a partitioning of this feature space into pools.*

Our goal is to learn partitions Π such that each element of a partition is a pool i.e., we want to partition the feature space by heterogeneity in the expected outcomes.

Definition 4 (Variants). *Two feature combinations k and k' are variants if they have the same value of features for all but one and they vary by exactly one intensity value (so they are orderable) i.e., $k_{-m} = k'_{-m}$ for all except some feature m , and k'_m takes a value that is the immediate next incremental value after k_m .*

At its core, heterogeneity boils down to whether variants have the same effect on the outcome of interest, at least on a scale relevant to the researcher or policymaker.

Some feature combinations can be considered unrelated to one another. Let us take an example, where researchers are exploring combinations of an antibiotic such as amoxicillin with an anti-inflammatory drug like ibuprofen. It makes sense to ask whether ibuprofen helps when it is prescribed alongside amoxicillin during a bacterial infection (e.g. whether it offers further temporary relief from the pain) or, when both are administered simultaneously, what happens when dosages

of both are increased (e.g., whether too strong a dose of both irritates the stomach). However, an amoxicillin treatment on its own would not usually be compared in its efficacy to ibuprofen treatment on its own – they are distinct drugs with distinct mechanisms. We will consider inadmissible pools consisting solely of unrelated feature combinations (here single drug features). We mathematically capture the (un)relatedness of feature combinations by first defining profiles in Definition 5.

Definition 5 (Profile). *A profile $\rho(k)$ is a binary vector indicating which of the M features have non-zero values, with the understanding that in a factorial design experiment, this indicates assignment to pure control and in a setting with heterogeneity we take (one of) the lowest value(s) as the base of 0.*

Returning to the example, if (a, b) captures dosages of amoxicillin and ibuprofen respectively, then combinations such as $k = (500 \text{ mg}, 100 \text{ mg})$ corresponds to the profile $\rho(k) = (1, 1)$, whereas $(500 \text{ mg}, 0)$ (amoxicillin on its own) corresponds to $\rho(k) = (1, 0)$ and $(0, 100 \text{ mg})$ (ibuprofen on its own) corresponds to the profile $\rho(k) = (0, 1)$. An admissible pool $\pi \in \Pi$ has to be contained within a single profile or thread across other profiles through either the profile $(0, 0)$ or $(1, 1)$.

As part of admissibility, we want to interpret a pool π as the (lack of) marginal changes when climbing up or down an ordering. Consider the profile where both amoxicillin and ibuprofen are administered, and where amoxicillin is administered in dosages from the ordered set $\{250 \text{ mg}, 500 \text{ mg}\}$ and ibuprofen is administered in dosages in the ordered set $\{200 \text{ mg}, 400 \text{ mg}\}$. This is depicted on the Hasse in Figure 2. Beginning from the lowest dosages of both $(250 \text{ mg}, 200 \text{ mg})$, we consider what happens when increasing the dosage of amoxicillin or ibuprofen. It could be that increasing amoxicillin has no effect (e.g. because the bacterial infection was highly localized) but increasing the dose of ibuprofen makes an appreciable difference (e.g., the patient feels much more relief from the pain). This is captured in Figure 2a. Since we are asking about changes in marginal values climbing up or down, admissible partitions pool contiguous features in the Hasse. In general, admissible pools are “convex” shapes in the Hasse.

Beyond just respecting the ordering, we also want admissible partitions to avoid brittle pools relying on measure zero events. Starting from the lowest dosage of an amoxicillin-ibuprofen treatment, $(250 \text{ mg}, 200 \text{ mg})$, suppose that either increasing the dosage of *just* amoxicillin or the dosage of *just* ibuprofen has an appreciable effect. This rules out Figure 2a. When amoxicillin and ibuprofen are both raised to their largest dosages simultaneously, the effect would be a combination of each drug’s individual dosage increase as well as an interaction effect between the two drugs. In a very special case, this interaction effect can exactly offset the effect of one drug’s increase in dosage.

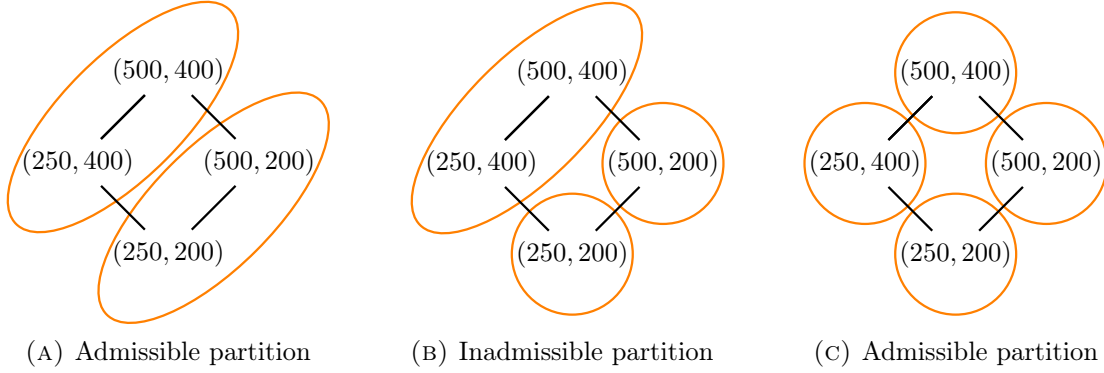


FIGURE 2. Hasse diagrams for amoxicillin and ibuprofen example. To see why Figure 2b fails Definition 6, consider $\pi_i = \{(250 \text{ mg}, 400 \text{ mg}), (500 \text{ mg}, 400 \text{ mg})\}$ and $\pi_j = \{(500 \text{ mg}, 200 \text{ mg})\}$ with incomparable minima $(250 \text{ mg}, 400 \text{ mg}) \not\preceq (500 \text{ mg}, 200 \text{ mg})$. This satisfies the antecedent but not the consequent of (3) (a).

For example, from a high 400 mg dose of ibuprofen, the benefits of a 250 mg dosage increase in amoxicillin (from 250 mg) can be *exactly* offset by an equal amount of stomach irritation that it causes so that 250 mg and 500 mg of amoxicillin have the exact same efficacy as 400 mg ibuprofen. Figure 2b captures this partition. However, this is a measure zero event. Almost surely, a stomach irritation does not *exactly* wash out the effect of a 250 mg dosage increase in amoxicillin. Any amount of estimation noise, which is inevitable, makes brittle pools like Figure 2b unreliable. Since partitions are discrete objects, it makes sense to ignore any partition that may arise from such measure zero events.⁷ In other words, an admissible partition needs to be robust to estimation noise in the marginal increments. This would mean that the dosage combination (500 mg, 400 mg) has to be in a distinct pool as in Figure 2c. Visually, this amounts to admissible partitions having to be “parallel” in the Hasse. The top pool $\{(250 \text{ mg}, 400 \text{ mg}), (500 \text{ mg}, 400 \text{ mg})\}$ in Figure 2b is not “parallel” to the other singleton pools below it. Figure 2a has two parallel pools, while Figure 2c has 4 parallel (singleton) pools.

Motivated by traversing the partial ordering while discarding all measure zero partitions, we present the formal definition of admissibility within a profile in Definition 6. We provide additional technical details with examples in Appendix A.

Definition 6 (Admissible partition of a profile). *A partition Π_0 of a profile ρ_0 is admissible if and only if*

- (1) every $\pi \in \Pi_0$ is a pool (cf. Definition 2),

⁷Other techniques such as Lasso or decision trees may falsely estimate a non-zero posterior probability for such unrealistic partitions. We give examples of this in Appendix A.

- (2) every $\pi \in \Pi_0$ is strongly convex i.e., $k, k' \in \pi$ and $k \geq k'' \geq k'$ implies $k'' \in \pi$, and $\min \pi$ and $\max \pi$ both exist and are unique (and possibly equal to each other), and
- (3) Π_0 respects parallel splits, i.e., for every pair of distinct pools $\pi_i, \pi_j \in \Pi_0$
- (a) if $\min \pi_i \not\leq \min \pi_j$, then there exists a $\pi' \in \Pi_0$ such that $\min \pi' = p'$, where for each feature m , $p'_m := \max\{p_m^{(i)}, p_m^{(j)}\}$ where $p^{(i)} = \min \pi_i$ and $p^{(j)} = \min \pi_j$, and
 - (b) if $\max \pi_i \not\geq \max \pi_j$, then there exists a $\pi'' \in \Pi_0$ such that $\max \pi'' = p''$, where for each feature m , $p''_m := \min\{\tilde{p}_m^{(i)}, \tilde{p}_m^{(j)}\}$ where $\tilde{p}^{(i)} = \max \pi_i$ and $\tilde{p}^{(j)} = \max \pi_j$.

Condition (1) is obvious. Condition (2) says pools must contain contiguous features. Condition (3) is more technical but says that pools must be parallel on the Hasse.

Suppose m arms are active with $R - 1$ non-control levels each. Then any admissible partition for a profile can be represented by a binary matrix, $\Sigma \in \{0, 1\}^{m \times (R-2)}$. Each element of Σ tells us whether a particular pair of adjacent levels in a feature is pooled. In particular, we define $\Sigma_{ij} = 1$ if and only if feature combinations with level j is pooled with feature combinations with factor $j + 1$ in feature i . We walk through some detailed examples of the setup in Appendix A.

Definition 6 captures admissibility within a single profile, but we also want to consider pooling across profiles. For example, Definition 6 does not speak to the question of pooling decisions for adding ibuprofen, as a temporary pain reliever, to a prescription of amoxicillin against a bacterial infection. Does introducing ibuprofen make an appreciable difference (offering the patient relief while waiting for the bacterial infection to work) or not (because the antibiotic itself offers pain relief by attacking the root cause)? In order to reason about this, we consider partially ordering of the profiles themselves using their binary representation in Definition 5. This also allows us to embed the profiles in an M -d unit hypercube with profiles as the vertices. By the same intuition behind convexity, we can pool two profiles if they are reachable on this hypercube. We formalize this in Definition 7.

Definition 7 (Admissible partition). *A partition Π of the entire feature space \mathcal{K} is admissible if and only if the following hold true:*

- (1) for every profile ρ_0 , the partition induced by Π on ρ_0 , $\Pi_0 = \{\pi \setminus \{k \mid \rho(k) \neq \rho_0\} \mid \pi \in \Pi\}$ is admissible by Definition 6,
- (2) every $\pi \in \Pi$ is connected in feature levels across profiles i.e., if $k_1, k_2 \in \pi$ such that $\rho_1 = \rho(k_1)$ and $\rho_2 = \rho(k_2)$ are adjacent on the hypercube, then there are feature combinations $k'_1, k'_2 \in \pi$ such that $\rho(k'_1) = \rho_1$, $\rho(k'_2) = \rho_2$ and $\|k'_1 - k'_2\|_1 = 1$,⁸ and

⁸Along with (1), this means that we can reach k_2 from k_1 by traversing the Hasse for ρ_1 to k'_1 , then jumping to k'_2 along an edge on the M -d hypercube, and then moving from k'_2 to k_2 while respecting the Hasse for ρ_2 .

(3) every $\pi \in \Pi$ is connected in profiles i.e., if π contains feature combinations from profiles ρ_0 and ρ_k where $\rho_0 < \rho_k$, then π also contains features in profiles $\rho_1, \dots, \rho_{k-1}$ such that $\|\rho_i - \rho_{i+1}\|_0 = 1$ for $i = 0, \dots, k - 1$.⁹

Specifically, by allowing to pool across different profiles, Definition 7 naturally allows us to explore heterogeneity in treatment effects where treatment and control are two distinct profiles. We illustrate its usefulness in the empirical data analysis of microcredit access in Section 7.

Just like the Σ matrix within each profile, we can also construct the intersection matrix Σ^\cap to denote how features are pooled across two adjacent profiles. Consider partitions induced by Π on two profiles ρ_1 and ρ_2 . Let us call these Π_1, Π_2 respectively. $\Sigma^\cap = \{0, 1, \infty\}^{|\Pi_1| \times |\Pi_2|}$ where $\Sigma_{i,j}^\cap = 0$ means that pools $\pi_i \in \Pi_1$ and $\pi_j \in \Pi_2$ are poolable according to (2) of Definition 7 but are not pooled together in Π . $\Sigma_{i,j}^\cap = 1$ means that these pools are poolable and are indeed pooled in Π . Finally, $\Sigma_{i,j}^\cap = \infty$ means that these pools are not poolable by Definition 7. Observe that if $\Sigma_{i,j}^\cap = 1$, then $\Sigma_{i,-j}^\cap = \infty$ and $\Sigma_{-i,j}^\cap = \infty$ in order to respect (1) of Definition 7. This object will be useful in our enumeration step in Algorithm 1.

In the remainder of this paper, we will consider only admissible partitions and may refer to them only as partitions (dropping the ‘‘admissible’’ quantifier) unless we need to distinguish them.

3. RASHOMON PARTITIONS

We elaborate on the statistical framework underlying the RPS. In Definition 1, we defined the RPS as the set of partitions obtaining at least some posterior probability threshold θ . Now, we obtain posteriors over the (functions of) effects of feature combinations. Given a unique partition Π with some probability $\mathbb{P}(\Pi | \mathbf{Z})$, it may be useful to know the likely effects of using that specific feature $k \in \pi \in \Pi$. This could be because, for instance, there may be scientific reasons to otherwise prefer one versus the other, heterogeneity in costs, logistical considerations, etc. There is also a statistical reason: the posterior may not be concentrated on just a few pools for some k but maybe for others. Therefore, we may be interested in the posterior over the entire set of admissible pools

$$P_{\beta|\mathbf{Z}}(\beta) = \sum_{\Pi \in \mathcal{P}^*} P_{\beta|\mathbf{Z}}(\beta | \Pi) \cdot \mathbb{P}(\Pi | \mathbf{Z}),$$

where $P_{\beta|\mathbf{Z}}$ is the distribution function of $\beta | \mathbf{Z}$. Throughout our analysis, we will assume that $P_{\beta|\mathbf{Z}}$ is a proper distribution i.e., it satisfies the Kolmogorov axioms. Our goal is to approximate

⁹Along with (1) and (2), this means that we can reach ρ_k from ρ_0 by traversing the M -d hypercube while staying within π and respecting the Hasse at each vertex of the hypercube.

functions of $P_{\beta|\mathbf{Z}}$ using only the RPS. That is,

$$P_{\beta|\mathbf{Z},\mathcal{P}_\theta}(\beta) = \sum_{\Pi \in \mathcal{P}_\theta} P_{\beta|\mathbf{Z},\mathcal{P}_\theta}(\beta | \Pi) \cdot \mathbb{P}(\Pi | \mathbf{Z}, \mathcal{P}_\theta), \quad \mathbb{P}(\Pi | \mathbf{Z}, \mathcal{P}_\theta) = \frac{\mathbb{P}(\Pi | \mathbf{Z})}{\sum_{\Pi' \in \mathcal{P}_\theta} \mathbb{P}(\Pi' | \mathbf{Z})},$$

meaning that the approximation only evaluates models in the RPS but is also normalized by the RPS. The quality of this approximation, of course, depends on both the shape of the posterior (i.e. how concentrated is the posterior around the highest probability models) and the structure of the RPS. Our first goal, then, is to describe how well we can approximate $P_{\beta|\mathbf{Z}}$ using the RPS. And then, we discuss how to construct the posterior over partitions, $\mathbb{P}(\Pi | \mathbf{Z})$, using generalized Bayesian inference. Technical details for results discussed here are deferred to Appendix B.

3.1. Posterior over effects. Consider the RPS, \mathcal{P}_θ . The Rashomon partitions allow for uniform approximation of the posterior over the effects vector β .

Theorem 1 (Rashomon approximation of posterior effects). *Let $f : \mathbb{R}^K \rightarrow \mathbb{R}^m$ be a measurable function of the effects β , where K is the number of unique feature combinations and $m \geq 1$. Then, the posterior distribution of $f(\beta)$ over the Rashomon Partition Set uniformly approximates the entire posterior of $f(\beta)$ in the sense that*

$$\sup_{\mathbf{t}} |F_{\beta|\mathbf{Z},\mathcal{P}_\theta}(\mathbf{t}) - F_{\beta|\mathbf{Z}}(\mathbf{t})| \leq \frac{1}{|\mathcal{P}_\theta|\theta} - |\mathcal{P}_\theta|\theta,$$

where $F_{\beta|\mathbf{Z}}$ is the distribution function of the transformation $f(\beta) | \mathbf{Z}$ and $F_{\beta|\mathbf{Z},\mathcal{P}_\theta}$ is the same but conditioned on the RPS.

With small θ or large \mathcal{P}_θ , this tends to 0, meaning that the posterior approximation can be quite close to that calculated over the full support. Essentially this is saying that if we have enough models of high enough posterior probability, then the error is low. This could arise as a result of having a few very highly likely models or having many models that are only fairly likely. We visualize the behavior of the $1/|\mathcal{P}_\theta|\theta$ term in our empirical data analyses in Section 7.

Notice that setting $f(\beta) = \beta$ recovers the posterior of β . f also covers other useful quantities derived from the vector β . An obvious example is $f(\beta) = \max_k \beta_k$ since conditional on a given variant k being estimated as the one with the maximum effect. There is a winner's curse since the selection of the maximum is positively biased, so the bias needs to be corrected (the posterior needs to be adjusted to have a lower mean) to undo this effect (Andrews et al., 2019). Other examples include the variability over outcomes across the feature combinations $\|\beta - \sum_K \beta_k / K\|_2^2$ and quantiles of the expected outcome distribution.

We now focus specifically on estimating the full posterior mean, $\mathbb{E}_{\Pi} \boldsymbol{\beta} = \sum_{\Pi \in \mathcal{P}^*} \boldsymbol{\beta}_{\Pi} \mathbb{P}(\Pi \mid \mathbf{Z})$, using the RPS. If we simply restricted ourselves to only models in the RPS, we would have $\mathbb{E}_{\Pi, \mathcal{P}_{\theta}} \boldsymbol{\beta} = \sum_{\Pi \in \mathcal{P}_{\theta}} \boldsymbol{\beta}_{\Pi} \mathbb{P}(\Pi \mid \mathbf{Z})$. As we discussed above, this quantity still depends on $\mathbb{P}(\Pi \mid \mathbf{Z})$, which involves normalizing over all admissible models and, thus, remains computationally infeasible. For some priors on $\boldsymbol{\beta}$, we could approximate $\mathbb{P}(\Pi \mid \mathbf{Z})$ but this requires specifying a prior on $\boldsymbol{\beta}$ and a corresponding approximation with adequate accuracy (Appendix F.1 gives an example using Gaussian priors and a Laplace approximation). More generally, the easiest quantity to compute is the expectation by taking the mean of the effects weighted by the self-normalized posterior probabilities as in Equation (4). Of course, if the RPS captures most of the posterior density, then this method can validly approximate the posterior mean but that is not the goal of this estimator. This estimator simply tells us what the effects are across the RPS.

$$(4) \quad \mathbb{E}_{\Pi | \mathcal{P}_{\theta}} \boldsymbol{\beta} = \sum_{\Pi \in \mathcal{P}_{\theta}} \boldsymbol{\beta}_{\Pi} \frac{\mathbb{P}(\Pi \mid \mathbf{Z}, \mathcal{P}_{\theta})}{\sum_{\Pi' \in \mathcal{P}_{\theta}} \mathbb{P}(\Pi' \mid \mathbf{Z}, \mathcal{P}_{\theta})}.$$

This approach contrasts with Bayesian and frequentist methods based on resampling trees. When resampling trees, under conditions where the mean is well-separated, we generally see the average to have appealing asymptotic properties. In any finite sample, though, we also expect that there will be several highly unappealing trees mixed in by chance. In our approach, in contrast, we look explicitly for trees with the highest posterior probability, forgoing exploring the entire space to instead focus on the partitions with the highest posterior probability. We can then characterize the quality of this approximation for a given RPS construction.

Corollary 1. *The mean conditional effect in Equation (4) approximates the posterior mean effect restricted to the Rashomon set, $\mathbb{E}_{\Pi, \mathcal{P}_{\theta}} \boldsymbol{\beta}$, as*

$$\frac{\|\mathbb{E}_{\Pi | \mathcal{P}_{\theta}} \boldsymbol{\beta} - \mathbb{E}_{\Pi, \mathcal{P}_{\theta}} \boldsymbol{\beta}\|}{\|\mathbb{E}_{\Pi, \mathcal{P}_{\theta}} \boldsymbol{\beta}\|} = \mathcal{O}\left(\frac{1}{|\mathcal{P}_{\theta}| \theta} - 1\right).$$

If we further have that the effects are bounded like $\|\boldsymbol{\beta}_{\Pi}\| < \infty$ for all $\Pi \in \mathcal{P}^$, then mean conditional effect in Equation (4) approximates the posterior mean effect, $\mathbb{E}_{\Pi} \boldsymbol{\beta}$, as*

$$\|\mathbb{E}_{\Pi | \mathcal{P}_{\theta}} \boldsymbol{\beta} - \mathbb{E}_{\Pi} \boldsymbol{\beta}\| = \mathcal{O}\left(\frac{1}{|\mathcal{P}_{\theta}| \theta} - |\mathcal{P}_{\theta}| \theta\right).$$

Corollary 1 says that our approximation is highly dependant on both the Rashomon threshold θ and the distribution of the models in the posterior space, which is indicated by $|\mathcal{P}_{\theta}|$. Of course, this result naturally extends to functions of $\boldsymbol{\beta}$ as well. To better understand Corollary 1, first assume that the models are uniformly distributed in the posterior probability space i.e., $|\mathcal{P}_{\theta}| \propto 1$

is independent of θ . As θ gets closer to 0, the RPS collects more admissible partitions. Therefore $|\mathcal{P}_\theta| \theta$ behaves like 1 and we get a better approximation using Equation (4). As θ gets closer to 1, the RPS is sparser. Therefore, $|\mathcal{P}_\theta| \theta$ behaves like 0 blowing up the error in our approximation. Now, we can consider a more complex model space where the models do not have a uniform posterior. Here, if our models are clustered near the *maximum a posteriori* (MAP) model, then a large θ will in fact give us a better approximation. Conversely, if models are clustered near a very small posterior probability, then a large θ will blow up our approximation error

3.2. Posterior over partitions. Now, we turn to the proverbial elephant of constructing a tractable posterior for Π , $\mathbb{P}(\Pi | \mathbf{Z}) \propto \mathbb{P}(\mathbf{y} | \mathbf{D}, \Pi) \cdot \mathbb{P}(\Pi)$. We need to model the likelihood component and the prior. Nested within $\mathbb{P}(\mathbf{y} | \mathbf{D}, \Pi)$ is a prior over β . In work on Bayesian tree models (e.g. [Chipman et al. \(2010\)](#)), the typical strategy is to define a prior over partitions and then define conjugate priors on β and related hyperparameters so that it is easy to evaluate each draw from the distribution over trees. We take a different approach based on generalized Bayesian inference ([Bissiri et al., 2016](#)), which requires specifying fewer distributions explicitly. However, in Appendix F.2, we also give an example of a fully specified Bayesian model where maximizing the likelihood $\mathbb{P}(\mathbf{y} | \mathbf{D}, \Pi)$ is equivalent to minimizing $\mathcal{L}(\Pi; \mathbf{Z})$, drawing a parallel with the previous work in the Bayesian literature. Let $\exp\{-\mathcal{L}(\Pi; \mathbf{Z})\}$ be the likelihood of \mathbf{Z} where $\mathcal{L}(\Pi; \mathbf{Z})$ is the loss incurred by the partition Π . Further, let $\exp\{-\lambda H(\Pi)\}$ be the prior over \mathcal{P}^* . Then, we have

$$(5) \quad \mathbb{P}(\Pi | \mathbf{Z}) \propto \exp\{-\mathcal{L}(\Pi; \mathbf{Z})\} \cdot \exp\{-\lambda H(\Pi)\} =: \exp\{-Q(\Pi)\}.$$

Specifically, we use the mean-squared error for the loss function,

$$(6) \quad \mathcal{L}(\Pi; \mathbf{Z}) = \frac{1}{n} \sum_{\pi \in \Pi} \sum_{k(i) \in \pi} (y_i - \hat{\mu}_\pi)^2, \quad \hat{\mu}_\pi = \frac{\sum_{k(i) \in \pi} y_i}{\sum_{k(i) \in \pi} 1}.$$

For the prior, we take the view that, unless directed otherwise by the specifics of the science in the context of the study, the researcher does not know the correlation structure between the various possible pools. That is they do not have a strong view on whether $\beta_k = \beta_{k'}$ is correlated with whether $\beta_{k''} = \beta_{k'}$. Therefore, we define the prior over the *number of distinct pools* i.e., $H(\Pi) = |\Pi|$, the size of the partition. The prior plays a regularizing role, putting more weight on less granular aggregations. It corresponds to the ℓ_0 penalty in a regression setting.

The RPS, taken together with the ℓ_0 penalty, is similar in spirit to the Occam's Window approach used in the context of Bayesian Model Averaging by [Madigan and Raftery \(1994\)](#) and [Madigan et al. \(1996\)](#). These papers use a stochastic search over the discrete space of models that ultimately results in a set of high posterior models and discards more complicated models if simpler models are found

to have higher posterior probability. Our approach, which does not do discrete model averaging, formalizes this notion by including a prior with an ℓ_0 penalty as part of the model, rather than using it to guide the search. In Theorem 2 we show that this choice of prior is minimax optimal and show how it lends to computational tractability in Section 4.

Now that we've developed language around describing the posterior probability of a partition through a loss function, it is useful to characterize the Rashomon threshold in the loss space. Specifically, we define $\theta := \theta(q, \epsilon) = q^{1+\epsilon} c^\epsilon$ where $c := c(\mathbf{Z})$ is some scaling constant depending on the observed data, q is the posterior probability of some good model, and ϵ is largest acceptable deviation from $\ln(1/(qc))$ i.e., the loss incurred by the good model. Then, the (q, ϵ) -Rashomon Partition Set (RPS), $\mathcal{P}_{q,\epsilon}$ is defined as

$$\mathcal{P}_{q,\epsilon} = \{\Pi \in \mathcal{P}^* : \mathbb{P}(\Pi | \mathbf{Z}) \geq q^{1+\epsilon} \cdot c^\epsilon\}.$$

This allows us to interpret Rashomon partitions with respect to a reference partition or pooling. Without any context, it is difficult to choose a threshold θ . However, if we have some reference model Π_0 that we know is good, then it makes sense to pick a threshold that is not much worse than the performance of Π_0 . In particular, using a reference Π_0 , we can define a measure of performance of model Π with respect to Π_0 as

$$(7) \quad \xi(\Pi, \Pi_0) = \frac{\log \mathbb{P}(\Pi | \mathbf{Z}) - \log \mathbb{P}(\Pi_0 | \mathbf{Z})}{\log \mathbb{P}(\Pi_0 | \mathbf{Z}) + \log \mathbb{P}(\mathbf{y} | \mathbf{X})} = \frac{Q(\Pi) - Q(\Pi_0)}{Q(\Pi_0)}.$$

ξ is essentially the log-likelihood ratio of the two models weighted by the log-likelihood of the reference model. For data that has a considerably higher likelihood (weighted by the likelihood of the model), the measure goes to 1. So when Π is a better fit than the reference, $\xi(\Pi, \Pi_0) < 0$. Conversely, when Π is a poorer fit than the reference, $\xi(\Pi, \Pi_0) > 0$. Note that if the two posteriors are identical, then $\xi(\Pi, \Pi_0) = 0$.

Suppose we know that Π_0 is a good model such that $\mathbb{P}(\Pi_0 | \mathbf{Z}) = q$. It makes sense to only look at partitions Π such that $\xi(\Pi, \Pi_0) \leq \epsilon$ for some $\epsilon > 0$. We show how to recover the RPS using (q, ϵ) in Proposition 1.¹⁰

Proposition 1. *Fix $\Pi_0 \in \mathcal{P}^*$ and let $q = \mathbb{P}(\Pi_0 | \mathbf{Z})$. Then $\mathcal{P}_{q,\epsilon} = \{\Pi \in \mathcal{P}^* : \xi(\Pi, \Pi_0) \leq \epsilon\}$.*

By construction, this result is almost trivial. Proposition 1 says that selecting the Rashomon threshold θ is equivalent to first selecting a reference model and choosing a tolerance ϵ relative to

¹⁰This is related to the candidate models for Bayesian model selection used by Madigan and Raftery (1994). Their set of models is $\mathcal{A} = \{\Pi : \mathbb{P}(\Pi_0 | \mathbf{Z})/\mathbb{P}(\Pi | \mathbf{Z}) \leq \tilde{c}\}$ where Π_0 is the *maximum a posteriori* estimate. In the language of Rashomon sets, $\tilde{c} = (\mathbb{P}(\Pi_0 | \mathbf{Z})\mathbb{P}(\mathbf{Z}))^{-\epsilon}$.

Notation	Definition
$\mathcal{P}_{ h}$	Set of admissible partitions with h pools
$Q \in \mathcal{Q}$	Prior over all β
$Q \in \mathcal{Q}_{ h}$	Prior over β such that there is some partition $\Pi_{\beta} \in \mathcal{P}_{ h}$
$Q \in \mathcal{Q}_{\mathcal{P}_{ h}}$	Prior for partitions $\Pi \in \mathcal{P}_{ h}$
P_{ℓ_0}	The uniform prior over $\mathcal{P}_{ h}$ (induced by ℓ_0 over \mathcal{P}^*)
$P_{Q, \mathbf{z}}$	Posterior density (over partitions or β) with prior Q
$\delta(P, Q)$	Total variation distance between P and Q

TABLE 1. Notation used in Theorem 2.

it. Regarding the choice of the reference model, consider any good initial estimate of a model. This could be for instance the MAP or a technique that converges to the MAP (e.g., regularization through the Lasso). Then the RPS will trace out, given a tolerance epsilon, all the models that have slightly lower or at least higher posterior values relative to the reference. This guarantees that we can essentially be robust against the Rashomon Effect and gives guidance on the choice.

4. SIZE OF THE RASHOMON SET

Given that we would like to enumerate \mathcal{P}_{θ} it is useful to calculate bounds on both its size and also \mathcal{P}^* . Since any admissible partition requires each profile to respect Definition 6, it is sufficient to consider each profile independently. To develop an upper bound, we will use m to denote the number of features with non-zero values in the profile we are focusing on, so $m \in \{1, \dots, M\}$. All technical details are deferred to Appendix C.

The first observation is that \mathcal{P}^* is small relative to the total number of potential partitions.

Proposition 2. *In each profile, the total number of:*

- (i) all possible partitions is $\mathcal{O}(2^{2(R-1)^m})$, and
- (ii) admissible partitions is $\mathcal{O}(2^{m(R-2)})$.

In the following sections, we motivate the choice of the ℓ_0 prior and discuss how this can be used to control the size of the Rashomon set.

4.1. Choosing a robust prior. Next, we select a prior. RPS can be built using other priors, but we advocate for using the robust one. We do not want to impose false independence or unwarranted assumptions on correlations on the relationship between the β s and instead want to be robust in an environment with possibly a complex and unknown correlational structure. We show that this corresponds to the ℓ_0 penalty: conditional on the number of pools in a partition, all admissible partitions are equally likely. Let \mathcal{Q} be a family of priors for some expected outcome β . For any

prior $Q \in \mathcal{Q}$, denote the posterior over β given some data \mathbf{Z} as $P_{Q,\mathbf{Z}}$, i.e.,

$$P_{Q,\mathbf{Z}}(\beta) = \mathbb{P}(\beta \mid \mathbf{Z}, \beta \sim Q) = \frac{\mathbb{P}(\mathbf{y} \mid \mathbf{X}, \beta)Q(\beta)}{\mathbb{P}(\mathbf{y} \mid \mathbf{X})}.$$

Let us fix the sparsity at h : there are h distinct pools in the partition. Define the restricted space of partitions as $\mathcal{P}_{|h} = \{\Pi \in \mathcal{P}^* : H(\Pi) = h\}$. Let $N(h) = |\mathcal{P}_{|h}|$. The ℓ_0 penalty imposes a sparsity restriction on the number of pools. Therefore, at a fixed sparsity h , the ℓ_0 penalty corresponds to a uniform prior over $\mathcal{P}_{|h}$. Denote the ℓ_0 prior as P_{ℓ_0} . So for any $\Pi \in \mathcal{P}_{|h}$, $P_{\ell_0}(\Pi) = 1/N(h)$.

For any given β , there is a corresponding admissible partition $\Pi_\beta \in \mathcal{P}^*$. Then we can define $\mathcal{Q}_{|h}$ be the family of priors for the restricted space of β such that there is some $\Pi_\beta \in \mathcal{P}_{|h}$. Let $\mathcal{Q}_{\mathcal{P}_{|h}}$ denote the family of priors, derived from $\mathcal{Q}_{|h}$, over partitions in $\mathcal{P}_{|h}$. We can traverse from $\mathcal{Q}_{|h}$ to $\mathcal{Q}_{\mathcal{P}_{|h}}$ by noticing that for a given β , there is a corresponding admissible partition $\Pi_\beta \in \mathcal{P}$ i.e, for any prior $Q \in \mathcal{Q}_{|h}$, we can define a prior over $\mathcal{P}_{|h}$,

$$Q_{\mathcal{P}_{|h}}(\Pi) = \int_{\beta} \mathbb{1}(\Pi_\beta = \Pi)Q(\beta)d\beta, \quad \Pi \in \mathcal{P}_{|h}.$$

For reference, we define the supports for various priors in Table 1.

For two priors $P, Q \in \mathcal{Q}_{\mathcal{P}_{|h}}$, define the total variation distance as

$$\delta(P, Q) = \sup_{\Pi \in \mathcal{P}_{|h}} |P_{P,\mathbf{Z}}(\Pi) - P_{Q,\mathbf{Z}}(\Pi)|.$$

Note that since \mathcal{P}^* is finite, the supremum and maximum over \mathcal{P}^* (and any of its subsets) are identical.

Theorem 2. *For a given sparsity h , the ℓ_0 penalty is minimax optimal in the sense that*

$$\sup_{Q \in \mathcal{Q}_{\mathcal{P}_{|h}}} \delta(P_{P_{\ell_0},\mathbf{Z}}, P_{Q,\mathbf{Z}}) = \inf_{P \in \mathcal{Q}_{\mathcal{P}_{|h}}} \sup_{Q \in \mathcal{Q}_{\mathcal{P}_{|h}}} \delta(P_{P,\mathbf{Z}}, P_{Q,\mathbf{Z}}).$$

In other words, if one is unwilling to commit to any correlation structure for the model coefficients, the ℓ_0 penalty, which puts a prior on the *number* of selected features, is optimal for model selection.

4.2. Implications for Calculations. We will show that the size of the Rashomon Partition Set for each profile is actually polynomial in M and R . First, in Lemma 1, we make a crucial observation that the number of pools in any RPS is bounded.

Lemma 1. *For a given probability q , maximum distance ϵ , and regularization parameter λ , any aggregation in the Rashomon set \mathcal{P}_θ can have at most $H_\theta(\lambda)$ pools,*

$$H_\theta(\lambda) = \left\lceil -\frac{\ln(c\theta)}{\lambda} \right\rceil,$$

where $c := c(\mathbf{Z})$ is a normalization constant that depends only on \mathbf{Z} and $\lfloor \cdot \rfloor$ is the floor function.

Essentially, the likelihood term, $c(\mathbf{Z})$, is driving all of the penalty on the maximum number of pools in a Rashomon partition. Since the likelihood of any given observation is small, it explodes as we collect more observations. As we collect more data, we gain more information with which we can distinguish finer partitions. Lemma 1 allows us to further reduce the size of the search space in Proposition 2 by considering only partitions that meet this requirement.

We show that the size of the Rashomon partition set is bounded polynomially in Theorem 3. Such a relationship between regularization and size of the model class was previously hypothesized and shown for empirical data by [Semenova et al. \(2022\)](#).

Theorem 3. *For a given Rashomon probability θ and regularization parameter λ , the size of the Rashomon Partition Set is bounded by*

$$|\mathcal{P}_{q,\epsilon}| \leq \sum_{h=1}^H N(h) = \begin{cases} \mathcal{O}(mR^{H-2}), & R > m^{1.41} \\ \mathcal{O}\left((mR)^{\log_2 H} (\log_2(mR))^{-1}\right), & \text{else} \end{cases},$$

where $H := H_\theta(\lambda)$ and $N(h)$ is the number of possible splits that generate h pools.

To illustrate the implications of Theorem 3, consider an example in which $M = 3$ and $R = 5$. Also, suppose that we can have at most $H = 8$ pools in any Rashomon partition. Theorem 3 says that the size of the RPS is $|\mathcal{P}_{q,\epsilon}| \leq 27$ using the first bound. The number of all admissible partitions is $2^{M(R-2)} = 512$. Now, imagine a setting where we add two more arms and another dosage intensity to get $M = 5$ and $R = 6$. While the size of the RPS is $|\mathcal{P}_{q,\epsilon}| \leq 800$, the total number of admissible partitions is 32,768. The RPS is less than 2% of the full search space. Let's turn $M = 10, R = 10$. Now, size of the RPS, 81,680, is only a fraction ($\approx 7 \times 10^{-20}$) of the full search space, $\approx 10^{24}$. As we will see in our empirical examples, combined with Theorem 1, with just hundreds of models, we can get very close to the full posterior.

5. ENUMERATING RASHOMON PARTITIONS

Since we do not pool across profiles, we can enumerate the Rashomon Partition for each profile independently and then finally combine them in the end. We will first develop intuition to present an algorithm to enumerate the RPS for a single profile. Then, we will discuss how to combine these profile-specific RPS to get our RPS across all profiles. The intuition behind our enumeration is that any split we make introduces a new set of pools. If for some reason this split is very bad, then no matter what other split we make, we can never recover. Theorems 4 and 5 help us identify

those poor splits. They rely on the fact that equivalent points having the exact same feature values will always belong to the same pool. However, equivalent units may not have the same outcome. Therefore, we will always incur some loss from these equivalent units (also see [Angelino et al. \(2017\)](#); [Xin et al. \(2022\)](#)). We defer technical details of the results to Appendix D.

First, we develop some notation. Let \mathcal{K} define the set of all $K = R^M$ possible feature combinations. For some $k \in \mathcal{K}$, let k_i denote the value that feature i takes for $i = 1, \dots, M$. Consider some partition matrix Σ for profile ρ , where the partition is given by $\Pi := \Pi(\Sigma)$. Given some data $\mathbf{Z} = (\mathbf{X}, \mathbf{y})$, we will use the mean squared error and the average outcome in pool $\pi \in \Pi$, $\hat{\mu}_\pi$, as defined in Equation (6). However, the results generalize to any non-negative loss function as we will see in Section 8 with weighted mean-squared error.

Consider the Σ matrix. Suppose we fix some indices \mathcal{M} in Σ . Define a new matrix $\Sigma_{\mathfrak{f}}$,

$$\Sigma_{\mathfrak{f},(i,j)} = \begin{cases} \Sigma_{(i,j)}, & (i,j) \in \mathcal{M} \\ 0, & \text{else} \end{cases}.$$

In other words, $\Sigma_{\mathfrak{f}}$ is a partition where all heterogeneity splits made by Σ corresponding to indices in \mathcal{M} are obeyed and we maximally split at all other places. Let $\Pi_{\mathfrak{f}} := \Pi(\Sigma_{\mathfrak{f}})$ correspond to this maximal partition respecting Σ at indices \mathcal{M} . Next, define

$$\pi_{\mathfrak{f}} = \{k \in \mathcal{K} \mid k_i \leq j + 1 \iff (i, j) \in \mathcal{M}\}$$

to be the set of all feature combinations covered by indices in \mathcal{M} . And we define the complement $\pi_{\mathfrak{f}}^c = \mathcal{K} \setminus \pi_{\mathfrak{f}}$. Finally, define $H(\Pi, \mathcal{M}) = \sum_{\pi \in \Pi} \mathbb{1}\{\pi \cap \pi_{\mathfrak{f}} \neq \emptyset\}$ to be the number of pools in Π consisting of feature combinations corresponding to indices \mathcal{M} .

Now consider a procedure where we keep Σ constant at \mathcal{M} and make further splits (not already implied by \mathcal{M}) at other indices only. Define $\text{child}(\Sigma, \mathcal{M})$ to be the set of all such Σ' .

Using the intuition we built earlier, our search algorithm in Algorithm D.1 starts at some partition and fixes some heterogeneity splits. Theorem 4 says that if the loss incurred by these fixed heterogeneity splits is already too high, then our search is doomed to begin with and we should abandon this partition.

Theorem 4. *Let θ_ϵ be the Rashomon threshold in the loss space i.e., $\Pi \in \mathcal{P}_{q,\epsilon}$ if and only if $Q(\Pi) < \theta_\epsilon$. Given a partition $\Pi := \Pi(\Sigma)$ for partition matrix Σ , a set of fixed indices \mathcal{M} , and data \mathbf{Z} consisting of n observations, define*

$$(8) \quad b(\Sigma, \mathcal{M}; \mathbf{Z}) = \frac{1}{n} \sum_{\pi \in \Pi_{\mathfrak{f}}} \sum_{k(i) \in \pi} \mathbb{1}\{k(i) \in \pi_{\mathfrak{f}}\} (y_i - \hat{\mu}_\pi)^2 + \lambda H(\Pi, \mathcal{M}).$$

If $b(\Sigma, \mathcal{M}; \mathbf{Z}) > \theta_\epsilon$, then Σ and all $\Sigma' \in \text{child}(\Sigma, \mathcal{M})$ are not in the Rashomon set $\mathcal{P}_{q,\epsilon}$.

Building on the same intuition, Theorem 5 “looks ahead” to see if this partition is of poor quality – if the loss incurred by feature combinations yet to be split is too high, then we should abandon this partition.

Theorem 5. *Consider the same setting as Theorem 4. Define*

$$(9) \quad b_{eq}(\Sigma, \mathcal{M}; \mathbf{Z}) = \frac{1}{n} \sum_{\pi \in \Pi_f} \sum_{k(i) \in \pi} \mathbb{1}\{k(i) \in \pi_f^c\} (y_i - \hat{\mu}_\pi)^2,$$

$$(10) \quad B(\Sigma, \mathcal{M}; \mathbf{Z}) = b(\Sigma, \mathcal{M}; \mathbf{Z}) + b_{eq}(\Sigma, \mathcal{M}; \mathbf{Z}).$$

If $B(\Sigma, \mathcal{M}; \mathbf{Z}) > \theta_\epsilon$, then Σ and all $\Sigma' \in \text{child}(\Sigma, \mathcal{M})$ are not in the Rashomon set $\mathcal{P}_{q,\epsilon}$.

Theorems 4 and 5 help aggressively cut down the search space by combining the lowest penalty on the splits already made and the lowest mean-squared error on the splits yet to be made. If this is already too high, then we abandon our search. We illustrate this in Algorithm D.1. Here, we start with all feature combinations pooled together. We begin our search at the first feature trying to split the two variants with the lowest dosages into separate pools. We keep a queue of possible splits to consider. Whenever we remove a possible split from the queue, we check its viability using Lemma 1, and Theorems 4 and 5. If this is a bad split, we go to the next split in the queue. And if this is a good split (so far), we check if it already meets the Rashomon threshold and recursively add other possible splits to this queue. We also maintain a cache of splits that have been added to the queue at some point to avoid doubling back on old splits.

The choice of starting position in Algorithm D.1 is arbitrary. No matter with which feature we start our search, Algorithm D.1 will eventually explore the feature space sufficiently to identify partitions outside the Rashomon set, at which point we abandon that search. Theorems 4 and 5 guarantee this. Algorithm D.1 will correctly enumerate the RPS independently of our starting search position.¹¹ As noted before, we can solve each profile independently. In Algorithm 1, we explicitly show how to do this. Note that in line 3, we once again leverage Theorem 5 by noting that each profile will always incur some loss.

Once we solve each profile independently, we can start pooling across profiles as dictated by Definition 7. The key insight here is the construction of the intersection matrix Σ^\cap we discussed earlier. Using this object, pooling across profiles can be achieved by a breadth-first search on the

¹¹Obviously, some starting positions may be computationally favorable i.e., we do not need to search for too long before we encounter low posterior partitions. We believe domain experts will have a better understanding of the context and may be able to choose a starting location that can reduce computation costs.

Algorithm 1 EnumerateRPS($M, R, H, \mathbf{Z}, \theta_\epsilon$)

Input: M features, R factors per feature, max pools H , data \mathbf{Z} , Rashomon threshold θ_ϵ
Output: Rashomon set $\mathcal{P}_{q,\epsilon}$

- 1: $\rho =$ all 2^M profiles
- 2: $H' = H - 2^M + 1$
- 3: $\mathcal{E} =$ [equivalent point bound of profile ρ_i for $\rho_i \in \rho$] $\triangleright b_{eq}$ in Theorem 5 with the zero matrix
- 4: $\mathcal{P} = \text{dict}()$
- 5: **for** $\rho_i \in \rho$ **do**
- 6: $\theta_i = \theta_\epsilon - \text{sum}(\mathcal{E}) + \mathcal{E}_{\rho_i}$
- 7: $M_i =$ active features in ρ_i
- 8: $R_i = R[M_i]$
- 9: $\mathcal{P}[\rho_i] = \text{EnumerateRPS_profile}(M_i, R_i, H', \mathbf{Z}, \theta_i)$ \triangleright See Algorithm D.1
- 10: Sort partition matrices in $\mathcal{P}[\rho_i]$ on loss
- 11: $\mathcal{P}' = \times_{\rho_i \in \rho} \mathcal{P}[\rho_i]$ \triangleright Obtain candidate partitions with Cartesian product
- 12: $\mathcal{P}_{q,\epsilon} = \text{PoolProfiles}(\mathcal{P}', \rho_0, \mathbf{Z}, \theta_\epsilon)$ \triangleright See Algorithm D.4
- 13: **return** $\mathcal{P}_{q,\epsilon}$

M -d unit hypercube by starting at the profile with all features inactive. During this breadth-first traversal, we recursively attempt to pool across neighbors in the hypercube using the intersection matrix. We describe this in Algorithm D.4.

Theorem 6. *Algorithm 1 correctly enumerates the Rashomon partition set.*

Given our setup, it is easy to see how Algorithm 1 can be parallelized by delegating each call to Algorithm D.1 to a separate thread. Since Algorithm D.4 is a breadth-first search, it can also be parallelized. Its correctness is shown in Appendix D.

6. SIMULATIONS

We conduct two simulation experiments. The first is the drug treatment setting we have been motivating throughout the paper. It demonstrates that in a very reasonable, real-world scenario – minimum dosages to be effective, strong interaction effects with excess amounts – regularization that relies on independence (Lasso) will fail to identify the best dosing policy. In contrast, the RPS will both tend to include the best drug combination (in addition to others of course) but also converge to the true best profile as the amount of data increases. The second illustrates the Rashomon effect. In a given sample, it is possible through random chance that a sub-optimal drug profile happens to be the best. The RPS contains the true best the vast majority of the time.

6.1. Simulation 1: An example in medicine. Imagine a setting where a pharmacist is interested in finding the best treatment as a combination of two drugs, A and B. In particular, we consider

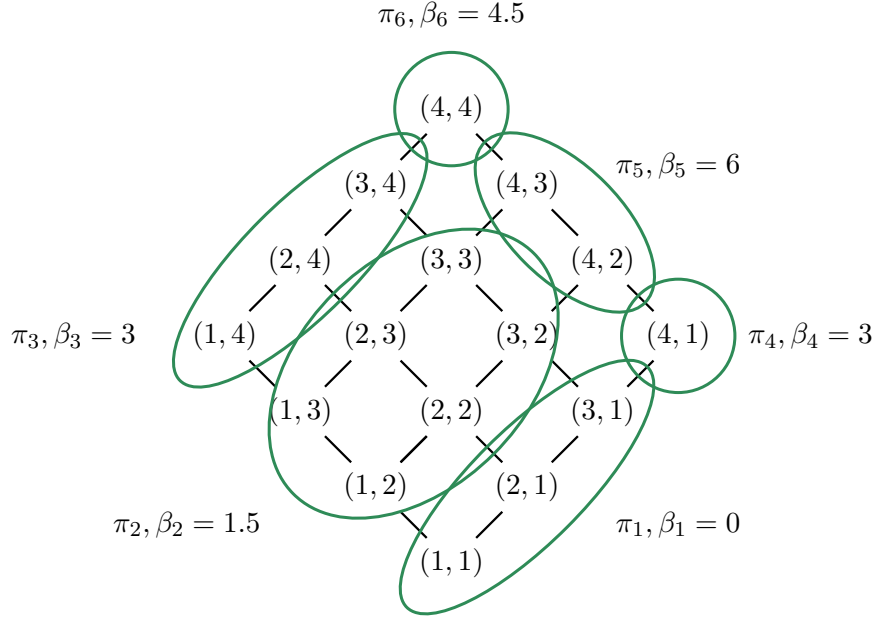


FIGURE 3. Hasse diagram illustrating partition used in Simulation 1.

a scenario where each drug needs a minimum dosage to be effective. However, when the dosages become too strong, the interaction between the drugs results in a reduced treatment effect.¹²

In this setup, suppose that each drug has 4 possible non-zero dosages $d \in \{1, 2, 3, 4\}$. We will denote each of $4^2 = 16$ unique drug cocktails by their dosage (d_A, d_B) . The treatment is not effective when $d_A < 4$ and $d_B = 1$. As we increase the dosages of the drugs, they become more effective. The treatment is most effective when drug A is maxed and drug B has a medium dosage i.e., $d_A = 4, d_B = 2, 3$. When both drugs are maxed, a drug interaction produces a sub-optimal effect. Our parameters and partition are summarized in Figure 3. Observe that, by design, all non-zero marginal increases in outcomes as we increase dosage levels are correlated. Therefore, we expect Lasso to perform poorly as it penalizes selecting correlated features. However, the ℓ_0 penalty does not presume any such false independence assumptions.

In each dataset, we fixed the number of samples per feature combination to n_k and outcomes for each feature were drawn from a $\mathcal{N}(\beta_i, 1)$ distribution. We varied $n_k \in \{10, 100, 1000, 5000\}$ and for each n_k simulated $r = 100$ datasets. For each dataset, we fit the Lasso model and found the RPS. The Rashomon threshold was chosen to be $1.5 \times \text{MSE}_{\text{Lasso}}$ where $\text{MSE}_{\text{Lasso}}$ is the MSE of the Lasso

¹²Such *antagonistic interactions* where one drug impedes the effect of another drug are not uncommon (see [Cascorbi, 2012](#); [Triplitt, 2006](#); [Wambaugh et al., 2020](#)). For example, ACE inhibitors (Angiotensin-converting enzyme inhibitors), used in treating high blood pressure, and Metformin, used in treating diabetes, are known to have negative interactions ([Blackburn and Wilson, 2006](#)); ACE inhibitors and NSAIDs (Non-steroidal anti-inflammatory drugs), and Aspirin and Ibuprofen have reduced effects when taken together ([Cascorbi, 2012](#)), and; effects of drug interactions in non-small cell lung cancer are highly context-specific ([Nair et al., 2023](#)).

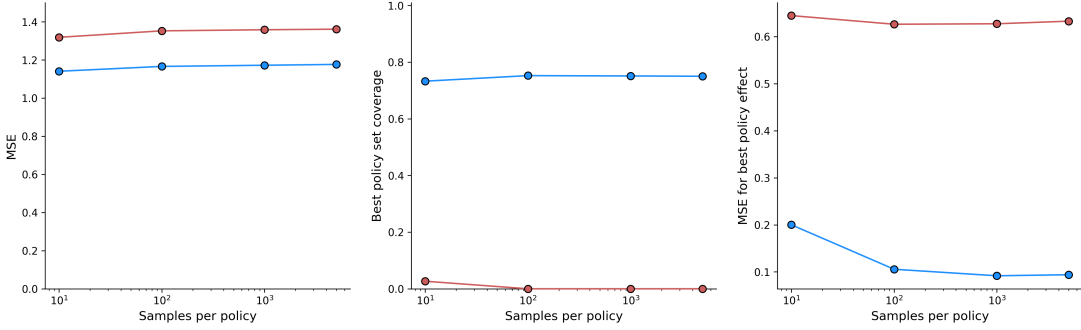


FIGURE 4. Results for Simulation 1. The blue points correspond to models in the Rashomon set and the red points correspond to Lasso estimates. From left to right: mean squared error, best policy set coverage and best policy mean squared error.

model with $n_k = 10$. We use the same regularization parameter $\lambda = 0.1$ for the Rashomon and Lasso models.

The results from the simulations are presented in Figure 4. The metrics reported here are described in Appendix G. It is clear that the “average” model in the RPS not only performs much better than Lasso in terms of overall MSE, but it is also able to recover the true best policy set. By looking only for the optimal model, Lasso consistently misses out on coverage for the best policies by incorrectly selecting features. However, when we look at the RPS of near-optimal models, we can recover the full best policy coverage almost always. Our results also reveal that the poor performance of Lasso is not a sample size issue. Lasso is simply not the right tool in situations with correlated parameters. Appendix G also visualizes the the Rashomon set through a 2D heatmap.

6.2. Simulation 2: The Rashomon effect. We now illustrate the Rashomon effect. By using just the optimal model, we miss out on insights into the true data-generating process offered by near-optimal models.

Consider a setting with four features. Each feature takes on four ordered factors including the control (which corresponds to zero, when the feature is inactive), $\{0, 1, 2, 3\}$. There are sixteen different feature profiles: $2^4 = 16$ possible combinations of active and inactive features. The control corresponds to the profile where all features are inactive.

Our data-generating process groups all feature combinations in a given profile into the same pool. We will assume that the following profiles have a non-zero outcome:

$$\beta_{(0,0,0,1)} = 4.4, \sigma_{(0,0,0,1)}^2 = 1, \beta_{(0,1,0,0)} = 4.3, \sigma_{(0,1,0,0)}^2 = 1, \beta_{(0,1,0,1)} = 4.45, \sigma_{(0,1,0,1)}^2 = 1,$$

$$\beta_{(1,0,1,0)} = 4.5, \sigma_{(1,0,1,0)}^2 = 1.5, \beta_{(1,1,1,1)} = 4.35, \sigma_{(1,1,1,1)}^2 = 1.$$

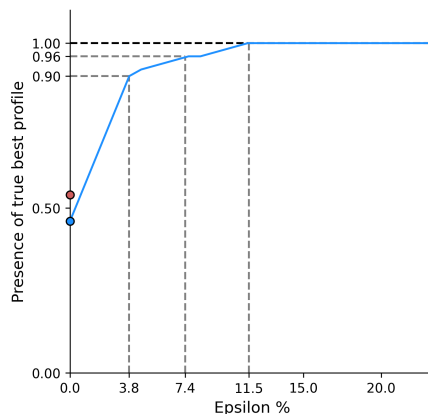


FIGURE 5. Results for Simulation 2. The plot shows often the true best profile is discovered as we increase the Rashomon threshold in the blue curve. With just $\epsilon \approx 0.038$, we recover the true best profile in the Rashomon set about 90% of the time. The red dot corresponds to how often Lasso recovers the true best profile.

All other feature profiles have outcome $\beta = 0$ and variance $\sigma^2 = 1$. Here, the feature profile $(1, 0, 1, 0)$ is the best. However, the other four profiles listed above are very close.

We generated data with $n_k = 30$ data points per feature combination. Each profile has a different number of feature combinations depending on how many features are active. Therefore, each profile will have a different number of data points. The outcomes were drawn from a $\mathcal{N}(\beta_i, \sigma_i^2)$ distribution. We averaged the results over $r = 100$ simulations.

Figure 5 tells us how often the true best feature profile is present in the Rashomon set as a function of the threshold ϵ . If we were to focus only on the best-fit model, we lose out on models that correctly recover the true best feature profile. However, by looking at the RPS, we can tease apart the nuances in the data-generating process. And as we increase ϵ , we increase the chance that we recover the true best profile.

7. EMPIRICAL DATA EXAMPLES

In three distinct environments – impact of price match on donations, heterogeneity in chromosomal structure, and the impact of microcredit on entrepreneurship – we emphasize robust conclusions, both affirming and challenging the established literature’s findings in each context through the use of RPS. This underscores the importance of our approach in shedding light on various research landscapes.

7.1. Does price matter in charitable giving? Our first example comes from the data of [Karlan and List \(2007\)](#) and concerns charitable giving. This is important for both basic research and policy considerations. Depending on the specific motivation for giving, whether or not there is a matching

gift for one's donation and how it scales with one's own donation may impact one's donation. Further, these patterns may correlate with political perspectives, which is of particular importance when the charity is a political NGO as is the case here.

Karlan and List (2007) conducted a field experiment to better understand the anatomy of charitable giving. They used mail solicitations to prior donors of a non-profit political organization to study the effect of price on charitable donations. The data contains 50,083 individuals in the United States who had previously donated to the organization. All individuals received a letter soliciting donations. Those in the treatment group (33,396 people) included an additional paragraph describing that their donation will be matched. The control group (16,687 subjects) did not receive this paragraph. The letters were identical otherwise.

The treatment consists of three different features: (i) the maximum size of the matching gift across all donations, (ii) the ratio of price match, and (iii) an example suggested donation amount. The maximum size of the matching gift took on four different values – \$25,000, \$50,000, \$100,000, or unspecified. The price match ratio took on three different values — \$1:\$1, \$2:\$1, or \$3:\$1. Here $\$a : \b means that the organization receives $\$a$ for every $\$b$ contribution. Finally, the suggested donation amount was dependent on the highest previous contribution (HPC) from that individual and took on three possible values – $1 \cdot \text{HPC}$, $1.25 \cdot \text{HPC}$ or $1.5 \cdot \text{HPC}$. This leads to a $4 \times 3 \times 3$ factorial design, excluding control, with fully ordered factors.¹³ All feature combinations were fully randomized.

Additionally, they also collected demographic census data (aggregated at the zip code level), state and county returns from the 2004 presidential election, and frequency of the organization's activities at the state level. They classify states as red or blue depending on whether they voted for George Bush or John Kerry in the 2004 U.S. presidential election. They note that political affiliation is the most robust indicator of the level of giving in the control group. Therefore, in our analysis, we include this as a demographic covariate. There were 35 data points whose political affiliation was missing and we removed these data points prior to our analysis. Thus, we have a $4 \times 3 \times 3 \times 2$ feature space. Our outcome is the amount, in hundreds of dollars, that were donated.

Karlan and List (2007) focus on two key findings. First, they find that (and puzzle over why) matching grants work in red but not blue states. Second, though having a match at all (relative to the control of none) has an effect, they argue that the matching ratio itself does not matter. That is, having an overly steep ratio is essentially wasteful.

¹³We assume $\$25,000 < \$50,000 < \$100,000 < \text{unspecified}$.

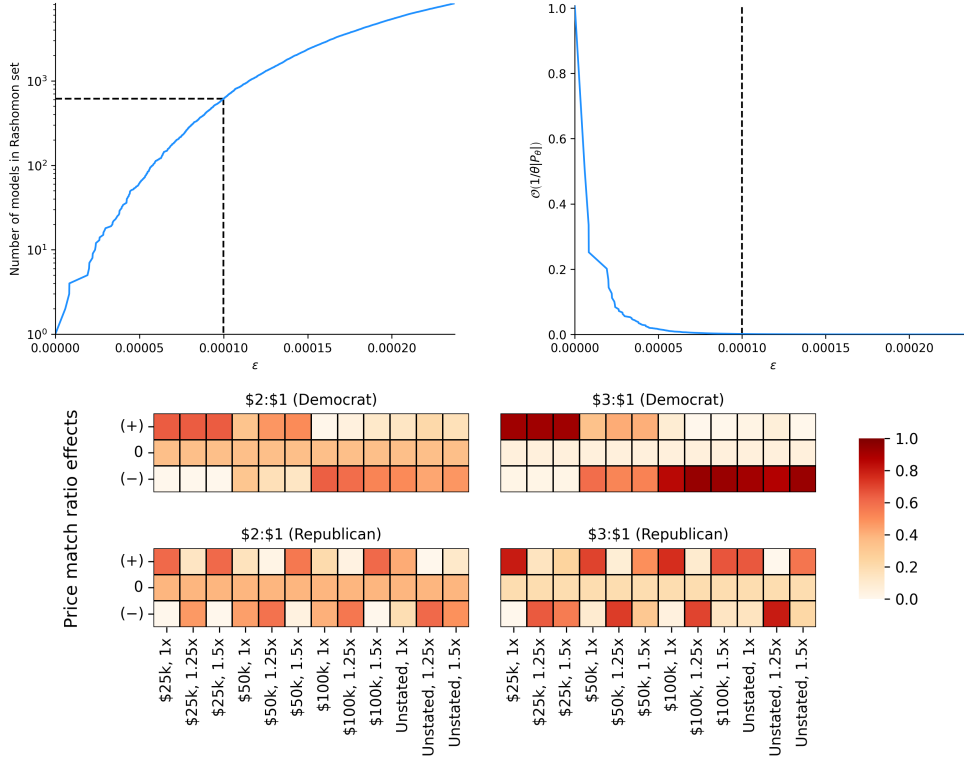


FIGURE 6. Results for the [Karlan and List \(2007\)](#) dataset. The top two panels show the size of the RPS and error term in Theorem 1 as a function of ϵ . Our choice of $\epsilon = 10^{-4}$ is highlighted by the black dashed line. The bottom panel shows the effect of price match of \$2:\$1 and \$3:\$1 relative to \$1:\$1 are stratified by political leaning and other treatments in the RPS.

We look at these two findings through the lens of the RPS. Figure 6 presents our choice of $\epsilon = 10^{-4}$ as well as how the set size and error bound change with ϵ . Figure 6 also shows the effect of price match of \$2:\$1 and \$3:\$1 relative to \$1:\$1 for all feature combinations.

We find the following. First, the treatment effect of matching is indeed differentially driven by red states alone from a robust perspective. In only less than 1% of the partitions in the RPS, we see that the treatment effect of matching is pooled between red and blue indicating robust heterogeneity of treatment effect across political affiliations. (This calculation is not directly presented in the figure, though it can be glimpsed from the fact that the patterns between red and blue states look different.)

Second, while having a match matters and is stratified across political affiliations, the matching ratio itself matters. That is, there is a split in the treatment effect between \$1:\$1 and $> \$1:$1 in 100% of the models in the RPS for blue states and 65% of the models in the red states. In each model in the RPS, we computed $\text{sign}\{\hat{y}(2:1, x, z, p) - \hat{y}(1:1, x, z, p)\}$ and $\text{sign}\{\hat{y}(3:1, x, z, p) - \hat{y}(1:1, x, z, p)\}$ for each maximum limit x , suggested donation z , and political affiliation p , where $\hat{y}(k)$ estimates$

$\mathbb{E}[Y_i(k)]$ with a sample mean.¹⁴ And we visualize the average of those quantities over the RPS in the bottom panel of Figure 6. We clearly see robust patterns in the sign of the match ratio effect. Specifically, for \$3:\$1 in blue states, we see a robust positive effect for a maximum limit of \$25,000 and a robust *negative* effect for \$100,000 or unspecified limits.¹⁵ In red states, we see a robust positive effect for a suggested donation of $1 \cdot \text{HPC}$ and a robust negative effect for $1.25 \cdot \text{HPC}$.

Our results demonstrate that [Karlan and List \(2007\)](#)’s assertion of the red-blue difference robustly holds. Meanwhile, contrary to their assertion (which is an artifact of their particular regression), we find that robustly match ratios matter and in particular this is the case with blue states across all feature combinations though holds true for most of the red state configurations as well. The result on match ratios mattering is of great policy relevance for the same reasons as argued in [Karlan and List \(2007\)](#): if they did not matter, low ratio matches could be used to save money, but if they robustly do matter, when they are positive high ratio matches ought to be leveraged and may have excess returns and when they are negative the costs are even more damaging.

7.2. Heterogeneity in telomere length. Telomeres are regions of repeated nucleotide sequences near the end of the chromosome that protect the chromosome from damage. Telomeres reduce in length every time a cell divides eventually becoming so short that the cell can no longer divide. Telomere length varies by cell type and more recent literature has begun to examine what features are associated with (or possibly cause) changes in telomere length. For instance, the shortening of telomeres has been linked to cellular senescence and aging and has been thought to hold biomarkers as targets for genetic predispositions and anti-cancer therapies ([Rossiello et al., 2022](#); [Srinivas et al., 2020](#)). While it was long believed that longer telomeres are “better,” recent research suggests that perhaps there is only a narrow range of telomere lengths that are healthy and anything that is extreme is at increased risk of immune system problems or cancer ([Alder et al., 2018](#); [Protsenko et al., 2020](#)). Research has found heterogeneity by race and ethnicity and, further, features such as stress and age have been associated with differences in telomere length ([Chae et al., 2014](#); [Geronimus et al., 2015](#); [Hamad et al., 2016](#); [Vyas et al., 2021](#)). Nonetheless, these analyses are large-scale associative statistical analyses rather than those derived from micro-experimental data.

Our RPS approach may be useful here as we can identify in data involving telomere length and various features, what *robust* associations can be made. This can give a micro-oriented experimental researcher guidance on where to focus, rather than relying on a specific machine learning exercise.

¹⁴We define $\text{sign}\{x\} = \mathbb{1}\{x > 0\} - \mathbb{1}\{x < 0\} \in \{1, 0, -1\}$.

¹⁵This robust discouragement effect is particularly interesting and may warrant further research.

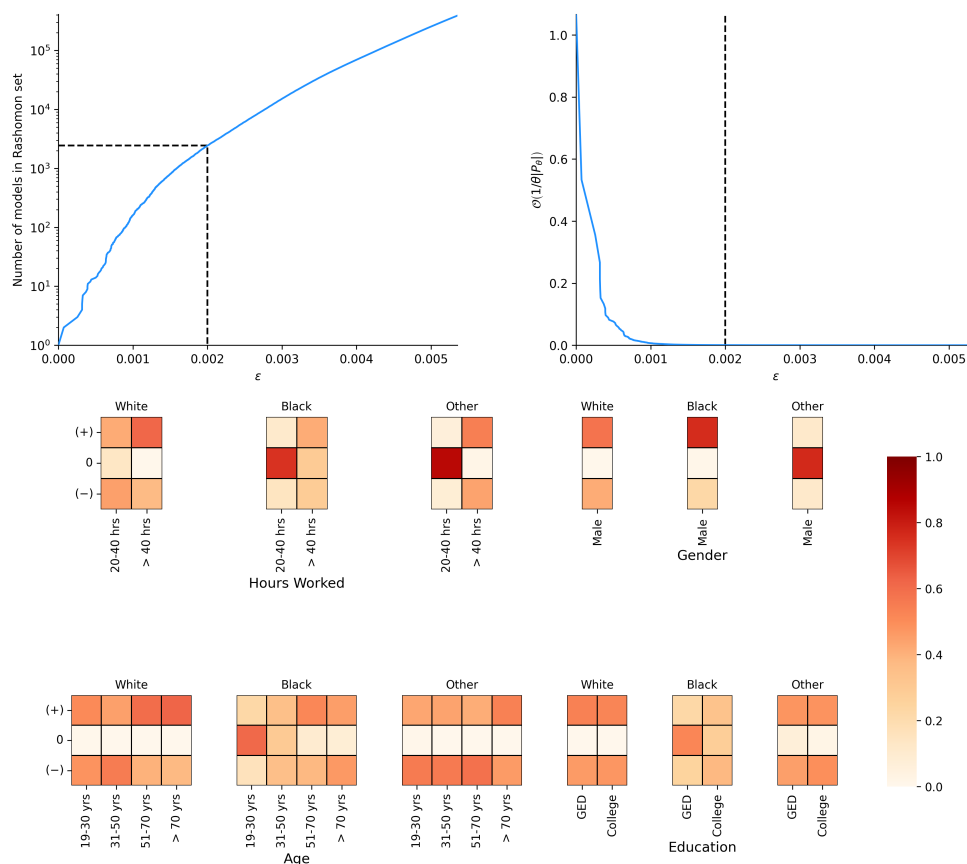


FIGURE 7. The top two panels show what happens as we increase ϵ in the NHANES dataset highlighting our choice of ϵ . In the bottom panel, we highlight heterogeneity in telomere length across the four features (hours worked, gender, age, and education) relative to the lowest level of that feature, sorted into race.

We use the National Health and Nutrition Examination Survey (NHANES) collected in 1999 and 2002. The survey included blood draws and from the samples DNA analyses were performed and telomere length was estimated. Specifically, the dataset reports the mean T/S ratio (telomere length relative to a standard reference DNA).¹⁶ The dataset also contains socio-economic variables. To speak to the emerging literature on telomere heterogeneity, we focus on hours worked (a proxy for stress), age, gender, race, and education. Our goal is to study the RPS of this heterogeneity on T/S.¹⁷

¹⁶See https://www.cdc.gov/nchs/nhanes/1999-2000/TELO_A.htm for details. Website last accessed on 2024-01-29.

¹⁷To operationalize, we removed all individuals who were missing data for our relevant covariates. We binned the number of hours worked into three ordered discrete factors – ≤ 20 hours, 21 – 40 hours, and ≥ 40 hours. Gender was unordered, and either Male or Female. Age was categorized into five ordered discrete factors – ≤ 18 years, 19 – 30 years, 31 – 50 years, 51 – 70 years, and > 70 years. Education was categorized into 3 ordered discrete factors – did not complete GED, finished GED but did not finish college, and received some college degree. Finally, race was categorized into three unordered factors – Black, White, and Other.

We show our choice of ϵ for the Rashomon threshold in the top two panels of Figure 7. In the RPS, we found robust heterogeneity in race – specifically, we found no partition that pools features across different races. So the remainder of the analysis will stratify based on race.

We found robust evidence of heterogeneity in gender only in White and Black races. All partitions for these races split males and females into separate pools. However, this was absent in Other races – only 23% of the partitions in the RPS split on gender.

Similar to the previous data exercise, for each race r , we find the length of telomeres stratified by each feature $m \in \{\text{Hours worked, Gender, Age, Education}\}$ relative to the lowest level of that feature, $\mathbb{E}[Y_i(x_m, \mathbf{x}_{-m}, r)] - \mathbb{E}[Y_i(1, \mathbf{x}_{-m}, r)]$.¹⁸ We use the sample mean estimates $\hat{y}(\mathbf{x}, r)$ and take its sign, $\text{sign}\{\hat{y}(x_m, \mathbf{x}_{-m}, r) - \hat{y}(1, \mathbf{x}_{-m}, r)\} \in \{1, 0, -1\}$. We average the counts of each sign over all partitions in the RPS and report them in the bottom panel of Figure 7. By visually inspecting this plot, we find very few robust patterns. As discussed earlier, we find robust differences in telomere lengths across males and females in the Black population and a robust non-difference in Other races. Similarly, we find a robust non-difference in Black and Other races in telomere lengths for people who work fewer than 40 hours.

Our findings reveal an absence of robust evidence supporting the patterns highlighted in existing literature. Moreover, of the few robust patterns we do identify, several findings contradict prior research. We find Black males have longer telomeres than females. Among White people, we find older people have longer telomeres, which also contradicts existing research. This underscores the necessity for further exploration in this field using comprehensive data and appropriate statistical methods.

7.3. Heterogeneity in the impact of microcredit access. A large literature has looked at the impact of microfinance on several outcomes, ranging from private consumption to business outcomes to social outcomes (e.g., female empowerment). Mostly, the literature has found little beyond basic consumption effects (Angelucci et al., 2015; Attanasio et al., 2015; Augsburg et al., 2015; Banerjee et al., 2015; Crépon et al., 2015; Tarozzi et al., 2015; Meager, 2019), though there is suggestive evidence of some potential heterogeneity. One specific heterogeneity of interest concerns entrepreneurs: those with pre-existing businesses may be particularly benefited by the access to microfinance loans (Banerjee et al., 2019). Another concerns family size (Baland et al., 2008): the returns to credit access may vary by whether the household has more children.

Developing an RPS is useful both for (a) developing theory about “archetypes” of potential borrowers: those who may respond heterogeneously due to credit access and (b) policymakers and

¹⁸For gender, we found telomere lengths of *Male* ($x_m = 2$) relative to *Female* ($x_m = 1$).

microcredit institution strategies. On the latter, the RPS may give policymakers pause about microcredit entry because they may worry about potential negative effects due to the complex nature of a credit injection. Our analysis allows the policymaker to take in robust advice: when no reasonable treatment of the data suggests negative effects, then policymakers can safely intervene. An RPS analysis provides a blueprint for robust intervention for a policymaker.

We study the Rashomon Partition Set in the [Banerjee et al. \(2015\)](#) data. The data is generated from a randomized controlled trial in which 102 neighborhoods in Hyderabad, India were randomly assigned to treatment or control, each with equal probability, where treatment meant that a partner microfinance organization, Spandana, entered. At baseline a number of characteristics of sampled individuals were collected, including the gender of the head of the household, the education status of the head of the household, the number of businesses previously owned by the household, and the number of children in the household. Additionally, at the neighborhood level, information about the share of households with debt, the share of households with businesses, total expenditure per capita in the region, and average literacy rates in the region were also collected at baseline. Amongst these regional characteristics, motivated by the literature we only look at the regional debt and business variables.

We look at outcomes from the second (longer term) endline, focusing on four spheres: (i) loans, (ii) household response (total expenditure, durables, temptation goods, labor supply), (iii) business (revenue, size, assets, profits), (iv) female empowerment (female business participation, education of daughters). We discretized the regional characteristics and the number of businesses previously owned into four levels based using quartiles. And we set the first quartile as the “base control” i.e., we consider that characteristic to be active if it is one of the higher three levels.

To study the impact of access to microcredit, we allow features across treatment and control profiles to be pooled together as per Definition 7. Then, we measure the heterogeneous impact as the conditional average treatment effect, $\text{CATE}(\mathbf{x}) = \mathbb{E}[Y_i(1, \mathbf{x})] - \mathbb{E}[Y_i(0, \mathbf{x})]$. We find the sample mean estimate $\widehat{\text{CATE}}(\mathbf{x}) = \widehat{y}(1, \mathbf{x}) - \widehat{y}(0, \mathbf{x})$ where $\widehat{y}(1, \mathbf{x})$ is the estimated potential outcome for a household assigned to treatment with feature combination \mathbf{x} , and $\widehat{y}(0, \mathbf{z})$ is the estimated potential outcome for a household assigned to control with feature combination \mathbf{z} . If feature \mathbf{x} is pooled across the treatment and control profiles, then $\widehat{\text{CATE}}(\mathbf{x}) = 0$ indicating no treatment effect heterogeneity in feature \mathbf{x} . Otherwise, $\widehat{\text{CATE}}(\mathbf{x}) \neq 0$ indicating treatment effect heterogeneity. Here we present $\text{sign}\{\widehat{\text{CATE}}(\mathbf{x})\} \in \{1, 0, -1\}$, which captures robust (or non-robust) qualitative patterns. We sort \mathbf{x} into various profiles and count the number of features in each profile that have a positive, zero, and negative effect, averaging the counts over all partitions in the RPS.

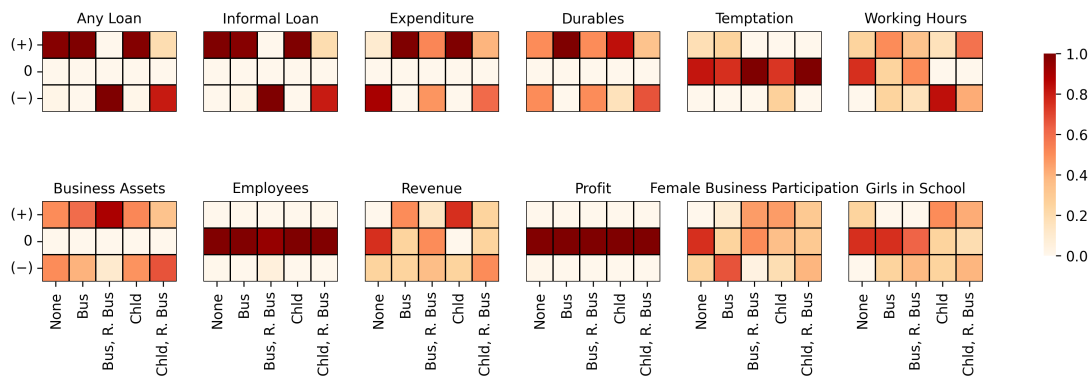


FIGURE 8. This plot visualizes the number of features with a positive, zero, or negative effect, averaged across partitions in the RPS. Each column corresponds to one of the five robust feature profiles described here where the label denotes which features are active (i.e., do not take the lowest level). “None” means that all features are taking these lowest values.

In Appendix H, Figure H.3 shows the full set of profiles and outcomes, demonstrating how non-robust many of the conclusions about many of the archetypes would actually be. These results indicate that there are no stable conclusions to be had for most profiles. Here, out of the 16 profiles, we highlight the 5 most robust ones, though arguably only the first is particularly robust. In each of these (and across all 16 profiles), profits and employees are robustly unaffected by microcredit. We describe the patterns for the most robust profile.

- (1) **Most robust archetype:** Large households, with no previous businesses, in a region with low baseline debt and business presence:
 - (a) take more loans (including informal).
 - (b) consume more, particularly durables but not temptation goods, and supply less labor.
 - (c) increase revenue, but nothing robust to note about business asset accumulation.
 - (d) see no changes in female empowerment.
- (2) **Other archetypes exhibiting some robustness:**
 - (a) Small households, with entrepreneurial experience, in a region with low baseline debt but high business presence.
 - (b) Small households, with no entrepreneurial experience, in a region with low baseline debt and business presence.
 - (c) Small households, with entrepreneurial experience, in a region with low baseline debt and business presence.
 - (d) Large households, with no previous businesses, in a region with high baseline debt but low business presence.

The RPS provides an avenue for the researcher to identify archetypes: profiles where the treatment effects are robust across many outcomes of interest. This provides an avenue for theory-building. It also clearly demonstrates when, for numerous profiles, there is little robustness to be said: the data, without strong priors, cannot really speak to the impacts of microcredit in most cases.

In Appendix H, we also look at the treatment effect heterogeneity by gender, which has been a point of interest in the literature. For the most part, we find no robust heterogeneity: the most robust conclusion is that there is no gender heterogeneity (a robust zero) in profits, business assets, and firm size. There are some minor robust differences in household expenditure response patterns, but the overall message is of non-robustness.

Finally, it is worth reiterating that beyond its value in theory-building, the RPS gives policymakers guidance on robust interventions. So for example, if the policymaker considered regions with high baseline debt, since robustly there are no positive profits and half the RPS suggests negative profits for entrepreneurs, they may not wish for the microcredit firm to enter in this market. But in contrast, in other markets, e.g., low debt and business presence, for large non-entrepreneurial families since there are robustly no effects on profits and robustly positive effects on consumption and leisure, they can proceed with confidence.

8. GENERALIZATIONS

Here, we consider two generalizations of the methods discussed so far. First, we consider a family of heterogeneous effects functions beyond just heterogeneity splits. For example, there might be some heterogeneity in *slopes* (and slopes of slopes, and so on). Second, we extend our method to pool on the space of the covariance between coefficients, rather than on the coefficients themselves. This means that coefficients no longer need to be exactly equal but, instead, related through a sparse covariance structure. We defer all technical details to Appendix D.

8.1. Pooling higher order derivatives. We ask whether, given some feature combination $k = (k_1, \dots, k_M)$, the marginal effect of increasing, say, k_1 has a linear effect. That is, we can just as simply allow for outcomes as we increase the intensity up a given feature that is not just a step function, but one that checks if there is a linear relationship.¹⁹ In this case, there is no “large” versus “small” effect and no natural pool in the space of levels. However, there is a natural low dimensional effect and even pools when considering the space of slopes. The result is a framework that captures extensions of Bayesian treed models (e.g., [Chipman et al. \(2002\)](#)).

Before we proceed, we first generalize the notion of pools described in Definition 2.

¹⁹Extensions of this kind can be made to accommodate higher order derivatives and other bases as well, e.g., sinusoidal effects.

Definition 8 (Generalization of pools). *Given M features taking on R partially ordered values each and some function $g(k, \boldsymbol{\beta})$, a pool π is a set of feature combinations k whose outcomes are given by $g(k, \boldsymbol{\beta}_\pi)$ where $\boldsymbol{\beta}_\pi$ depends on π .*

It is easy to see that the original pool defined in Definition 2 is recovered by setting $g(k, \boldsymbol{\beta}_\pi) = \beta_\pi$.

For instance, suppose we are interested in linear effects. Then the regression equation for pool π

$$y = g(k, \boldsymbol{\beta}_\pi) = \beta_{\pi,0} + \sum_{m=1}^M \beta_{\pi,m} k_m = \beta_{\pi,0} + \boldsymbol{\beta}_\pi^\top k$$

where $\boldsymbol{\beta}_\pi$ is the linear slope within that pool. The estimated outcome for feature combination $k \in \pi$ is $\hat{y} = f(k, \hat{\boldsymbol{\beta}}_\pi; \Pi)$, where $\hat{\boldsymbol{\beta}}_\pi$ is estimated within each pool using some procedure like least squares.

For some partition Π , define the block vector $\boldsymbol{\beta} = [\boldsymbol{\beta}_{\pi_1}, \dots, \boldsymbol{\beta}_{\pi_{|\Pi|}}]$ where $\pi_i \in \Pi$. Then, the general outcome function for any feature combination k can be written as

$$y = g(k, \boldsymbol{\beta}; \Pi) = \sum_{\pi \in \Pi} \mathbb{1}\{k \in \pi\} g(k, \boldsymbol{\beta}_\pi).$$

The practitioner is free to choose any domain-specific parametric function. For example, g could be a higher-order Taylor series-like expansion. Or, g could even be sinusoidal because the practitioner believes the outcomes are (piece-wise) sinusoidal. Of course, the more complex the estimation procedure for $\boldsymbol{\beta}$, the harder it is to enumerate the RPS.

Observe that the form of the posterior remains the same,

$$\mathbb{P}(\Pi \mid \mathbf{Z}) \propto \exp \{-\mathcal{L}(\mathbf{Z}) + \lambda H(\Pi)\} = \exp \left\{ -\frac{1}{n} \sum_{i=1}^n (y_i - \hat{y}_i)^2 + \lambda H(\Pi) \right\}.$$

Therefore, the results in Section 3 still hold. We can freely choose any other non-negative loss function, $\mathcal{L}(\mathbf{Z})$, and still use the same framework and algorithm to enumerate the RPS.

Further, the results in Section 5 are also valid when using an arbitrary parametric outcome function as discussed here. We summarize this in Theorem 7.

Theorem 7. *Suppose the outcome function is $g(k, \boldsymbol{\beta}; \Pi)$ for feature combination k , admissible partition Π , and some unknown parameter $\boldsymbol{\beta}$. Let us denote the estimated outcome for unit i with feature combination k by $\hat{y}_i = g(k, \hat{\boldsymbol{\beta}}; \Pi)$ where $\hat{\boldsymbol{\beta}}$ is estimated from the data. If we use \hat{y}_i instead of $\hat{\mu}_\pi$ in Equations 8 and 10, then*

- (i) *Theorem 4 is still true,*
- (ii) *Theorem 5 is still true, and*
- (iii) *Algorithm 1 correctly enumerates the Rashomon partitions for outcome function f .*

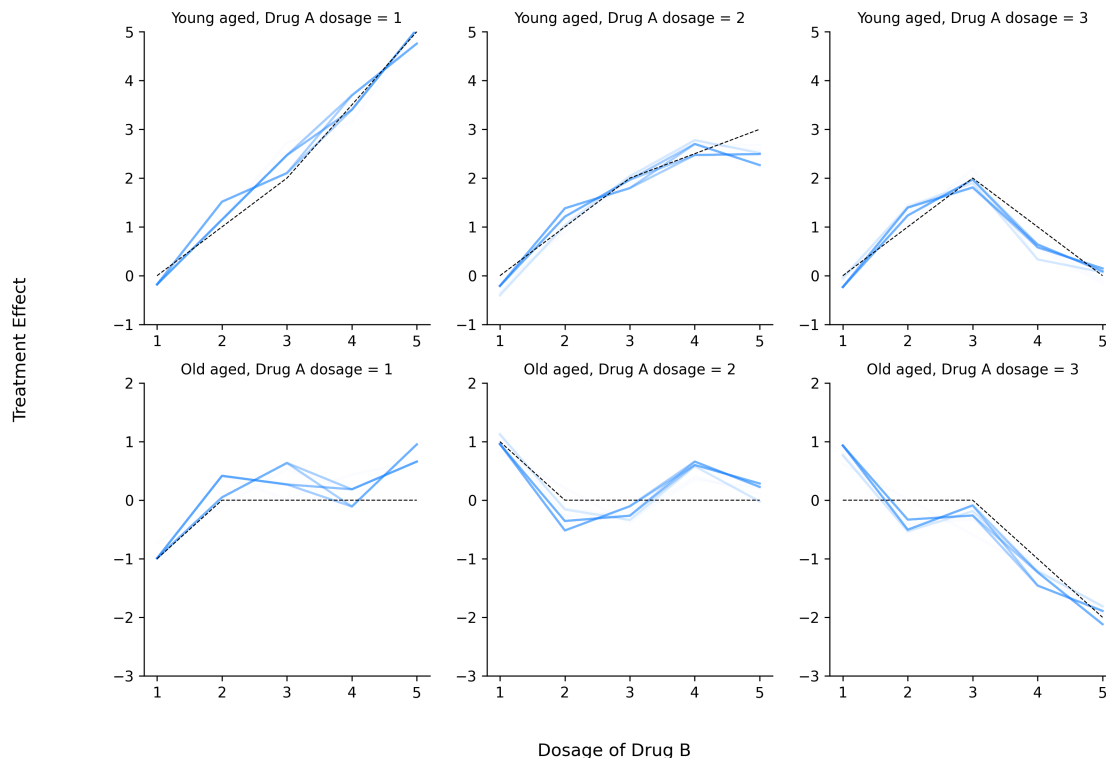


FIGURE 9. The black line corresponds to the true data-generating process and the blue lines correspond to effects estimated in each model in the Rashomon set. We estimate the outcome of each pool as a linear function of the features. The denser the blue line, the more often it appears in the Rashomon set.

To see the usefulness of the generalization, suppose we are interested in how a person’s age affects their response to a treatment consisting of a combination of two drugs, A and B. Suppose that there are four possible dosages for drug A, $\{0, 1, 2, 3\}$, six possible dosages for drug B, $\{0, 1, 2, 3, 4, 5\}$, and people are classified as young aged or old aged where 0 indicates control. Suppose that the treatment effects are piecewise linear (which generalizes the stepwise effects that we’ve assumed in previous simulations). We illustrate the treatment effects for different combinations in black dashed lines in Figure 9. By choosing a linear function as the outcome for each pool, we can find the Rashomon set. In Figure 9, we show the estimated linear curves in 100 models present in the Rashomon set ($\epsilon \approx 5 \times 10^{-4}$) in blue. The denser the blue line, the more often it appears in the Rashomon set. We discuss the exact simulation setup in Appendix G.

8.2. Sparse correlation structure between coefficients. Next, we explore the space of potential (sparse) covariance matrices between the coefficients. We now apply the Hasse structure to the elements of the variance-covariance matrix and pool on the space of covariances rather than the

coefficients themselves. This generalization requires an additional distributional assumption on the coefficients. Specifically, assume that

$$\boldsymbol{\beta} \mid \boldsymbol{\mu}, \boldsymbol{\Lambda} \sim \mathcal{N}(\boldsymbol{\mu}, \boldsymbol{\Lambda})$$

where $\boldsymbol{\mu}$ is some mean matrix and $\boldsymbol{\Lambda}$ is some covariance matrix. Then the posterior has the form

$$\mathbb{P}(\boldsymbol{\beta}, \boldsymbol{\Lambda}, \Pi \mid \mathbf{Z}) \propto \mathbb{P}(\mathbf{y} \mid \boldsymbol{\beta}, \boldsymbol{\Lambda}, \mathbf{D}, \Pi) \cdot \mathbb{P}(\boldsymbol{\beta}, \boldsymbol{\Lambda}, \Pi)$$

The likelihood component of the loss is

$$\mathbb{P}(\mathbf{y} \mid \boldsymbol{\beta}, \boldsymbol{\Lambda}, \mathbf{D}, \Pi) \propto \exp \left\{ -\frac{1}{N} (\mathbf{y} - \mathbf{D}\boldsymbol{\beta})^\top \boldsymbol{\Lambda} (\mathbf{y} - \mathbf{D}\boldsymbol{\beta}) \right\},$$

where N is the number of observed data points.

We do not have additional information about the covariance structure (though this could of course also be included in a prior) beyond the following three assumptions. First, we think that $\boldsymbol{\Lambda}$ is dense i.e., $\boldsymbol{\Lambda}$ is sparse in the number of uncorrelated outcomes. Second, we neither know nor want to know the correlation: it is an ℓ_0 problem. Third, we assume independence across the mean and correlation conditional on the covariance pooling. That is, Π is sufficient for the existence of dependence. Then

$$\mathbb{P}(\boldsymbol{\beta}, \boldsymbol{\Lambda}, \Pi) = \mathbb{P}(\boldsymbol{\beta} \mid \boldsymbol{\Lambda}, \Pi) \cdot \mathbb{P}(\boldsymbol{\Lambda} \mid \Pi) \cdot \mathbb{P}(\Pi)$$

Suppose that we have a partition $\Pi = \{\pi_1, \dots, \pi_H\}$ where $H = |\Pi|$ and Π now is defined in the space of covariance matrices, so pooling setting elements of the covariance matrix to be equal. Then, consider the following procedure for drawing the covariance matrix, $\boldsymbol{\Lambda} \in \mathbb{R}^{K \times K}$. For each pool $\pi_i \in \Pi$, draw $\boldsymbol{\Lambda}_i \sim f_i$ independently where f_i is some prior (for example, inverse Wishart). Then, $\boldsymbol{\Lambda} = \text{diag}(\boldsymbol{\Lambda}_1, \dots, \boldsymbol{\Lambda}_H)$. The number of non-zero elements of $\boldsymbol{\Lambda}$ is given by $\|\boldsymbol{\Lambda}\|_0 = \sum_{i=1}^H h_i^2$. Therefore, we penalize the number of zero elements, $K^2 - \sum_{i=1}^H h_i^2$. Thus, the prior is

$$\mathbb{P}(\Pi) \propto \exp \left\{ -\lambda \left(K^2 - \sum_{i=1}^H h_i^2 \right) \right\}.$$

So our penalized loss function is just weighted mean-squared error penalized differently,

$$(11) \quad Q(\Pi; \mathbf{Z}) = \mathcal{L}(\Pi; \mathbf{Z}) + \lambda H(\Pi) = \frac{1}{n} (\mathbf{y} - \mathbf{D}\boldsymbol{\beta})^\top \boldsymbol{\Lambda} (\mathbf{y} - \mathbf{D}\boldsymbol{\beta}) + \lambda \left(K^2 - \sum_{i=1}^H h_i^2 \right).$$

Theorem 8. *Consider the same setup in Section 5 except the loss function is weighted mean squared error penalized by the number of zeros in the covariance matrix as in Equation 11. Specifically,*

Equations (8) and (9) are modified, respectively, as

$$(12) \quad b(\Sigma, \mathcal{M}; \mathbf{Z}) = \frac{1}{n} \sum_{\pi \in \Pi_f} \sum_{k(i) \in \pi} \mathbb{1}\{k(i) \in \pi_f\} \widehat{\Lambda}_{k(i),k(i)}^2 (y_i - \widehat{\mu}_\pi)^2 + \lambda H(\Pi, \mathcal{M}),$$

$$(13) \quad b_{eq}(\Sigma, \mathcal{M}; \mathbf{Z}) = \frac{1}{n} \sum_{\pi \in \Pi_f} \sum_{k(i) \in \pi} \mathbb{1}\{k(i) \in \pi_f^c\} \widehat{\Lambda}_{k(i),k(i)}^2 (y_i - \widehat{\mu}_\pi)^2.$$

where $\widehat{\Lambda}_{k,k}^2$ is the estimated variance of feature combination k .

Then

- (i) Theorem 4 is still true,
- (ii) Theorem 5 is still true, and
- (iii) Algorithm 1 correctly enumerates the Rashomon partitions.

9. RELATED WORK

Our work contributes based on ideas that are present in several vibrant literatures. In this section, we contextualize our work in reference to three lines of existing work. We also provide a more thorough discussion of four specific alternative approaches in Appendix E.

9.1. Related work on the Rashomon effect. Our work is, of course, related to literature prior work grappling with the Rashomon effect (Chatfield, 1995; Breiman, 2001; McAllister, 2007; Tulabandhula and Rudin, 2014; D’Amour et al., 2022; Zhong et al., 2023). One line, reminiscent of dealing with p-hacking, identifies sets of estimands that generate similar objective function values (Marx et al., 2020; Coker et al., 2021; Watson-Daniels et al., 2023) and has been explored in the context of variable importance (Fisher et al., 2019; Dong and Rudin, 2020). Model multiplicity is now being recognized as an important problem in fields such as fairness and causal inference (Black et al., 2022; Pawelczyk et al., 2020; Kobylińska et al., 2023). The most related is Xin et al. (2022), who identify ϵ -Rashomon sets and a decision tree algorithm to enumerate the set of estimands (trees) that have squared loss smaller than a threshold slightly higher than that of a reference model.

Our work considers the Rashomon effect when addressing pressing questions in statistical inference and decision-making. We develop a Bayesian framework and define the RPS as the set of models with high posterior probability. This framework allows for unified inference across partitions and for specific effects. We can also provide a bound on the error in estimating the posterior using only the RPS. We show how to practically estimate the effects of different policies or feature combinations using the RPS and show that the error vanishes quickly in our empirical simulations. We show how to enumerate the entire RPS in the regression setting using scientifically sensible restrictions to cut down our search space. Finally, we formalize the notion of simple models using

the ℓ_0 penalty as a sparsity constraint. We show in Theorem 2 that, in the absence of information about the correlation structure of the parameters, the ℓ_0 penalty is minimax optimal. [Semenova et al. \(2022\)](#) hypothesized and showed using empirical simulations that regularization changes the size of the RPS. We establish and prove this relationship for the ℓ_0 penalty in Theorem 3.

9.2. Related work on Bayesian model uncertainty. In our work, we address uncertainty across plausible models of heterogeneity. Our goal is to identify cases where distinct elements of the factorial have (nearly) indistinguishable outcomes, which we accomplish by creating partitions of the space of covariate interactions (though we generalize our approach to smoothing covariance matrices in Section 8). In this sense, our setup is reminiscent of other work on Bayesian tree models that leverage priors over partitions, or trees (e.g., [Chipman et al. \(1998\)](#), [Denison et al. \(1998\)](#), [Wu et al. \(2007\)](#) or Bayesian Additive Regression Trees (BART) ([Chipman et al., 2010](#))). Like this work, we put priors over complexity in the space of trees. In contrast to many subsequent papers in this line of work, our goal is not solely or even principally prediction, but the identification of sets of combinations of characteristics that are heterogeneous with respect to the outcome. We use Hasse diagrams that obey admissibility criteria and, critically, our computational approach does not involve sampling from the posterior, but rather identifying partitions that make up the RPS. Enumerating the RPS allows researchers to focus on a set of the highest posterior explanations for heterogeneity while avoiding the computational issues associated with sampling the extremely large space of trees. We also demonstrate in Section 8 how to extend our framework to functions across pools (see, for example [Chipman et al. \(2002\)](#)). Our approach is also related to Bayesian Model Averaging (BMA), where each element of the model space is inherently meaningful ([Raftery et al., 1997](#); [Clyde, 2003](#)). The notion of using a small set of simple models with high posterior probability models arises in [Madigan and Raftery \(1994\)](#) in the context of BMA for graphical models and more generally in [Madigan et al. \(1996\)](#). Unlike BMA, though, the dimension of β stays fixed throughout, though there are restrictions on β given a particular partition. This feature avoids the need for the computational issues associated with searching the extremely large space of highly correlated models of different dimensions ([Raftery et al., 1997](#); [Hans et al., 2007](#); [Onorante and Raftery, 2016](#)) while preserving interpretability and a unified Bayesian inference framework. Analogously, [Tian and He \(2009\)](#) and [Chen and Tian \(2014\)](#) use this for causal discovery by finding high posterior equivalence classes of causal Bayesian networks.

9.3. Related work on learning treatment heterogeneity with machine learning tools. A rapidly growing literature leverages ideas from machine learning to estimate treatment effect heterogeneity. Our approach is most closely related to [Banerjee et al. \(2021\)](#) (prior work in part by

Chandrasekhar and Sankar), which developed the Hasse representation for treatment variant aggregation for a factorial randomized controlled trial. Their technique employs ℓ_1 regularization (Lasso) to pool treatment combinations. To grapple with the correlations in the design matrix from the factorial data, they employ a Puffer transformation (Jia and Rohe, 2015) to satisfy irrepresentability. They only prove that this transformation can be used for fully crossed RCTs since it is not obvious that the conditions are satisfied for generically factorialized covariate data. Our approach differs fundamentally in several ways, beyond taking a Bayesian rather than frequentist approach. First, we focus on robustness and allow for uncertainty in the selected model through the RPS. There is no such approach in their work. Second, regularizing using an ℓ_1 penalty imposes independence across adjacent models. This is exactly the opposite of what we would expect in practice (two treatment conditions with the same drugs at slightly different levels should have related outcomes). Third, their approach to robustness is to perturb the ℓ_1 penalization parameter. But this traces out a limited family of models for two reasons. To see this, notice that fundamentally the Rashomon Effect is about multimodality: the ℓ_1 approach privileges modes that are more consistent with independent priors irrespective of the penalization parameter. So this approach does not address the Rashomon Effect. Further, the Lasso approach in some sense is limited by roughly being a greedy algorithm: misleading local minima can severely affect which model is selected as optimal since it cannot explore robust alternatives. Our robust prior approach immediately takes us to a decision tree strategy that can explore beyond local minima. Fourth, their regression approach requires recovering irrepresentability from a correlated design matrix, and the techniques are shown to work only in the crossed RCT setting. Our approach with the decision tree strategy and ℓ_0 prior applies to arbitrary factorial data structures since it is agnostic to the correlational structure.

Our work is also related to existing tree-based methods (e.g. the seminal work of Wager and Athey (2018) on causal forests in the context of treatment heterogeneity). Wager and Athey (2018) construct regression trees (every tree corresponding to some partition Π in our language) to describe heterogeneity in the space of covariates and then sample from the distribution over trees to (honestly) estimate conditional average treatment effects. Honesty here refers to an iterative sample splitting strategy to alleviate issues with estimating the tree and then doing inference using the same data. Both their thought experiments and goals are distinct. Beyond being Bayesian (which philosophically addresses “honesty”), our approach departs in several ways. First, in our setting, data are partially ordered, a restriction that is not captured in the regression trees. Second, we have a coherency requirement: without admissibility restrictions, unrestricted decision trees will put considerable mass on and arrive at partitions that are not real-world meaningful and yet be

incorporated into their estimator. This is not desirable and we rule this out. Third, the sampling over trees means that there is no guarantee that the selected trees (or Π s) will be high quality. We provide guarantees, by definition of the RPS, on the quality of the selected partitions and we enumerate all of them. Fourth, to understand whether two adjacent feature combinations should be pooled, in their approach each of these queries must be tested individually which quickly runs into multiple hypothesis issues when done in mass. But our approach natively returns a posterior over all partitions and therefore jointly over all poolings. This delivers output amenable to theory-building: “archetypes” of pools that robustly exhibit certain effects. Fifth, the manner in which tree depth is controlled involves ensuring leafs (pools) have enough observations. This is sensible from a certain perspective, but for our purposes corresponds to the statistician having a prior that their data collection process stratifies observations against *unknown* true partition structure. This is both not a reasonable prior on first principles and also one that changes as one samples more data, since its shape is defined by the data collection itself. Taken together, these features make it impossible to explore multiple potential models for heterogeneity, which is a fundamental goal of our work.

Finally, we contrast our work with recent work in econometrics that uses machine learning “proxies” to study heterogeneity in treatment effects. The logic is that in settings with a moderate-to-high dimensional covariate structure and little information about the relationship between covariates, machine learning tools can effectively capture patterns of how covariates are associated with heterogeneity in treatment effects rather than the exact covariate-based effects. A novel method developed in Chernozhukov et al. (2018), for example, constructs a framework for inference using proxies constructed by an arbitrary machine learning model. After constructing proxies (predictions of the outcome using features flexibly), Chernozhukov et al. (2018) cluster respondents into groups with the highest and lowest treatment efficacy using treatment outcomes predicted based on the proxies. These clusters, which are derived from amalgamating covariates through “black box” machine learning algorithms, can then be related back to observable covariates. We are interested in a different set of goals: rather than finding what features are associated with heterogeneity (and more extreme effects), we want to identify robust poolings.²⁰ The outputs of the proxy techniques do not lend themselves to addressing these questions nor do they readily provide any comment on robustness for the same reasons as those faced by the causal forests techniques previously discussed. Our work shows that admissibility restrictions and the geometry of the underlying problem provide enough

²⁰Further, robustness is an exact finite sample n calculation, so in some sense, we are not worried about the high dimensional case of the number of parameters exploding relative to the number of observations.

structure to make search in the space of covariates possible and interpretable, alleviating the need to use black box algorithms to summarize relationships between covariates through proxies.

10. DISCUSSION

In this paper, we present an approach for estimating heterogeneity in outcomes based on a set of discrete covariates. We derive a fully Bayesian framework and an algorithm to identify *all* possible pooling across feature combinations with the highest posterior density: the Rashomon Partition Set. We provide bounds on the portion of the posterior captured by models for heterogeneity in this set, allowing researchers to compute posteriors for marginal effects and evaluate specific treatment combinations. Appealing to a Bayesian framework addresses the issue of multiple testing/selection that leaves practitioners with the unappealing choice between invalid inference and procedures such as data splitting that have implications for power, which are particularly problematic in settings where we expect the cost of data collection to be high. Meanwhile, by identifying a set of high posterior models rather than sampling from the entire posterior, we avoid the inefficiency and impracticality of existing Bayesian approaches to model uncertainty. By only considering scientifically plausible pools in a geometry that allows for partial ordering (Hasse diagrams), we substantially reduce the number of possible explanations for heterogeneity without sacrificing flexibility. Additionally, and critically, these choices mean that the resulting high posterior partitions are *interpretable* and useful for researchers and policymakers when designing future interventions or generalizations.

We now highlight two additional philosophical points about our approach. First, our approach is fundamentally generative in the sense that it produces insights that are directly interpretable. As we highlight in our empirical examples, we expect that Rashomon partitions themselves will be of interest for researchers or policymakers. They allow for the identification of the most robust conclusions, settings where policymakers can intervene without worrying about likely negative consequences, and defining “archetypes” for theory-building.

In this way, our work contributes to a growing literature in artificial intelligence and machine learning that pushes back on the use of black box algorithms to make high-stakes decisions (see e.g., [Rudin \(2019\)](#)). While machine learning models may be effective at estimating complex relationships between covariates, they also often do so in ways that obfuscate the influence of particular features (or combinations of features). Our approach presents an alternative strategy that generates insights about sources of treatment effect heterogeneity based on combinations of observed covariates. Our work shows that admissibility restrictions and the geometry of the underlying problem provide enough structure to make search in the space of covariates possible, alleviating the need to use black box algorithms to summarize relationships between covariates through proxies.

Second, our work highlights the aperture that exists between statistical and practical decision-making. We take as given that in many moderate to high dimensional settings there will be interactions between features. With finite data, the result is a set of possible models for heterogeneity whose statistical performance is indistinguishable. Said another way, our work posits that the quest for the “best” statistical model is Sisyphean in essentially any scientifically interesting setting. While this may seem dire, it actually presents an opportunity to involve additional factors beyond model performance that are often critical in practice for making decisions. Amongst models in the RPS, a policymaker could choose based on, for example, implementation cost, equity considerations, or preserving privacy without sacrificing statistical performance.

There are many promising areas for future work in extending the framework we present here. First, we present results in terms of a posterior in a Bayesian framework. We could, however, also construct a similar structure under a frequentist paradigm. In such a setup, we would need to explore a re-splitting strategy (see [Wager and Athey \(2018\)](#), for example) to construct an “honest” set of Hasse diagrams. Furthermore, we could use our approach to identify groups that are systematically underrepresented in randomized trials (see [Parikh et al. \(2024\)](#), for example) and, as a further generalization, to compare results across trials (see for example [Meager \(2019\)](#)). Finally, our computational approach could be more generally valuable in a wide range of settings. In the context of model selection for graphical models, for example [Madigan and Raftery \(1994\)](#) suggest a stochastic search strategy that leverages the structure of the graph. Unlike ours, however, their approach averages over discrete models, leaving open the potential for an approach similar to ours in the context of graphical models or discrete model averaging more generally.

REFERENCES

- Aakvik, A., Salvanes, K. G., and Vaage, K. (2010). Measuring heterogeneity in the returns to education using an education reform. *European Economic Review*, 54(4):483–500.
- Agrawal, D., Pote, Y., and Meel, K. S. (2021). Partition function estimation: A quantitative study. *arXiv preprint arXiv:2105.11132*.
- Alder, J. K., Hanumanthu, V. S., Strong, M. A., DeZern, A. E., Stanley, S. E., Takemoto, C. M., Danilova, L., Applegate, C. D., Bolton, S. G., Mohr, D. W., et al. (2018). Diagnostic utility of telomere length testing in a hospital-based setting. *Proceedings of the National Academy of Sciences*, 115(10):E2358–E2365.
- Andrews, I., Kitagawa, T., and McCloskey, A. (2019). Inference on winners. Technical report, National Bureau of Economic Research.
- Angelino, E., Larus-Stone, N., Alabi, D., Seltzer, M., and Rudin, C. (2017). Learning certifiably optimal rule lists. In *Proceedings of the 23rd ACM SIGKDD International Conference on Knowledge Discovery and Data Mining*, pages 35–44.
- Angelucci, M., Karlan, D., and Zinman, J. (2015). Microcredit impacts: Evidence from a randomized microcredit program placement experiment by compartamos banco. *American Economic Journal: Applied Economics*, 7(1):151–182.
- Attanasio, O., Augsburg, B., De Haas, R., Fitzsimons, E., and Harmgart, H. (2015). The impacts of microfinance: Evidence from joint-liability lending in mongolia. *American Economic Journal: Applied Economics*, 7(1):90–122.
- Augsburg, B., De Haas, R., Harmgart, H., and Meghir, C. (2015). The impacts of microcredit: Evidence from bosnia and herzegovina. *American Economic Journal: Applied Economics*, 7(1):183–203.
- Baland, J.-M., Somanathan, R., Vandewalle, L., et al. (2008). Microfinance lifespans: A study of attrition and exclusion in self-help groups in india. In *India policy forum*, volume 4, pages 159–210. National Council of Applied Economic Research.
- Banerjee, A., Breza, E., Duflo, E., and Kinnan, C. (2019). Can microfinance unlock a poverty trap for some entrepreneurs? Technical report, National Bureau of Economic Research.
- Banerjee, A., Chandrasekhar, A. G., Dalpath, S., Duflo, E., Floretta, J., Jackson, M. O., Kannan, H., Loza, F. N., Sankar, A., Schrimpf, A., et al. (2021). Selecting the most effective nudge: Evidence from a large-scale experiment on immunization. Technical report, National Bureau of Economic Research.

- Banerjee, A., Duflo, E., Glennerster, R., and Kinnan, C. (2015). The miracle of microfinance? evidence from a randomized evaluation. *American economic journal: Applied economics*, 7(1):22–53.
- Bénard, C. and Josse, J. (2023). Variable importance for causal forests: breaking down the heterogeneity of treatment effects. *arXiv preprint arXiv:2308.03369*.
- Bissiri, P. G., Holmes, C. C., and Walker, S. G. (2016). A general framework for updating belief distributions. *Journal of the Royal Statistical Society Series B: Statistical Methodology*, 78(5):1103–1130.
- Black, E., Raghavan, M., and Barocas, S. (2022). Model multiplicity: Opportunities, concerns, and solutions. In *Proceedings of the 2022 ACM Conference on Fairness, Accountability, and Transparency*, pages 850–863.
- Blackburn, D. F. and Wilson, T. W. (2006). Antihypertensive medications and blood sugar: theories and implications. *Canadian Journal of Cardiology*, 22(3):229–233.
- Breiman, L. (2001). Statistical modeling: The two cultures (with comments and a rejoinder by the author). *Statistical Science*, 16(3):199–231.
- Cascorbi, I. (2012). Drug interactions – principles, examples and clinical consequences. *Deutsches Ärzteblatt International*, 109(33-34):546.
- Chae, D. H., Nuru-Jeter, A. M., Adler, N. E., Brody, G. H., Lin, J., Blackburn, E. H., and Epel, E. S. (2014). Discrimination, racial bias, and telomere length in african-american men. *American journal of preventive medicine*, 46(2):103–111.
- Chatfield, C. (1995). Model uncertainty, data mining and statistical inference. *Journal of the Royal Statistical Society Series A: Statistics in Society*, 158(3):419–444.
- Chen, Y. and Tian, J. (2014). Finding the k-best equivalence classes of bayesian network structures for model averaging. In *Proceedings of the AAAI conference on artificial intelligence*, volume 28.
- Chernozhukov, V., Demirer, M., Duflo, E., and Fernandez-Val, I. (2018). Generic machine learning inference on heterogeneous treatment effects in randomized experiments, with an application to immunization in India. Technical report, National Bureau of Economic Research.
- Chipman, H. A., George, E. I., and McCulloch, R. E. (1998). Bayesian CART model search. *Journal of the American Statistical Association*, 93(443):935–948.
- Chipman, H. A., George, E. I., and McCulloch, R. E. (2002). Bayesian treed models. *Machine Learning*, 48:299–320.
- Chipman, H. A., George, E. I., and McCulloch, R. E. (2010). BART: Bayesian additive regression trees. *The Annals of Applied Statistics*, 4(1).

- Clyde, M. (2003). Model averaging. *Subjective and objective Bayesian statistics*, pages 636–642.
- Coker, B., Rudin, C., and King, G. (2021). A theory of statistical inference for ensuring the robustness of scientific results. *Management Science*, 67(10):6174–6197.
- Crépon, B., Devoto, F., Duflo, E., and Parienté, W. (2015). Estimating the impact of microcredit on those who take it up: Evidence from a randomized experiment in morocco. *American Economic Journal: Applied Economics*, 7(1):123–150.
- D’Amour, A., Heller, K., Moldovan, D., Adlam, B., Alipanahi, B., Beutel, A., Chen, C., Deaton, J., Eisenstein, J., Hoffman, M. D., et al. (2022). Underspecification presents challenges for credibility in modern machine learning. *The Journal of Machine Learning Research*, 23(1):10237–10297.
- Denison, D. G., Mallick, B. K., and Smith, A. F. (1998). A bayesian CART algorithm. *Biometrika*, 85(2):363–377.
- Dong, J. and Rudin, C. (2020). Exploring the cloud of variable importance for the set of all good models. *Nature Machine Intelligence*, 2(12):810–824.
- Fisher, A., Rudin, C., and Dominici, F. (2019). All models are wrong, but many are useful: Learning a variable’s importance by studying an entire class of prediction models simultaneously. *J. Mach. Learn. Res.*, 20(177):1–81.
- Flajolet, P. and Sedgewick, R. (2009). *Analytic Combinatorics*. Cambridge University Press.
- Forster, A. G., van de Werfhorst, H. G., and Leopold, T. (2021). Who benefits most from college? dimensions of selection and heterogeneous returns to higher education in the united states and the netherlands. *Research in Social Stratification and Mobility*, 73:100607.
- Gelman, A. (2006). Prior distributions for variance parameters in hierarchical models (comment on article by browne and draper).
- Geronimus, A. T., Pearson, J. A., Linnenbringer, E., Schulz, A. J., Reyes, A. G., Epel, E. S., Lin, J., and Blackburn, E. H. (2015). Race-ethnicity, poverty, urban stressors, and telomere length in a detroit community-based sample. *Journal of health and social behavior*, 56(2):199–224.
- Hahn, P. R., Murray, J. S., and Carvalho, C. M. (2020). Bayesian regression tree models for causal inference: Regularization, confounding, and heterogeneous effects (with discussion). *Bayesian Analysis*, 15(3):965–1056.
- Hamad, R., Tuljapurkar, S., and Rehkopf, D. H. (2016). Racial and socioeconomic variation in genetic markers of telomere length: a cross-sectional study of us older adults. *EBioMedicine*, 11:296–301.
- Hammer, S. M., Squires, K. E., Hughes, M. D., Grimes, J. M., Demeter, L. M., Currier, J. S., Eron Jr, J. J., Feinberg, J. E., Balfour Jr, H. H., Deyton, L. R., et al. (1997). A controlled

- trial of two nucleoside analogues plus indinavir in persons with human immunodeficiency virus infection and cd4 cell counts of 200 per cubic millimeter or less. *New England Journal of Medicine*, 337(11):725–733.
- Hans, C., Dobra, A., and West, M. (2007). Shotgun stochastic search for “large p” regression. *Journal of the American Statistical Association*, 102(478):507–516.
- Hu, X., Rudin, C., and Seltzer, M. (2019). Optimal sparse decision trees. *Advances in Neural Information Processing Systems*, 32.
- Jia, J. and Rohe, K. (2015). Preconditioning the lasso for sign consistency. *Electronic Journal of Statistics*, 9:1150–1172.
- Karlan, D. and List, J. A. (2007). Does price matter in charitable giving? evidence from a large-scale natural field experiment. *American Economic Review*, 97(5):1774–1793.
- Karlan, D. and Zinman, J. (2010). Expanding credit access: Using randomized supply decisions to estimate the impacts. *The Review of Financial Studies*, 23(1):433–464.
- Kobylińska, K., Krzyżiński, M., Machowicz, R., Adamek, M., and Biecek, P. (2023). Exploration of rashomon set assists explanations for medical data. *arXiv preprint arXiv:2308.11446*.
- Madigan, D. and Raftery, A. E. (1994). Model selection and accounting for model uncertainty in graphical models using occam’s window. *Journal of the American Statistical Association*, 89(428):1535–1546.
- Madigan, D., Raftery, A. E., Volinsky, C. T., and Hoeting, J. A. (1996). Bayesian model averaging. *Integrating Multiple Learned Models (IMLM-96)*, (P. Chan, S. Stolfo, and D. Wolpert, eds).
- Marx, C., Calmon, F., and Ustun, B. (2020). Predictive multiplicity in classification. In III, H. D. and Singh, A., editors, *Proceedings of the 37th International Conference on Machine Learning*, volume 119 of *Proceedings of Machine Learning Research*, pages 6765–6774. PMLR.
- McAllister, J. W. (2007). Model selection and the multiplicity of patterns in empirical data. *Philosophy of Science*, 74(5):884–894.
- Meager, R. (2019). Understanding the average impact of microcredit expansions: A bayesian hierarchical analysis of seven randomized experiments. *American Economic Journal: Applied Economics*, 11(1):57–91.
- Mincer, J. (1958). Investment in human capital and personal income distribution. *Journal of Political Economy*, 66(4):281–302.
- Nair, N. U., Greninger, P., Zhang, X., Friedman, A. A., Amzallag, A., Cortez, E., Sahu, A. D., Lee, J. S., Dastur, A., Egan, R. K., et al. (2023). A landscape of response to drug combinations in non-small cell lung cancer. *Nature Communications*, 14(1):3830.

- Onorante, L. and Raftery, A. E. (2016). Dynamic model averaging in large model spaces using dynamic occam’s window. *European Economic Review*, 81:2–14.
- Parikh, H., Ross, R., Stuart, E., and Rudolph, K. (2024). Who are we missing? a principled approach to characterizing the underrepresented population. *arXiv preprint arXiv:2401.14512*.
- Pawelczyk, M., Broelemann, K., and Kasneci, G. (2020). On counterfactual explanations under predictive multiplicity. In Peters, J. and Sontag, D., editors, *Proceedings of the 36th Conference on Uncertainty in Artificial Intelligence (UAI)*, volume 124 of *Proceedings of Machine Learning Research*, pages 809–818. PMLR.
- Protsenko, E., Rehkopf, D., Prather, A. A., Epel, E., and Lin, J. (2020). Are long telomeres better than short? relative contributions of genetically predicted telomere length to neoplastic and non-neoplastic disease risk and population health burden. *PloS one*, 15(10):e0240185.
- Raftery, A. E., Madigan, D., and Hoeting, J. A. (1997). Bayesian model averaging for linear regression models. *Journal of the American Statistical Association*, 92(437):179–191.
- Rossiello, F., Jurk, D., Passos, J. F., and d’Adda di Fagagna, F. (2022). Telomere dysfunction in ageing and age-related diseases. *Nature cell biology*, 24(2):135–147.
- Rubin, D. B. (1981). Estimation in parallel randomized experiments. *Journal of Educational Statistics*, 6(4):377–401.
- Rudin, C. (2019). Stop explaining black box machine learning models for high stakes decisions and use interpretable models instead. *Nature machine intelligence*, 1(5):206–215.
- Semenova, L., Rudin, C., and Parr, R. (2022). On the existence of simpler machine learning models. In *Proceedings of the 2022 ACM Conference on Fairness, Accountability, and Transparency*, pages 1827–1858.
- Srinivas, N., Rachakonda, S., and Kumar, R. (2020). Telomeres and telomere length: a general overview. *Cancers*, 12(3):558.
- Tarozzi, A., Desai, J., and Johnson, K. (2015). The impacts of microcredit: Evidence from ethiopia. *American Economic Journal: Applied Economics*, 7(1):54–89.
- Tian, J. and He, R. (2009). Computing posterior probabilities of structural features in bayesian networks. In *Proceedings of the Twenty-Fifth Conference on Uncertainty in Artificial Intelligence, UAI ’09*, pages 538–547, Arlington, Virginia, USA. AUAI Press.
- Topley, K. (2016). Computationally efficient bounds for the sum of catalan numbers. *arXiv preprint arXiv:1601.04223*.
- Triplitt, C. (2006). Drug interactions of medications commonly used in diabetes. *Diabetes Spectrum*, 19(4):202.

- Tulabandhula, T. and Rudin, C. (2014). Robust optimization using machine learning for uncertainty sets. *arXiv preprint arXiv:1407.1097*.
- Vyas, C. M., Ogata, S., Reynolds, C. F., Mischoulon, D., Chang, G., Cook, N. R., Manson, J. E., Crous-Bou, M., De Vivo, I., and Okereke, O. I. (2021). Telomere length and its relationships with lifestyle and behavioural factors: variations by sex and race/ethnicity. *Age and ageing*, 50(3):838–846.
- Wager, S. and Athey, S. (2018). Estimation and inference of heterogeneous treatment effects using random forests. *Journal of the American Statistical Association*, 113(523):1228–1242.
- Wambaugh, M. A., Denham, S. T., Ayala, M., Brammer, B., Stonhill, M. A., and Brown, J. C. (2020). Synergistic and antagonistic drug interactions in the treatment of systemic fungal infections. *Elife*, 9:e54160.
- Watson-Daniels, J., Parkes, D. C., and Ustun, B. (2023). Predictive multiplicity in probabilistic classification. In *Proceedings of the AAAI Conference on Artificial Intelligence*, volume 37, pages 10306–10314.
- Wu, Y., Tjelmeland, H., and West, M. (2007). Bayesian CART: Prior specification and posterior simulation. *Journal of Computational and Graphical Statistics*, 16(1):44–66.
- Xin, R., Zhong, C., Chen, Z., Takagi, T., Seltzer, M., and Rudin, C. (2022). Exploring the whole rashomon set of sparse decision trees. *Advances in Neural Information Processing Systems*, 35:14071–14084.
- Zhao, P. and Yu, B. (2006). On model selection consistency of lasso. *The Journal of Machine Learning Research*, 7:2541–2563.
- Zhong, C., Chen, Z., Seltzer, M., and Rudin, C. (2023). Exploring and interacting with the set of good sparse generalized additive models. *arXiv e-prints*, pages arXiv–2303.

APPENDIX A. ADMISSIBILITY AND HASSE DIAGRAMS

One way to understand admissibility is by arranging the data of feature combination assignments into a *feature variant aggregation design matrix*, $\mathbf{F} \in \{0, 1\}^{n, K}$. The entries of the matrix are as follows. If $k(i)$ is the feature combination that i is assigned to, we set

$$F_{i\ell} := \mathbb{1}\{k(i) \geq \ell \cap \rho(k(i)) = \rho(\ell)\}.$$

So the variant design matrix switches on a dummy variable for all variants that are subordinate to $k(i)$. The utility is that it allows for us to understand the marginal value of climbing the ordering up from $k(i)$, as in the *treatment variant aggregation* (TVA) procedure of [Banerjee et al. \(2021\)](#).

To see this, it is useful to rewrite Equation (1) in its variant form,

$$(A.1) \quad \mathbf{y} = \mathbf{F}\boldsymbol{\alpha} + \epsilon,$$

which is just a linear transformation of Equation (1), so that:

$$(A.2) \quad \beta_k = \sum_{k' \leq k; \rho(k) = \rho(k')} \alpha_{k'}$$

This says that an expected outcome of a feature combination is the sum of expected marginal values leading up to it.

It is useful to represent our framework in a Hasse diagram. The Hasse draws links between features in the direction of the partial ordering. We imagine that moving from one node to its adjacent node in Hasse inherits a value that corresponds to the marginal change in the outcome moving from an immediate subordinate variant to the present variant. In a setup with two features, by Equation (A.2) the node (r, r') has value $\alpha_{r, r'} = (\beta_{r, r'} - \beta_{r, r'-1}) - (\beta_{r-1, r'} - \beta_{r-1, r'-1})$ wherever these indices on the right-hand side are not 0 (wherever the index is 0, we drop the corresponding β_k term on the right-hand side – basically because the corresponding feature combination is in a different profile). These will either capture a main effect of increasing a dosage (as on the sides of the Hasse) or an interaction effect between multiple dosage increases (as in the interior of the Hasse).

We discuss specific examples in [Example A.1](#) and [Example A.2](#) below.

Example A.1. Consider an example with $M = 2$ features, each with $R = 3$ discrete values, $\{1, 2, 3\}$. Then there are $K = R^M = 9$ different feature combinations. The Hasse diagram is shown in [Figure A.1](#). So, we end up pooling $(2, 2)$ with $(3, 2)$ and $(2, 3)$ with $(3, 3)$. The corresponding $\boldsymbol{\Sigma} \in \{0, 1\}^{2 \times 2}$

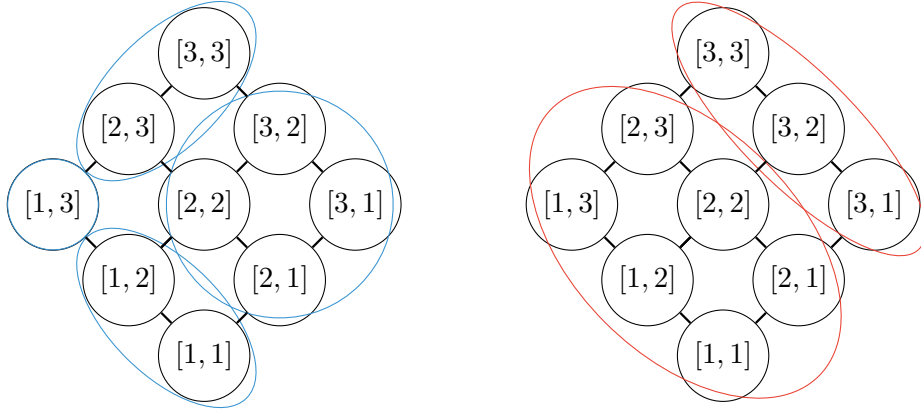


FIGURE A.1. Hasse diagram for Examples A.1 and A.2. The partition described in Example A.1 is shown in blue ellipses on the left panel. The right panel describes a different admissible partition in red ellipses seen in Example A.2

matrix for this profile is

$$\Sigma = \begin{bmatrix} 0 & 1 \\ 1 & 0 \end{bmatrix}.$$

This indicates that we split variants with value 1 from value 2 in the first feature (by $\Sigma_{11} = 0$) and pool variants of value 2 with value 3 in the first feature (by $\Sigma_{12} = 1$). Further, we pool variants with value 1 and value 2 in the second feature (by $\Sigma_{21} = 1$) and split variants with value 2 from value 3 in the second features (by $\Sigma_{22} = 0$).

Example A.2. Consider the same setup in Example A.1 with $M = 2$ features, each with $R = 3$ discrete values, $\{1, 2, 3\}$. Another admissible partition can be defined by the matrix

$$\Sigma = \begin{bmatrix} 1 & 0 \\ 1 & 1 \end{bmatrix}.$$

The pools are $\pi_1 = \{(a, b) \mid a = \{1, 2\}, b = \{1, 2, 3\}\}$ and $\pi_2 = \{(a, b) \mid a = \{3\}, b = \{1, 2, 3\}\}$. This is illustrated in the right panel of Figure A.1.

Now, we turn to admissibility as defined in Definition 6. Case (1) simply comes from the definition of a pool (cf. Definition 2). To understand the necessity of strong convexity in case (2) and the parallel splitting criteria in case (3), we need to understand how the marginal increments α_k affect the overall outcome $\beta_{k'}$. Observe that α_k affect $\beta_{k'}$ for all feature combinations $k' \geq k$ by Equation A.2. We can define this “sphere of influence” of k as $A_k = \{k' \in \mathcal{K} \mid \rho(k) = \rho(k'), k' \geq k\}$. Further, when we are interested in the outcomes $\beta_{k'}$, it is sufficient to consider only spheres A_k where $\alpha_k > 0$ i.e., the “active spheres.” Therefore, the intersection of all active spheres (taken either directly or

through its complement) will give rise to a set of feature combinations with the same outcome i.e., a pool. It is easy to see that any such sphere is strongly convex in our sense. Therefore, any pool will also be strongly convex.

The parallel splitting criteria “from above” in Case ((3)a) of Definition 6, also follows from these spheres of influence interpretation of the active α_k . Specifically, tracking the active α_k ensures that if a segment through a Hasse is pooled, then any segment both parallel to it and below it must be pooled as well. For the sake of contradiction, assume to the contrary that the top segment is pooled while a parallel bottom segment is cleaved. There must be some node along the bottom segment that was responsible for this cleaving through its marginal effect. However, the sphere of influence of this marginal effect cuts through the top segment too, cleaving the top segment into distinct pooled sets, a contradiction.

Of course, as mentioned in Section 2, it is possible to have exact marginal increments exactly offset each other so that despite two feature combinations k_1, k_2 influenced by two different spheres of action, $\beta_{k_1} = \beta_{k_2}$. However, we do not want to pool these features together because adding very little noise to one of the corresponding active $\alpha_{k'}$ will immediately render $\beta_{k_1} \neq \beta_{k_2}$ i.e., this is a measure zero event.

The above shows that admissibility (with case (3) limited to case ((3)a)) is necessary from just using the spheres of influence of marginal effects, and nothing more. However, this version of admissibility is also sufficient: any admissible partition Π_0 (as per Definition 6) can be shown to derive from a common set of nodes k_1, \dots, k_n so that each $\pi \in \Pi_0 = A_{k_1}^{a_1} \cap \dots \cap A_{k_n}^{a_n}$, where $a_i \in \{1, c\}$, i.e. denoting either the sphere of influence or its complement. A quick proof sketch is as follows. First, we define the spheres through Π_0 . For each $\pi_i \in \Pi_0$, take $k_i = \min \pi_i$ its unique minimum. These k_i will be the nodes that generate the spheres of influence. We will show that for any $p_1, p_2 \in \pi_i \in \Pi_0$, $p_1 \in A_{k_j} \iff p_2 \in A_{k_j}$. Observe that for any $p \in \pi_i$, then trivially $p \in A_{k_i}$. Now consider the case when $p \in A_{k_j}$ for $k_j \neq k_i$. Then, $p > k_j$. It is not possible that $k_j \not\leq k_i$ as this would violate the parallel splits criteria (one can show there would be another $\pi' \in \Pi_0$ containing p). It is also not possible for $k_j > k_i$ as this would violate convexity ($p > k_j > k_i$ would imply $k_j \in \pi_i$). Thus, if $p \in \pi_i$ and $p \in A_{k_j}$, then necessarily $k_j \leq k_i$. Then, it follows that if $p_1, p_2 \in \pi_i$, then $p_1 \in A_{k_j} \iff p_2 \in A_{k_j}$. Therefore, all members of each $\pi \in \Pi_0$ are in the same unique intersection of spheres of influence, so each $\pi \in \Pi_0$ is uniquely represented as $\pi = A_{k_1}^{a_1} \cap \dots \cap A_{k_n}^{a_n}$.

Of course, in this particular parameterization of β , we chose to climb *up* the Hasse. We could have alternatively chosen to climb *down* the Hasse as

$$(A.3) \quad \mathbf{y} = \mathbf{G}\boldsymbol{\gamma} + \boldsymbol{\epsilon},$$

$$(A.4) \quad \beta_k = \sum_{k' \geq k; \rho(k) = \rho(k')} \gamma_{k'},$$

where $G_{i\ell} := \mathbb{1}\{k(i) \leq \ell \cap \rho(k(i)) = \rho(\ell)\}$. The difference from Equation A.2 is in the indexing of the sum, $k' \geq k$. It is easy to see with an analogous sphere of influence argument with γ that admissibility (With case (3) limited to ((3)b) this time) is necessary and sufficient characterization of pools from active marginals in γ .

When the goal of the problem is to identify heterogeneity in β , there is no reason to prefer one parameterization of climbing the Hasse over the other. Seeing that the parallel splitting criteria is linked to robustly estimating the pools of heterogeneity, we want to obey both of them together at the same time. This does run the risk of generating more granular partitions as a result of stronger restrictions, but this is a small price to pay for robustly estimating heterogeneity when one wishes to be agnostic about the system. Hence the full criterion for admissibility Definition 6, respecting parallel splits from both above (case ((3)a)) and below (case ((3)b)).

One might imagine that asking for more restrictions can complicate the search process. However, a by-product of being agnostic to the direction of Hasse traversal is that there is a bijective mapping between the Σ partition matrices and admissible partitions. We show in Proposition 2 that this significantly reduces the size of the model class, and later show in Theorem 3 that the size of the RPS, which is our primary estimation goal, is only polynomial. This has very important practical implications for computational feasibility.

One can quickly verify that Examples A.1 and A.2 satisfy the admissibility as defined in Definition 6 by visual inspection and identify the corresponding Σ matrices. In Example A.3 below, we show an example of an inadmissible partition. Interestingly, there is a valid decision tree that arrives at this partition.

Example A.3. *Consider the same setup in Example A.1 with $M = 2$ features, each with $R = 3$ discrete values, $\{1, 2, 3\}$. In Figure A.2, we illustrate an inadmissible partition. This is inadmissible because we have pools $\pi_1 = \{(1, 1), (1, 2), (1, 3)\}$, $\pi_2 = \{(2, 1), (2, 2)\}$, $\pi_3 = \{(3, 1), (3, 2)\}$, and $\pi_4 = \{(2, 3), (3, 3)\}$. Admissibility (see condition (3) of Definition 6) says that if π_1 is in the partition, then feature combinations $(\cdot, 2)$ and $(\cdot, 3)$ should always be pooled together. This contradicts what we observe in π_2 , π_3 , and π_4 . Similarly, if π_4 is in the partition, admissibility would require that feature combinations $(2, \cdot)$ and $(3, \cdot)$ need to be pooled together which contradicts π_2 and π_3 . Since this partition is inadmissible, we cannot represent it using the Σ matrix.*

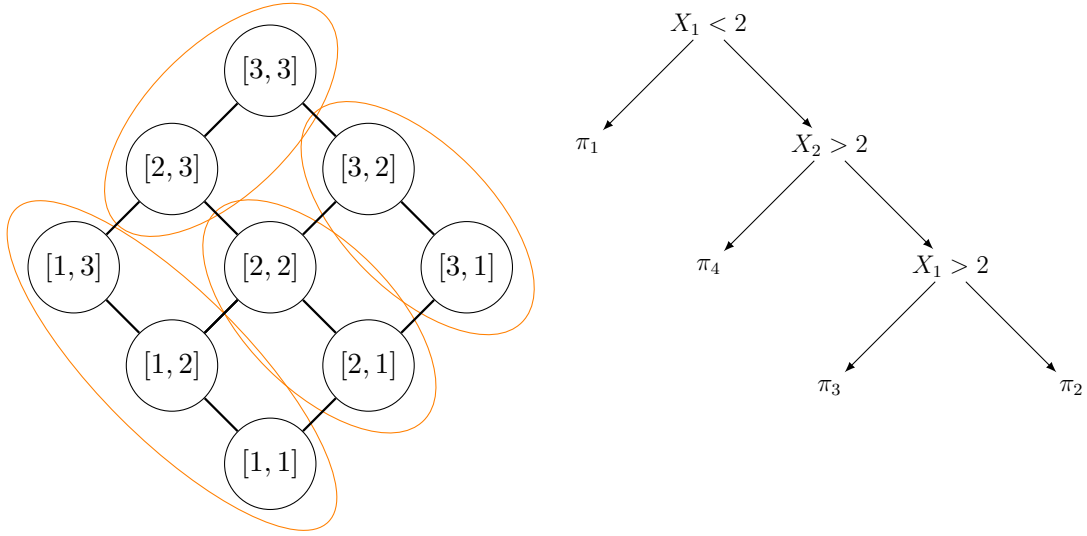


FIGURE A.2. Hasse diagram with the inadmissible partition described in Example A.3. The pools are $\pi_1 = \{(1, 1), (1, 2), (1, 3)\}$, $\pi_2 = \{(2, 1), (2, 2)\}$, $\pi_3 = \{(3, 1), (3, 2)\}$, and $\pi_4 = \{(2, 3), (3, 3)\}$. The decision tree illustrates how to generate this partition.

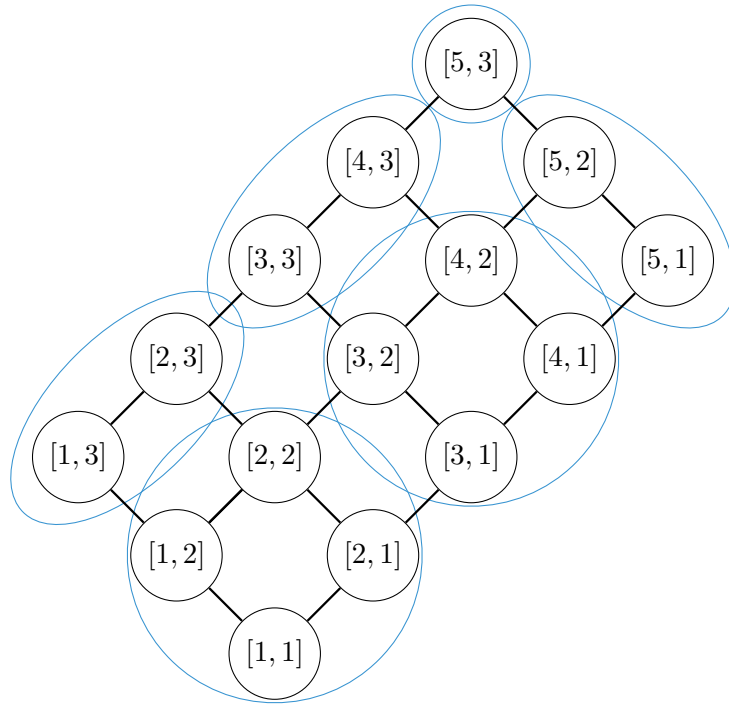


FIGURE A.3. Hasse diagram for Example A.4. The inadmissible partition is shown in blue ellipses.

To see why this is inadmissible from the marginal perspective, let us look at π_3 and π_4 . From these pools, it is evident that $\alpha_{2,3} \neq 0$, $\alpha_{3,1} \neq 0$, and $\alpha_{3,3} \neq 0$. And we know that,

$$\beta_{3,3} = \alpha_{3,3} + \alpha_{3,2} + \alpha_{3,1} + \alpha_{2,3} + C$$

$$\beta_{2,3} = \alpha_{2,3} + C,$$

where the term C is common to both equations. In the pooling currently, it so happens that $\beta_{3,3} = \beta_{2,3}$ – the terms $\alpha_{3,3}, \alpha_{3,2}, \alpha_{3,1}$ jointly make this true by $\alpha_{3,3} + \alpha_{3,2} + \alpha_{3,1} = 0$. However, we know that $\alpha_{3,1} \neq 0$. So if we add some noise $\varepsilon > 0$ to $\alpha_{3,1}$ to get $\alpha'_{3,1} := \alpha_{3,1} + \varepsilon$. Then, $\beta_{3,3} \neq \beta_{2,3}$ anymore. In other words, the pool π_4 is not robust to noise in the non-zero marginals as any noise will almost surely break π_4 into $\{(2, 3)\}$ and $\{(3, 3)\}$ as separate pools. Hence, this partition is inadmissible.

Decision trees are not robust in this sense as they may generate inadmissible partitions. The right panel of Figure A.2 illustrates a decision tree that generates the inadmissible partition discussed in this example.

Example A.4. Consider a different setup with $M = 2$ features, The first feature takes on $R_1 = 5$ discrete values $\{1, 2, 3, 4, 5\}$ and the second feature takes on $R_2 = 3$ discrete values, $\{1, 2, 3\}$. An admissible partition can be defined by the matrix

$$\Sigma = \begin{bmatrix} 1 & 0 & 1 & 0 \\ 1 & 0 & - & - \end{bmatrix},$$

where we use “–” to denote that the second feature does not have dosages corresponding to those entries in the Σ matrix. The pools are $\pi_1 = \{(a, b) \mid a, b \leq 2\}$, $\pi_2 = \{(a, b) \mid a \leq 2, b = 3\}$, $\pi_3 = \{(a, b) \mid a = 3, 4, b \leq 2\}$, $\pi_4 = \{(a, b) \mid a = 3, 4, b = 3\}$, $\pi_5 = \{(a, b) \mid a = 5, b \leq 2\}$, and $\pi_6 = \{(5, 3)\}$. This is illustrated in Figure A.3.

So far, we have been describing how to pool different feature combinations if they belong to the same profile. Now, we turn our attention to pooling *across* profiles. The marginal representation in Equation A.1 does not allow for features to be pooled together if they are in different profiles. We now describe a similar representation that allows features to be pooled across profiles if and only if they are variants,

$$(A.5) \quad \mathbf{y} = \mathbf{F}\boldsymbol{\alpha} + \mathbf{A}\boldsymbol{\delta} + \boldsymbol{\epsilon},$$

$$(A.6) \quad A_{i,(\ell,\rho)} = \mathbb{1}\{k(i) > \ell \cap \rho(k(i)) > \rho(\ell) = \rho\},$$

$$\beta_k = \sum_{k' \leq k; \rho(k) = \rho(k')} \alpha_{k'} + \sum_{k' < k} \sum_{\rho; \rho(k') < \rho(k)} \delta_{k', \rho}.$$

By setting $\boldsymbol{\delta} = \mathbf{0}$, we can immediately see that Equation (A.5) is a generalization of Equation (A.1). In fact, if depending on the context, we do not want to pool profile ρ_1 with ρ_2 , then this

corresponds to setting the appropriate entries in δ to 0. This is exactly what [Banerjee et al. \(2021\)](#) do in their analysis of cross-randomized behavioral nudges for improving immunization.

This representation agrees with our admissibility in Definition 7. Case (1) follows from the fact that this is a generalization of Equation A.1. Cases (2) and (3) follow from the definition of the \mathbf{A} matrix. For example, consider two features k_1, k_2 that belong to two different profiles. We can only pool variants i.e., $\|k_1 - k_2\|_1 = 1$. If they are variants, then the two profiles must be adjacent on the M -d hypercube.

At this point, it is important to note that there are no restrictions such as the parallel splitting criteria across different profiles. This is because the marginal δ_k only contributes to the outcome across profiles i.e., from the perspective within a profile, the sphere of influence of δ_k is indistinguishable from the sphere of influence of $\alpha_{k'}$ where k' is at the lower boundary of the Hasse adjacent to the Hasse of k . Since each pair of feature variants from different profiles have different across-profile marginals δ_k , they are not coupled together like the α marginals are.

APPENDIX B. APPROXIMATING THE POSTERIOR

Proof of Theorem 1. By the triangle inequality, we can write

$$\begin{aligned} \sup_{\mathbf{t}} |F_{\beta|\mathbf{Z}, \mathcal{P}_\theta}(\mathbf{t}) - F_{\beta|\mathbf{Z}}(\mathbf{t})| &= \sup_{\mathbf{t}} \left| \sum_{\Pi \in \mathcal{P}_\theta} F_{\beta|\mathbf{Z}}(\mathbf{t} | \Pi) \frac{\mathbb{P}(\Pi | \mathbf{Z})}{\sum_{\Pi' \in \mathcal{P}_\theta} \mathbb{P}(\Pi' | \mathbf{Z})} - \sum_{\Pi \in \mathcal{P}^*} F_{\beta|\mathbf{Z}}(\mathbf{t} | \Pi) \mathbb{P}(\Pi | \mathbf{Z}) \right|, \\ &\leq \text{(I)} + \text{(II)} \\ \text{I} &= \sup_{\mathbf{t}} \left| \sum_{\Pi \in \mathcal{P}_\theta} F_{\beta|\mathbf{Z}}(\mathbf{t} | \Pi) \frac{\mathbb{P}(\Pi | \mathbf{Z})}{\sum_{\Pi' \in \mathcal{P}_\theta} \mathbb{P}(\Pi' | \mathbf{Z})} - \sum_{\Pi \in \mathcal{P}_\theta} F_{\beta|\mathbf{Z}}(\mathbf{t} | \Pi) \mathbb{P}(\Pi | \mathbf{Z}) \right|, \\ \text{II} &= \sup_{\mathbf{t}} \left| \sum_{\Pi \in \mathcal{P}_\theta} F_{\beta|\mathbf{Z}}(\mathbf{t} | \Pi) \mathbb{P}(\Pi | \mathbf{Z}) - \sum_{\Pi \in \mathcal{P}^*} F_{\beta|\mathbf{Z}}(\mathbf{t} | \Pi) \mathbb{P}(\Pi | \mathbf{Z}) \right| \end{aligned}$$

Let us denote $K = \sum_{\Pi' \in \mathcal{P}_\theta} \mathbb{P}(\Pi' | \mathbf{Z})$. Then the first term is,

$$\begin{aligned} \text{(I)} &= \sup_{\mathbf{t}} \left| \sum_{\Pi \in \mathcal{P}_\theta} F_{\beta|\mathbf{Z}}(\mathbf{t} | \Pi) \frac{\mathbb{P}(\Pi | \mathbf{Z})}{K} - \sum_{\Pi \in \mathcal{P}_\theta} F_{\beta|\mathbf{Z}}(\mathbf{t} | \Pi) \mathbb{P}(\Pi | \mathbf{Z}) \right| \\ &\leq \left| \frac{1}{K} - 1 \right| \sup_{\mathbf{t}} \left| \sum_{\Pi \in \mathcal{P}_\theta} F_{\beta|\mathbf{Z}}(\mathbf{t} | \Pi) \mathbb{P}(\Pi | \mathbf{Z}) \right| \\ &\leq \left| \frac{1}{K} - 1 \right| \sup_{\mathbf{t}} \left| \sum_{\Pi \in \mathcal{P}_\theta} \mathbb{P}(\Pi | \mathbf{Z}) \right| \end{aligned}$$

$$\leq \left| \frac{1}{K} - 1 \right| = \frac{1}{K} - 1,$$

where in the third line, we trivially bound $F_{\beta|\mathbf{Z}}(\mathbf{t} | \Pi) \leq 1$ as it is a distribution function and in the last time we bound $\sum_{\Pi \in \mathcal{P}_\theta} \mathbb{P}(\Pi | \mathbf{Z}) \leq 1$ since it is a probability mass function. Note that we were able to remove the absolute values because $K \leq 1$ giving us $1/K - 1 > 0$. Note that, by definition, $K \geq |\mathcal{P}_\theta| \theta$. Therefore,

$$(I) \leq \frac{1}{|\mathcal{P}_\theta| \theta} - 1.$$

Moving on to the second term,

$$\begin{aligned} (II) &= \sup_{\mathbf{t}} \left| \sum_{\Pi \in \mathcal{P}_\theta} F_{\beta|\mathbf{Z}}(\mathbf{t} | \Pi) \cdot \mathbb{P}(\Pi | \mathbf{Z}) - \sum_{\Pi \in \mathcal{P}^*} F_{\beta|\mathbf{Z}}(\mathbf{t} | \Pi) \cdot \mathbb{P}(\Pi | \mathbf{Z}) \right| \\ &= \sup_{\mathbf{t}} \left| \sum_{\Pi \in \mathcal{P}^* \setminus \mathcal{P}_\theta} F_{\beta|\mathbf{Z}}(\mathbf{t} | \Pi) \cdot \mathbb{P}(\Pi | \mathbf{Z}) \right| \\ &\leq \sup_{\mathbf{t}} \left| \sum_{\Pi \in \mathcal{P}^* \setminus \mathcal{P}_\theta} 1 \cdot \mathbb{P}(\Pi | \mathbf{Z}) \right| \\ &= \sum_{\Pi \in \mathcal{P}^* \setminus \mathcal{P}_\theta} \mathbb{P}(\Pi | \mathbf{Z}) \\ &\leq 1 - |\mathcal{P}_\theta| \theta, \end{aligned}$$

where in the third line, we again bound $F_{\beta|\mathbf{Z}}(\mathbf{t} | \Pi) \leq 1$, and in the final step, we use the definition of \mathcal{P}_θ .

Therefore,

$$\sup_{\mathbf{t}} |F_{\beta|\mathbf{Z}, \mathcal{P}_\theta}(\mathbf{t}) - F_{\beta|\mathbf{Z}}(\mathbf{t})| \leq (I) + (II) \leq \frac{1}{|\mathcal{P}_\theta| \theta} - |\mathcal{P}_\theta| \theta.$$

□

Proof of Corollary 1. This argument is identical to Theorem 1 except for how we bound the expectations. We have

$$\begin{aligned} \|\mathbb{E}_{\Pi|\mathcal{P}_\theta} \beta - \mathbb{E}_{\Pi, \mathcal{P}_\theta} \beta\| &= \left\| \sum_{\Pi \in \mathcal{P}_\theta} \beta_\Pi \frac{\mathbb{P}(\Pi | \mathbf{Z})}{\sum_{\Pi' \in \mathcal{P}_\theta} \mathbb{P}(\Pi' | \mathbf{Z})} - \sum_{\Pi \in \mathcal{P}_\theta} \beta_\Pi \mathbb{P}(\Pi | \mathbf{Z}) \right\| \\ &= \left\| \frac{1}{\sum_{\Pi' \in \mathcal{P}_\theta} \mathbb{P}(\Pi' | \mathbf{Z})} - 1 \right\| \left\| \sum_{\Pi \in \mathcal{P}_\theta} \beta_\Pi \mathbb{P}(\Pi | \mathbf{Z}) \right\| \end{aligned}$$

$$= \left| \frac{1}{K} - 1 \right| \|\mathbb{E}_{\Pi, \mathcal{P}_\theta} \boldsymbol{\beta}\|,$$

where $K = \sum_{\Pi' \in \mathcal{P}_\theta} \mathbb{P}(\Pi' | \mathbf{Z})$. Note that by definition, $K \geq |\mathcal{P}_\theta| \theta$. Further, $K \leq 1$ gives us $1/K - 1 > 0$. Therefore,

$$\begin{aligned} \|\mathbb{E}_{\Pi | \mathcal{P}_\theta} \boldsymbol{\beta} - \mathbb{E}_{\Pi, \mathcal{P}_\theta} \boldsymbol{\beta}\| &\leq \left(\frac{1}{|\mathcal{P}_\theta| \theta} - 1 \right) \|\mathbb{E}_{\Pi, \mathcal{P}_\theta} \boldsymbol{\beta}\| \\ \implies \frac{\|\mathbb{E}_{\Pi | \mathcal{P}_\theta} \boldsymbol{\beta} - \mathbb{E}_{\Pi, \mathcal{P}_\theta} \boldsymbol{\beta}\|}{\|\mathbb{E}_{\Pi, \mathcal{P}_\theta} \boldsymbol{\beta}\|} &= \mathcal{O} \left(\frac{1}{|\mathcal{P}_\theta| \theta} - 1 \right). \end{aligned}$$

If we assume that $\|\boldsymbol{\beta}_\Pi\| < \infty$, then define $C = \max_{\Pi \in \mathcal{P}^*} \|\boldsymbol{\beta}_\Pi\| < \infty$. Then, we have

$$\|\mathbb{E}_{\Pi | \mathcal{P}_\theta} \boldsymbol{\beta} - \mathbb{E}_{\Pi, \mathcal{P}_\theta} \boldsymbol{\beta}\| = \mathcal{O} \left(\frac{1}{|\mathcal{P}_\theta| \theta} - 1 \right).$$

Further,

$$\begin{aligned} \|\mathbb{E}_{\Pi, \mathcal{P}_\theta} \boldsymbol{\beta} - \mathbb{E}_\Pi \boldsymbol{\beta}\| &= \left\| \sum_{\Pi \in \mathcal{P}_\theta} \boldsymbol{\beta}_\Pi \mathbb{P}(\Pi | \mathbf{Z}) - \sum_{\Pi \in \mathcal{P}^*} \boldsymbol{\beta}_\Pi \mathbb{P}(\Pi | \mathbf{Z}) \right\| \\ &= \left\| \sum_{\Pi \in \mathcal{P}^* \setminus \mathcal{P}_\theta} \boldsymbol{\beta}_\Pi \mathbb{P}(\Pi | \mathbf{Z}) \right\| \\ &\leq C \sum_{\Pi \in \mathcal{P}^* \setminus \mathcal{P}_\theta} \mathbb{P}(\Pi | \mathbf{Z}) \\ &= \mathcal{O}(1 - |\mathcal{P}_\theta| \theta), \end{aligned}$$

where in the last line we used the definition of Rashomon sets.. Therefore,

$$\begin{aligned} \|\mathbb{E}_{\Pi | \mathcal{P}_\theta} \boldsymbol{\beta} - \mathbb{E}_\Pi \boldsymbol{\beta}\| &\leq \|\mathbb{E}_{\Pi | \mathcal{P}_\theta} \boldsymbol{\beta} - \mathbb{E}_{\Pi, \mathcal{P}_\theta} \boldsymbol{\beta}\| + \|\mathbb{E}_{\Pi, \mathcal{P}_\theta} \boldsymbol{\beta} - \mathbb{E}_\Pi \boldsymbol{\beta}\| \\ &= \mathcal{O} \left(\frac{1}{|\mathcal{P}_\theta| \theta} - |\mathcal{P}_\theta| \theta \right). \end{aligned}$$

□

Proof of Proposition 1. We can easily see that

$$\begin{aligned} \xi(\Pi, \Pi_0) &\leq \epsilon \\ \iff \exp(-Q(\Pi)) &\geq \exp(-Q(\Pi_0))(1 + \epsilon) \\ \iff \mathbb{P}(\Pi | \mathbf{Z}) &\geq \mathbb{P}(\Pi_0 | \mathbf{Z})^{1+\epsilon} c^\epsilon, \end{aligned}$$

where $c := c(\mathbf{Z})$ is the normalization constant.

□

APPENDIX C. APPENDIX TO SIZE OF THE RASHOMON SET

Proof of Proposition 2.

- (i) To count the number of all possible partitions, we cast this as a decision tree problem. There are $(R-1)^m$ possible treatment policies in the profile with all arms turned on. These constitute possible nodes in a binary decision tree. The leaves in the decision tree are the pools. The number of binary trees with n nodes is given by

$$C_n = \frac{1}{n+1} \binom{2n}{n},$$

where C_n is the Catalan number (see *An Invitation to Analytic Combinatorics* from [Flajolet and Sedgewick, 2009](#)). Therefore, the number of trees we can construct (that may or may not be admissible) is

$$T = \sum_{n=1}^{(R-1)^m} C_n = \mathcal{O}\left(2^{2(R-1)^m}\right),$$

where the big-O bound is given by [Topley \(2016\)](#).

- (ii) To count the number of admissible aggregations, conceptualize the binary matrix, $\Sigma \in \{0, 1\}^{m \times (R-2)}$ again. Each element of Σ tells us whether a particular pair of adjacent levels in a feature is pooled. In particular, we define $\Sigma_{ij} = 1$ if and only if feature combinations with dosage j are pooled with feature combinations with factor $j+1$ in feature i . Therefore, Σ enumerates all admissible partitions. This gives us the desired result. □

Proof of Theorem 2. For any prior $P \in \mathcal{Q}_{\mathcal{P}|h}$, we have,

$$\begin{aligned} \sup_{Q \in \mathcal{Q}_{\mathcal{P}|h}} \delta(P_{P, \mathbf{Z}}, P_{Q, \mathbf{Z}}) &= \sup_{Q \in \mathcal{Q}_{\mathcal{P}|h}} \sup_{\Pi \in \mathcal{P}|h} |P_{P, \mathbf{Z}}(\Pi) - P_{Q, \mathbf{Z}}(\Pi)| \\ &= \sup_{\Pi \in \mathcal{P}|h} \sup_{Q \in \mathcal{Q}_{\mathcal{P}|h}} |P_{P, \mathbf{Z}}(\Pi) - P_{Q, \mathbf{Z}}(\Pi)| \\ &= \frac{1}{\mathbb{P}(\mathbf{y} | \mathbf{X})} \sup_{\Pi \in \mathcal{P}|h} \mathbb{P}(\mathbf{y} | \mathbf{X}, \Pi) \sup_{Q \in \mathcal{Q}_{\mathcal{P}|h}} |P(\Pi) - Q(\Pi)|. \end{aligned}$$

First, consider the ℓ_0 prior.

$$\sup_{Q \in \mathcal{Q}_{\mathcal{P}|h}} \delta(P_{P_{\ell_0}, \mathbf{Z}}, P_{Q, \mathbf{Z}}) = \frac{1}{\mathbb{P}(\mathbf{y} | \mathbf{X})} \sup_{\Pi \in \mathcal{P}|h} \mathbb{P}(\mathbf{y} | \mathbf{X}, \Pi) \sup_{Q \in \mathcal{Q}_{\mathcal{P}|h}} \left| \frac{1}{N(h)} - Q(\Pi) \right|.$$

Choose an adversarial prior Q^* such that $Q^*(\Pi^*) = 1$ for some arbitrary $\Pi^* \in \mathcal{P}|_h$. Then,

$$\begin{aligned} & \sup_{Q \in \mathcal{Q}_{\mathcal{P}|_h}} \left| \frac{1}{N(h)} - Q(\Pi) \right| = \left| \frac{1}{N(h)} - Q^*(\Pi^*) \right| = 1 - \frac{1}{N(h)} \\ \implies & \sup_{Q \in \mathcal{Q}_{\mathcal{P}|_h}} \delta(P_{P_{\ell_0}, \mathbf{Z}}, P_{Q, \mathbf{Z}}) = \left(1 - \frac{1}{N(h)} \right) \frac{\sup_{\Pi \in \mathcal{P}|_h} \mathbb{P}(\mathbf{y} | \mathbf{X}, \Pi)}{\mathbb{P}(\mathbf{y} | \mathbf{X})} \end{aligned}$$

Next, consider any other prior $P \in \mathcal{Q}_{\mathcal{P}|_h}$, $P \neq P_{\ell_0}$. Let $\Pi_m = \operatorname{argmin}_{\Pi} P(\Pi)$. Denote $P(\Pi_m) = p$. Observe that $p < 1/N(h)$ because $P \neq P_{\ell_0}$. Construct an adversarial prior Q^* such that $Q^*(\Pi_m) = 1$. Therefore,

$$\begin{aligned} & \sup_{Q \in \mathcal{Q}_{\mathcal{P}|_h}} |P(\Pi) - Q(\Pi)| = |P(\Pi_m) - Q^*(\Pi_m)| = 1 - p \\ \implies & \sup_{Q \in \mathcal{Q}_{\mathcal{P}|_h}} \delta(P_{P, \mathbf{Z}}, P_{Q, \mathbf{Z}}) = \frac{1}{\mathbb{P}(\mathbf{y} | \mathbf{X})} \sup_{\Pi \in \mathcal{P}|_h} \mathbb{P}(\mathbf{y} | \mathbf{X}, \Pi)(1 - p) \\ & = (1 - p) \frac{\sup_{\Pi \in \mathcal{P}|_h} \mathbb{P}(\mathbf{y} | \mathbf{X}, \Pi)}{\mathbb{P}(\mathbf{y} | \mathbf{X})} \\ & > \sup_{Q \in \mathcal{Q}_{\mathcal{P}|_h}} \delta(P_{P_{\ell_0}, \mathbf{Z}}, P_{Q, \mathbf{Z}}). \end{aligned}$$

Thus, the ℓ_0 prior is minimax optimal,

$$\sup_{Q \in \mathcal{Q}_{\mathcal{P}|_h}} \delta(P_{P_{\ell_0}, \mathbf{Z}}, P_{Q, \mathbf{Z}}) = \inf_{P \in \mathcal{Q}_{\mathcal{P}|_h}} \sup_{Q \in \mathcal{Q}_{\mathcal{P}|_h}} \delta(P_{P, \mathbf{Z}}, P_{Q, \mathbf{Z}}).$$

□

Proof of Lemma 1. From the definition of the Rashomon set, if $\Pi \in \mathcal{P}_\theta$, then

$$\begin{aligned} & \mathbb{P}(\Pi | \mathbf{Z}) \geq \theta \\ \implies & \frac{\exp \{-\mathcal{L}(\Pi) - \lambda H(\Pi)\}}{c} \geq \theta \\ \implies & \exp \{-\lambda H(\Pi)\} \geq c\theta \\ \implies & H(\Pi) \leq -\frac{\ln(c\theta)}{\lambda}, \end{aligned}$$

which gives our desired result. □

Proof of Theorem 3. Suppose we have h pools in some partition. Let $N(h)$ be the number of possible splits that generate h pools. And define $H := H_\theta(\lambda)$ for brevity. Then, the total number of Rashomon partitions is bounded by

$$|\mathcal{P}_\theta| \leq \sum_{h=1}^H N(h).$$

Now, we use the asymptotic bound in Lemma C.3. When $R > m^{1.41}$, we have the sum of a finite geometric series,

$$\sum_{h=1}^H mR^{h-1} = m \frac{R^H - 1}{R(R-1)} = \mathcal{O}(mR^{H-2}).$$

For the other case, we bound it by the integral,

$$\begin{aligned} \sum_{h=1}^H (mR)^{\log_2 h} &\leq \int_{h=1}^H (mR)^{\log_2 h} dh = \frac{H(mR)^{\log_2 H} - 1}{1 + \log_2(mR)} \\ &= \mathcal{O}\left((mR)^{\log_2 H} (\log_2(mR))^{-1}\right), \end{aligned}$$

where the integral is evaluated in Lemma C.4. This gives us the desired result. \square

C.1. Helpful results. We state a useful result that helps us count the number of pools generated by a partition matrix Σ .

Lemma C.1. *Let Σ be the partition matrix for a profile with m active features. Suppose there are z_i 1's in the i -th row of Σ . Then the number of pools created by Σ is,*

$$\begin{aligned} H(\Sigma) &= (R-1)^m - (R-1)^{m-1} \sum_i z_i + (R-1)^{m-2} \sum_{i_1 < i_2} z_{i_1} z_{i_2} \\ &\quad - (R-1)^{m-3} \sum_{i_1 < i_2 < i_3} z_{i_1} z_{i_2} z_{i_3} + \dots + (-1)^m z_1 \dots z_m. \end{aligned}$$

Proof of Lemma C.1. Observe that there are $(R-1)^m$ feature combinations in total ($R-1$ because we are assuming the R discrete values include the control). Suppose, we set $\Sigma_{ij} = 1$, then we are pooling policies of type $[r_1, \dots, r_{i-1}, j, r_{i+1}, \dots, r_m]$ with $[r_1, \dots, r_{i-1}, j-1, r_{i+1}, \dots, r_m]$, where $r_{j'}$ can take on $R-1$ values. Therefore, $(R-1)^{m-1}$ policies are pooled. So, if there are in $\text{nnz}(\Sigma) = \sum_i z_i$, then $(R-1)^{m-1} \sum_i z_i$ policies are pooled.

However, if some of those 1's are in a different treatment arm, then we end up double counting those. For example, if $\Sigma_{i_1, j} = 1$ and $\Sigma_{i_2, j'} = 1$, then we remove policies of type $[r_1, \dots, j, \dots, j', \dots, r_m]$ twice where j and j' are at indices i_1 and i_2 . So, we need to add them back. Similarly, the remaining non-linear terms account for this ‘‘double counting.’’ \square

Lemma C.1 tells us how to count the number of pools given a partition matrix. We now state another result that bounds the sparsity of the partition matrix given some number of pools in Lemma C.2.

Lemma C.2. *Let Σ be the matrix defined in Proposition 2 for a profile with m active features. Suppose there are H pools. Then,*

$$\sum_i z_i \leq \frac{(2R-3)^m + 1 - 2H}{2(R-1)^{m-1}}$$

Proof of Lemma C.2. Rearranging and dropping negative terms from Lemma C.1,

$$\begin{aligned} (R-1)^{m-1} \sum_i z_i &\leq -H + (R-1)^m + (R-1)^{m-2} \sum_{i_1 < i_2} z_{i_1} z_{i_2} \\ &\quad + (R-1)^{m-4} \sum_{i_1 < \dots < i_4} z_{i_1} z_{i_2} z_{i_3} z_{i_4} + \dots \\ &\leq -H + (R-1)^m + (R-1)^{m-2} (R-2)^2 \sum_{i_1 < i_2} 1 \\ &\quad + (R-1)^{m-4} (R-2)^4 \sum_{i_1 < \dots < i_4} 1 + \dots \\ &= -H + \sum_{n \text{ even}} \binom{m}{n} (R-1)^{m-n} (R-2)^n \\ \implies \sum_i z_i &\leq \frac{(2R-3)^m + 1 - 2H}{2(R-1)^{m-1}}, \end{aligned}$$

where the second inequality uses $z_j \leq R-2$ and the last step uses the well-known identity

$$\sum_{k \text{ even}} \binom{n}{k} a^{n-k} b^k = \frac{1}{2} ((a+b)^n + (a-b)^n).$$

□

We state a stronger result in Lemma C.3 that tells us exactly how many partition matrices could have generated a given number of pools. This result is crucial in bounding the size of the RPS in a practically meaningful way as in Theorem 3.

Lemma C.3. *Let Σ be the matrix defined in Proposition 2 for a profile with m active features. Then the number of Σ matrices that generate h pools is given by*

$$N(h) = \sum_{k=0}^m \binom{m}{k} \sum_{\prod_{i=1}^k (z_i+1)=h} \prod_{i=1}^k \binom{R-2}{z_i},$$

where we define $N(1) = 1$ and $\binom{n}{k} = 0$ for $k > n$.

As $m, R \rightarrow \infty$, we have

$$N(h) = \begin{cases} \mathcal{O}(mR^{h-1}), & R > m^{1.41} \\ \mathcal{O}((mR)^{\log_2 h}), & \text{else} \end{cases}.$$

Proof of Lemma C.3. This is an exercise in counting. When we make z splits in one feature, we generate $z + 1$ pools. When we make z_i splits in feature i and z_j splits in feature j , we generate $(z_i + 1)(z_j + 2)$ pools.

When we want to generate h pools, we first choose the features where we want the splits to occur. This is what the first summation is doing. Suppose that we've chosen k features where we want to perform splits. Next, we need to identify how many splits can be made in each feature. This is what the inner summation is doing with the condition $\prod_{i=1}^k (z_i + 1) = h$. Finally, we need to identify where those splits are made, which is where the binomial coefficient comes in.

To get the asymptotic bound, we first consider the term where the exponent on R is the largest. This is when we choose all splits in the same feature. Next, we consider the term where the exponent on m is the largest. For this to happen, we need to choose as many arms as possible i.e., make the smallest number of non-zero splits in each feature. This corresponds to making 1 split in each feature i.e., selecting $\log_2 h$ feature. Hence, we get the asymptotic bound $\mathcal{O}(\max\{mR^{h-1}, (mR)^{\log_2 h}\})$.

Observe that

$$mR^{h-1} > (mR)^{\log_2 h} \iff R > m^{\frac{\log_2 h - 1}{h - \log_2 h - 1}}.$$

The exponent on m is a decreasing function in h . When $h = 2$, $mR^{h-1} = (mR)^{\log_2 h}$. And when $h = 3$, the exponent is approximately 1.41. Therefore $mR^{h-1} > (mR)^{\log_2 h}$ whenever $R > m^{1.41}$, which gives our desired result. \square

Lemma C.3 has a nice implication. When h is a prime number, we expect $N(h)$ to be small because all of the splits need to be made in the same feature. On the other hand, when $h = 2^k$ is a power-of-two, we expect $N(h)$ to be very large since we can make splits in multiple features at the same time.

Lemma C.4. For $a > 1$,

$$\int_x a^{\log_2 x} dx = \frac{xa^{\log_2 x}}{1 + \log_2 a} + C.$$

Proof of Lemma C.4. We use integration by parts to solve this,

$$\int_x a^{\log_2 x} dx = a^{\log_2 x} \int_x dx - \int_x x \cdot \frac{a^{\log_2 x} \log_2 a}{x} dx$$

$$\begin{aligned}
&= xa^{\log_2 x} - \log_2 a \int_x a^{\log_2 x} dx \\
\implies \int_x a^{\log_2 x} dx &= \frac{xa^{\log_2 x}}{1 + \log_2 a} + C.
\end{aligned}$$

□

APPENDIX D. APPENDIX TO RASHOMON SET ENUMERATION AND GENERALIZATIONS

We organize this appendix into proofs for results in Section 5, additional algorithms used in Section 5, and proofs for results in Section 8.

D.1. Proofs in Section 5.

Proof of Theorem 4. By definition,

$$b(\Sigma, \mathcal{M}; \mathbf{Z}) \leq \frac{1}{n} \sum_{\pi \in \Pi_f} \sum_{k(i) \in \pi} (y_i - \hat{\mu}_\pi)^2 + \lambda H(\Pi, \mathcal{M})$$

Notice that $|\Pi| \geq H(\Pi, \mathcal{M})$. Further, by making more splits, we can only reduce the total mean-squared error incurred. Therefore,

$$\begin{aligned}
Q(\Pi; \mathbf{Z}) &= \mathcal{L}(\Pi; \mathbf{Z}) + \lambda |\Pi| \\
&= \frac{1}{n} \sum_{\pi \in \Pi} \sum_{k(i) \in \pi} (y_i - \hat{\mu}_\pi)^2 + \lambda |\Pi| \\
&\geq \frac{1}{n} \sum_{\pi \in \Pi} \sum_{k(i) \in \pi} \mathbb{1}\{k(i) \cap \pi_f \neq \emptyset\} (y_i - \hat{\mu}_\pi)^2 + \lambda |\Pi| \\
&\geq \frac{1}{n} \sum_{\pi \in \Pi_f} \sum_{k(i) \in \pi} \mathbb{1}\{k(i) \cap \pi_f \neq \emptyset\} (y_i - \hat{\mu}_\pi)^2 + \lambda |\Pi| \\
&\geq \frac{1}{n} \sum_{\pi \in \Pi_f} \sum_{k(i) \in \pi} \mathbb{1}\{k(i) \cap \pi_f \neq \emptyset\} (y_i - \hat{\mu}_\pi)^2 + \lambda H(\Pi, \mathcal{M}) \\
&= b(\Sigma_f; \mathbf{Z}).
\end{aligned}$$

So if $b(\Sigma, \mathcal{M}; \mathbf{Z}) > \theta_\epsilon$, then Σ is not in the Rashomon set. Now consider $\Sigma' \in \text{child}(\Sigma, \mathcal{M})$. Notice that the size of the fixed set of indices \mathcal{M}' in any child of Σ increases (because there are fewer places to make further splits). With any further split we make in \mathcal{M} , the number of pools increases. Finally, the loss is non-negative. These together imply,

$$\begin{aligned}
b(\Sigma', \mathcal{M}'; \mathbf{Z}) &\geq b(\Sigma, \mathcal{M}; \mathbf{Z}) \\
\implies Q(\Pi(\Sigma'); \mathbf{Z}) &\geq b(\Sigma', \mathcal{M}'; \mathbf{Z}) \geq b(\Sigma, \mathcal{M}; \mathbf{Z}).
\end{aligned}$$

Therefore, if $b(\Sigma, \mathcal{M}; \mathbf{Z}) > \theta_\epsilon$, then Σ and all $\Sigma' \in \text{child}(\Sigma, \mathcal{M})$ are not in the Rashomon set. \square

Proof of Theorem 5. By definition of b_{eq} ,

$$b_{eq}(\Sigma, \mathcal{M}; \mathbf{Z}) \leq \frac{1}{n} \sum_{\pi \in \Pi} \sum_{k(i) \in \pi} \mathbb{1}\{k(i) \cap \pi_{\dagger}^c \neq \emptyset\} (y_i - \hat{\mu}_\pi)^2.$$

The idea in the inequality above is that any further split we make must obey the splits made at \mathcal{M} .

$$\begin{aligned} Q(\Pi; \mathbf{Z}) &= \mathcal{L}(\Pi; \mathbf{Z}) + \lambda |\Pi| \\ &= \frac{1}{n} \sum_{\pi \in \Pi} \sum_{k(i) \in \pi} \mathbb{1}\{k(i) \cap \pi_{\dagger} \neq \emptyset\} (y_i - \hat{\mu}_\pi)^2 + \lambda |\Pi| + \\ &\quad \frac{1}{n} \sum_{\pi \in \Pi} \sum_{k(i) \in \pi} \mathbb{1}\{k(i) \cap \pi_{\dagger}^c \neq \emptyset\} (y_i - \hat{\mu}_\pi)^2 \\ &\geq b(\Sigma, \mathcal{M}; \mathbf{Z}) + b_{eq}(\Sigma, \mathcal{M}; \mathbf{Z}) \\ &= B(\Sigma, \mathcal{M}; \mathbf{Z}). \end{aligned}$$

Therefore, if $B(\Sigma, \mathcal{M}; \mathbf{Z}) > \theta_\epsilon$, then $Q(\Pi; \mathbf{Z}) > \theta_\epsilon$ and $\Sigma' \in \text{child}(\Sigma, \mathcal{M})$. Let $\Pi' := \Pi(\Sigma')$. Then,

$$\begin{aligned} Q(\Pi'; \mathbf{Z}) &= \mathcal{L}(\Pi'; \mathbf{Z}) + \lambda |\Pi'| \\ &= \frac{1}{n} \sum_{\pi \in \Pi'} \sum_{k(i) \in \pi} \mathbb{1}\{k(i) \cap \pi_{\dagger} \neq \emptyset\} (y_i - \hat{\mu}_\pi)^2 + \lambda |\Pi'| + \\ &\quad \frac{1}{n} \sum_{\pi \in \Pi'} \sum_{k(i) \in \pi} \mathbb{1}\{k(i) \cap \pi_{\dagger}^c \neq \emptyset\} (y_i - \hat{\mu}_\pi)^2 \\ &\geq b(\Sigma, \mathcal{M}; \mathbf{Z}) + \frac{1}{n} \sum_{\pi \in \Pi'} \sum_{k(i) \in \pi} \mathbb{1}\{k(i) \cap \pi_{\dagger}^c \neq \emptyset\} (y_i - \hat{\mu}_\pi)^2 \\ &\geq b(\Sigma, \mathcal{M}; \mathbf{Z}) + b_{eq}(\Sigma, \mathcal{M}; \mathbf{Z}) \\ &= B(\Sigma, \mathcal{M}; \mathbf{Z}). \end{aligned}$$

In the steps above, we used the fact that making any split will increase the number of pools to say that $|\Pi'| \geq |\Pi|$. We also used the definition of b_{eq} and the idea of a minimum loss incurred by equivalent units in the final step.

Therefore, if $B(\Sigma, \mathcal{M}; \mathbf{Z}) > \theta_\epsilon$, then $Q(\Pi'; \mathbf{Z}) > \theta_\epsilon$ for any $\Sigma' \in \text{child}(\Sigma, \mathcal{M})$. So Σ and all such Σ' are not in the Rashomon set. \square

Proof of Theorem 6. First note that Algorithm D.1 correctly enumerates the Rashomon set for any given profile. This follows directly from Lemma 1, and Theorems 4 and 5.

Next, Algorithm D.4 performs a breadth-first search starting at the control profile. Since the M -d hypercube has a unique source (the control profile) and sink (the profile with all features active), the breadth-first search will terminate after a finite time and traverse every possible path in the hypercube. When traversing an edge in the hypercube, Algorithm D.3 attempts to pool adjacent profiles using the intersection matrix Σ^\cap while obeying (1) and (2) of Definition 7. This pooling attempt is done recursively guaranteeing that all admissible partitions are considered for the Rashomon set.

The choice of Rashomon thresholds for each profile, described in Line 3, is justified by the usage of Theorem 5.

Correctness of Algorithm 1 immediately follows. \square

D.2. Additional algorithms. Algorithm 1 calls upon two important algorithms and uses a specific caching object that we describe here. First, Algorithm D.1 describes how to enumerate the Rashomon partitions for a single profile. Second, Algorithm D.4 describes a breadth-first search to enumerate partitions across different profiles by traversing the M -d hypercube. This algorithm in turn relies on Algorithm D.2 to obtain the intersection matrix between partitions of adjacent profiles and Algorithm D.3 to pool adjacent profiles recursively. Finally, Algorithm D.5 describes the implementation of the caching object used in Algorithm 1.

D.3. Proofs in Section 8.

Proof of Theorem 7. The results follow directly from Theorems 4, 5, and 6. \square

Proof of Theorem 8. The results follow directly from Theorems 4, 5, and 6. \square

APPENDIX E. FURTHER DETAILS ON RELATED WORK

It is useful to contrast our method with several other (some recent) approaches to study heterogeneity. Specifically, we are interested in their application to settings with partial orderings (e.g., factorial structure and admissibility) which is easily interpretable.

We will focus on four main related approaches: (1) canonical Bayesian Hierarchical Models (BHM) (Rubin, 1981; Gelman, 2006; Meager, 2019); (2) ℓ_1 regularization of marginal effects to identify heterogeneity (Banerjee et al., 2021); (3) causal forests (Wager and Athey, 2018); and (4) machine learned proxies (Chernozhukov et al., 2018). We intend this discussion to be a guide for practitioners considering implementing our proposed method or one of these state-of-the-art alternatives. We discuss conceptually related work (e.g. Bayesian decision trees) in previous sections. Let us for the moment set aside the following immediate differences. Our focus on robustness, profiles, and enumerating the entire Rashomon Partition are all novel. Instead, it is useful to identify the

Algorithm D.1 EnumerateRPS_profile($M, R, H, \mathbf{Z}, \theta_\epsilon$)**Input:** M features, R factors per feature, max pools H , data \mathbf{Z} , Rashomon threshold θ_ϵ **Output:** Rashomon set $\mathcal{P}_{q,\epsilon}$

```

1:  $\mathcal{P}_{q,\epsilon} = \emptyset$ 
2:  $\mathcal{S} = \text{cache}()$  ▷ See Algorithm D.5
3:  $\mathcal{Q} = \text{queue}()$ 
4:  $\Sigma = \{1\}^{M \times (R-2)}$ 
5:  $\mathcal{Q}.\text{push}(\Sigma, 1, 1)$  ▷ Can start at any arbitrary arm
6: while  $\mathcal{Q}$  is not empty do
7:    $(\Sigma, i, j) = \mathcal{Q}.\text{dequeue}()$ 
8:   if  $\mathcal{S}.\text{seen}(\Sigma, i, j)$  then continue
9:    $\mathcal{S}.\text{insert}((\Sigma, i, j))$ 
10:  if  $H(\Sigma) > H$  then continue
11:   $\Sigma_1 = \Sigma, \Sigma_{1,i,j} = 1$ 
12:   $\Sigma_0 = \Sigma, \Sigma_{0,i,j} = 1$ 
13:  for  $m \leq M$  do ▷ Branch and search
14:     $j_1 = \min\{j \leq R-2 \mid \text{not } \mathcal{S}.\text{seen}(\Sigma_1, m, j)\}$ 
15:    if  $j_1 \neq \emptyset$  then  $\mathcal{Q}.\text{enqueue}(\Sigma_1, m, j_1)$ 
16:     $j_0 = \min\{j \leq R-2 \mid \text{not } \mathcal{S}.\text{seen}(\Sigma_0, m, j)\}$ 
17:    if  $j_0 \neq \emptyset$  then  $\mathcal{Q}.\text{enqueue}(\Sigma_0, m, j_0)$ 
18:  if  $B(\Sigma, i, j; \mathbf{Z}) > \theta_\epsilon$  then continue
19:  if  $Q(\Sigma_1) \leq \theta_\epsilon$  then  $\mathcal{P}_{q,\epsilon}.\text{add}(\Sigma_1)$ 
20:  if  $Q(\Sigma_0) \leq \theta_\epsilon$  and  $H(\Sigma_0) \leq H$  then  $\mathcal{P}_{q,\epsilon}.\text{add}(\Sigma_0)$ 
21:  if  $j < R-2$  then ▷ Search deeper
22:    if not  $\mathcal{S}.\text{seen}(\Sigma_1, i, j+1)$  then  $\mathcal{Q}.\text{enqueue}(\Sigma_1, i, j+1)$ 
23:    if not  $\mathcal{S}.\text{seen}(\Sigma_0, i, j+1)$  then  $\mathcal{Q}.\text{enqueue}(\Sigma_0, i, j+1)$ 
24: return  $\mathcal{P}_{q,\epsilon}$ 

```

Algorithm D.2 IntersectionMatrix(Π, ρ_i, ρ_j)**Input:** Partition Π , Adjacent profiles ρ_i, ρ_j such that $\rho_i < \rho_j$ **Output:** Intersection matrix Σ^\cap

```

1:  $\mathbf{m} = \rho_i \wedge \rho_j$  ▷ Indices of features active in both profiles
2:  $m' = \rho_i \oplus \rho_j$  ▷ Index where  $\rho_i, \rho_j$  differ
3:  $\Pi_{\rho_i} = \{\pi \setminus \{k \mid \rho(k) \neq \rho_i\} \mid \pi \in \Pi\}$ 
4:  $\Pi_{\rho_j} = \{\pi \setminus \{k \mid \rho(k) \neq \rho_j\} \mid \pi \in \Pi\}$ 
5:  $\Sigma^\cap = [\infty]^{|\Pi_{\rho_i}| \times |\Pi_{\rho_j}|}$ 
6: for  $\pi_k \in \Pi_{\rho_i}$  do
7:   for  $\pi_{k'} \in \Pi_{\rho_j}$  do ▷ Features with lowest non-zero level in  $m'$ 
8:      $\mathcal{A} = \sum_{a_1 \in \pi_k} \sum_{a_2 \in \pi_{k'}} \mathbb{1}\{\|\mathbf{x}(a_1) - \mathbf{x}(a_2)\|_1 = 1\}$ 
9:     if  $\mathcal{A} \neq \emptyset$  then
10:        $\Sigma_{k,k'}^\cap = 0$ 
11: return  $\Sigma^\cap$ 

```

philosophical differences across the various approaches and how they relate to us. Every approach, as we will note, effectively uses partitions Π at some point to determine which data to pool or not. The specific techniques create distributions, possibly degenerate, over these partitions, and these

Algorithm D.3 PoolAdjacentProfiles($\mathcal{P}_{q,\epsilon}, \Pi, \mathbf{z}, \Sigma^\cap, \mathbf{Z}, \theta$)

Input: Rashomon set $\mathcal{P}_{q,\epsilon}$, partition Π , list of pools that can be pooled across profiles \mathbf{z} , data \mathbf{Z} , Rashomon threshold θ , intersection matrices already seen \mathcal{S}

Output: Rashomon set $\mathcal{P}_{q,\epsilon}$

```

1: while  $\mathbf{z} \neq \emptyset$  do
2:    $(k, k') = \mathbf{z}.\text{pop}()$ 
3:    $\mathcal{P}_{q,\epsilon} = \text{PoolAdjacentProfiles}(\mathcal{P}_{q,\epsilon}, \Pi, \mathbf{z}, \Sigma^\cap, \theta)$ 
4:    $\Sigma^{\cap, \prime} = \Sigma^\cap$ 
5:    $\Sigma_{k,k'}^{\cap, \prime} = 1$ 
6:    $\Sigma_{k,-k'}^{\cap, \prime} = \infty, \Sigma_{-k,k'}^{\cap, \prime} = \infty$   $\triangleright$  Cannot pool  $\pi_k$  or  $\pi_{k'}$  with any other pool
7:    $\Pi' = (\Pi \setminus \{\pi_k, \pi_{k'}\}) \cup (\pi_k \cup \pi_{k'})$   $\triangleright$  Update  $\Pi$ 
8:   if  $Q(\Pi'; \mathbf{Z}) \leq \theta$  then
9:      $\mathcal{P}_{q,\epsilon} = \Pi' \cup \text{PoolAdjacentProfiles}(\mathcal{P}_{q,\epsilon}, \Pi', \mathbf{z}, \Sigma^{\cap, \prime}, \theta)$ 
10: return  $\mathcal{P}_{q,\epsilon}$ 

```

Algorithm D.4 PoolProfiles($\mathcal{P}, \rho_0, \mathbf{Z}, \theta$)

Input: Candidates for Rashomon set \mathcal{P} , control profile ρ_0 , data \mathbf{Z} , Rashomon threshold θ

Output: Rashomon set $\mathcal{P}_{q,\epsilon}$

```

1:  $\mathcal{P}_{q,\epsilon} = \emptyset$ 
2:  $\mathcal{Q} = \text{queue}()$ 
3: while  $\mathcal{Q} \neq \emptyset$  do
4:    $\rho_i = \mathcal{Q}.\text{dequeue}()$ 
5:    $\mathcal{N}(\rho_i) = \{\rho_j \mid \|\rho_i - \rho_j\|_0 = 1, \rho_j > \rho_i\}$   $\triangleright$  Neighbors of  $\rho_i$  with additional active feature
6:   for  $\rho_j \in \mathcal{N}(\rho_i)$  do
7:      $\mathcal{Q}.\text{enqueue}(\rho_j)$ 
8:     for  $\Pi \in \mathcal{P}'$  do
9:        $\Sigma^\cap = \text{IntersectionMatrix}(\Pi, \rho_i, \rho_j)$   $\triangleright$  See Algorithm D.2
10:       $\mathbf{z} = \{(k, k') \mid \Sigma_{k,k'}^\cap = 0\}$ 
11:       $\mathcal{P}_{q,\epsilon} = \text{PoolAdjacentProfiles}(\mathcal{P}_{q,\epsilon}, \Pi, \mathbf{z}, \Sigma^\cap, \mathbf{Z}, \theta)$   $\triangleright$  See Algorithm D.3
12: return  $\mathcal{P}_{q,\epsilon}$ 

```

Algorithm D.5 Implementation of caching object used in Algorithm D.1

```

 $\mathcal{S} = \text{cache}()$   $\triangleright$  Initialize caching object
 $C = \{\}$ 
 $\mathcal{S}.\text{insert}(\Sigma, i, j)$   $\triangleright$  Extract and insert  $\Sigma_i$ 
   $\Sigma[i, j : (R-2)] = \text{NA}$ 
   $C = C \cup \{\Sigma\}$ 
 $\mathcal{S}.\text{seen}(\Sigma, i, j)$   $\triangleright$  Extract and check presence of  $\Sigma_i$ 
   $\Sigma[i, j : (R-2)] = \text{NA}$ 
return  $\Sigma \in C$ 

```

distributions are sampled from and marginalized to estimate treatment effects β_k . The interesting thing therefore is in how one builds a distribution over Π .

Algorithm D.6 `select_feasible_combinations(K, θ)`

Input: K list of n sorted lists containing a numerical score, θ threshold**Output:** F , list of lists of length n with indices of elements from each of K_i such that their sum is less than θ

```

1:  $F = \{\}$ 
2:  $n = \text{len}(K)$ 
3: if  $n = 0$  then return  $\{\}$ 
4:  $K_{1,\text{feasible indices}} = \{i \mid K_1[i] \leq \theta\}$ 
5: if  $n = 1$  then
6:    $F = \{K_{1,\text{feasible indices}}\}$ 
   return  $F$ 
7:  $x = \sum_{j=2}^n K_j[1]$ 
8: for  $i \in K_{1,\text{feasible indices}}$  do
9:    $\theta_i = \theta - K_1[i]$ 
10:  if  $\theta_i < x$  then break
11:   $F_i = \text{select\_feasible\_combinations}(K[2:], \theta_i)$ 
12:  for  $f \in F_i$  do
13:     $F.\text{insert}([i].\text{append}(f))$ 
return  $F$ 

```

E.1. **Bayesian Hierarchical Models.** We now discuss how our work relates to a canonical representation of a Bayesian Hierarchical Model. As discussed previously, our work is more similar to Bayesian Tree(d) models than to other methods for accounting for learning heterogeneity, such as Bayesian Model Averaging. For context, however, we present how our approach compares to the canonical Bayesian approach. The Bayesian perspective provides a compromise between complete and partial pooling. Partial pooling occurs by encouraging similarity in the values for parameters without requiring strict equality. Using the notation from our model, for example, we could construct a model where

$$\mathbf{y} \sim N(\mathbf{D}\boldsymbol{\beta}, \sigma_y^2)$$

and, for the sake of exposition, all β are drawn independently from

$$\boldsymbol{\beta} \sim N(\mu_\beta, \sigma_\beta^2).$$

Requiring that all values of $\boldsymbol{\beta}$ come from the same distribution encourages sharing information across potential feature combinations and encourages the effects on heterogeneity to be similar (but not identical). Meager (2019) uses this approach when comparing treatment effects across multiple domains. In that paper, the goal is not to pool across potentially similar treatment conditions but instead to (partially) pool across geographic areas.

As one example of the classical model, Meager (2019) has outcomes for household i in study k modeled as

$$y_{ik} \sim N(\mu_k + \tau_k \mathbf{T}_{ik}, \sigma_{yk}^2) \quad \forall i, k$$

$$\begin{pmatrix} \mu_k \\ \tau_k \end{pmatrix} \sim N \left[\begin{pmatrix} \mu \\ \tau \end{pmatrix}, \begin{pmatrix} \sigma_\mu^2 & \sigma_{\mu\tau} \\ \sigma_{\mu\tau} & \sigma_\tau^2 \end{pmatrix} \right] \quad \forall i, k$$

where τ_k, μ_k are the overall mean and treatment effect at area k , respectively. The vector \mathbf{T}_{ik} is the treatment indicator for household i in study k .

One way to measure the degree of pooling is the (partial) ‘‘pooling factor’’ metric defined in Gelman (2006), $\omega(\boldsymbol{\beta}) = \sigma_y^2 / \sigma_y^2 + \sigma_\beta^2$. The partial pooling metric quantifies how much the effect of treatment combinations varies compared to the overall heterogeneity in the outcomes. The partial pooling metric, the Meager (2019) context refers to the relative variation related to differences between studies compared to sampling variability.

In contrast, we could think of our approach as using a prior on $\boldsymbol{\beta}$ conditional on the partitions that potentially force some values of β_k, β'_k to be equal. In Appendix F.2, we show that the objective function we use in Equation 5 corresponds to a hierarchical model where we draw the $\boldsymbol{\beta}$ vector as

$$\boldsymbol{\beta} \mid \Pi \sim \mathcal{N}(\boldsymbol{\mu}_\Pi, \boldsymbol{\Lambda}),$$

where $\boldsymbol{\mu}_\Pi$ is structured such that $\mu_k = \mu_{k'}$ for any $k, k' \in \pi \in \Pi$. Then, given some feature combinations \mathbf{D} , we draw the outcomes as

$$\mathbf{y} \mid \mathbf{D}, \boldsymbol{\beta} \sim \mathcal{N}(\mathbf{D}\boldsymbol{\beta}, \boldsymbol{\Sigma}).$$

To understand the variation within the $\boldsymbol{\beta}$ vector, we need to average across potential partitions, since some partitions will set $\beta_k = \beta'_k$ and others will not. This amounts to replacing the σ_β^2 in the pooling factor with the variance of the distribution of $\mathbb{P}(\boldsymbol{\beta} \mid Z)$, which is defined in Equation 3.

We could also conceptualize the above derivation in terms of equality on $\boldsymbol{\beta}$ rather than the means $\boldsymbol{\mu}_\Pi$. If, for example, we replace $\boldsymbol{\Lambda}$ with $\boldsymbol{\Lambda}_\Pi$ where $\text{Var}(\mu_k, \mu'_k) = 0$ for any $k, k' \in \pi \in \Pi$ (or equivalently, when $\mu_k = \mu_{k'}$) then we enforce that $\beta_k = \beta'_k$. Of course, if we go the opposite direction and let the diagonal of $\boldsymbol{\Lambda}_\Pi$ be unconstrained then there is essentially no sharing of information across feature combinations.

Finally, hierarchical models of this type are, of course, quite flexible and we could construct more complex models that capture features of our pooling approach. Among those options would be to use the Bayesian version of penalized regression, such as the Bayesian Lasso, which would be philosophically related to the approach we describe in the next section.

E.2. Lasso regularization. This is the approach taken in prior work by several of the authors of the present paper, in [Banerjee et al. \(2021\)](#). There the setting was one in which the researcher faced a factorial experimental design: a crossed randomized controlled trial (RCT). The paper developed the Hasse structure described above and an approach that required transforming \mathbf{D} into an equivalent form presented in Equation (A.1) in Appendix A. Here every parameter α_k represents the marginal difference between β_k and $\beta_{k'}$ where $\rho(k) = \rho(k')$ (they are the same profile) and k exactly differs from k' on one arm by one dose. The parameter vector $\boldsymbol{\alpha}$ records the marginal effects. Notice the support of $\boldsymbol{\alpha}$ therefore identifies Π (since non-zero entries determine splits).

The first difficulty in applying this to general settings of heterogeneity is that ℓ_1 regularization requires irreducibility: that there is limited correlation between the regressors so that the support may be consistently recovered ([Zhao and Yu, 2006](#)). Unfortunately, the regression implied by the Hasse does not satisfy this so some pre-processing is required. [Banerjee et al. \(2021\)](#) apply the Puffer transformation of [Jia and Rohe \(2015\)](#) to retain irreducibility and estimate the Lasso model. However, this is not free: the approach requires conditions on the minimum singular value of the design matrix. The authors leverage the structure of a crossed randomized controlled trial (which places considerable restriction on the design matrix) to argue that indeed these conditions are met. There is no guarantee and it is unlikely to be the case that these conditions are met for general factorial data of arbitrary covariates. So, tackling the much more general structure required moving away from regression (we use decision trees) and changing the regularization (we use ℓ_0).

The second key observation is that the Bayesian lasso means that the ℓ_1 penalty corresponds to priors $\mathbb{P}(\boldsymbol{\alpha})$ that are i.i.d. Laplace on every dimension k . That is

$$-\log \mathbb{P}(\boldsymbol{\alpha}) = \log \prod_k \mathbb{P}(\alpha_k) = \log \prod_k \exp(-\lambda |\alpha_k|) = \lambda \sum_k |\alpha_k|.$$

Note that this is true whether one uses regular lasso, Puffer transformed lasso, spike-and-slab lasso, group lasso (up to the group level) and so on. No matter at whatever level the ℓ_1 sum is being taken, it corresponds to independence at that level in the prior.

In practice what this means is that given two partitions Π and Π' , which have the same number of pools and which have the same loss value, if one is more consistent with independent values of α_k than the other, it will receive a higher posterior. There are at least two problems.

The main philosophical problem is that there is no reason to place the meta-structure that the marginal differences between adjacent variants should have an i.i.d. distribution. In fact, one might think that the basic science or social science dictates *exactly the opposite*. Independence means that a marginal increase in dosage of drug A, holding fixed B and C at some level, is thought to be *independent* of increasing A holding fixed B and C at (potentially very similar) different levels. Similarly, the marginal value of receiving a slightly larger loan given that the recipient has 10 years of schooling and started 5 previous businesses is *independent* of receiving a slightly larger loan if the recipient had 10 years of schooling and started 6 previous businesses. Independence is unreasonable in both examples.

There is a second issue in that if an object of interest is Π , this approach provides no way forward. Regularization delivers posteriors over α : $\mathbb{P}(\alpha \mid \mathbf{y}, \mathbf{X})$. This implies a posterior over S_α . The map from S_α to Π is deterministic, and is given by some $\phi(S_\alpha) = \Pi$, which means that

$$\mathbb{P}(\Pi \mid \mathbf{y}, \mathbf{X}) = \int_{\alpha} \mathbf{1}\{\phi(S_\alpha) = \Pi\} \cdot \mathbb{P}(\alpha \mid \mathbf{y}, \mathbf{X})$$

is the actual calculation of interest.

So the regularization approach requires the statistician to take all the marginal parameters to be i.i.d., and given this, integrate over possible coefficient vectors that are consistent with this specific aggregation. This makes calculating an RPS very difficult.

E.3. Causal Random Forests. We now compare our approach to Causal Random Forests (CRFs) introduced by [Wager and Athey \(2018\)](#). CRFs construct regression trees over the space of potential combinations of covariates. Trees partition the space of covariates into “leaves.” Unlike our setting, trees are hierarchical; the procedure to construct trees involves splitting the observed data in two based on X_i being above or below a threshold. They then partition recursively, dividing each subsequent group until the leaves contain very few observations. This approach can also be thought of as finding nearest neighbors, where the number of neighbors is the number of observations in the leaf and using distance on the tree as the closeness metric. CRFs construct a conditional average treatment effect at a pre-determined point $X = x$, $\tau(x) = \mathbb{E}[Y(1) - Y(0) \mid X = x]$ where $Y(1)$ is potential outcome for the treated and $Y(0)$ is the potential outcome for the control.

Relating this back to our work, take T to be a tree and $\pi \in \Pi(T)$ to be a leaf in the tree, which corresponds to a pool in our language. Then, the estimated expected outcomes for each leaf is

$$\hat{\beta}_\pi = \frac{1}{|\{i : X_i \in \pi\}|} \sum_{\{i : X_i \in \pi\}} Y_i.$$

Further, taking τ_π to be the treatment effect of observations in pool (leaf) π and W_i as the treatment indicator, which we assume orthogonal to X and Y , the estimated treatment effect for π is

$$\hat{\tau}_\pi = \frac{1}{|\{i : W_i = 1, X_i \in \pi\}|} \sum_{\{i:W_i=1,X_i \in \pi\}} Y_i - \frac{1}{|\{i : W_i = 0, X_i \in \pi\}|} \sum_{\{i:W_i=0,X_i \in \pi\}} Y_i.$$

To summarize, the approach for forming trees splits the observed covariate space into partitions, known as leaves. Each leaf consists of a mix of people in treatment and control groups and, in fact, the specification of the tree depends on this balance across treatment and control groups since the algorithm requires that splitting be done in a way that preserves a minimum number of treatment and control in each leaf. To compute a treatment effect conditional on a particular value of X , look at the difference in outcome between treated and control people in a given leaf. Outcomes are not considered with constructing the tree (in contrast to our proposed approach) and treatment status is not used to split explicitly but does influence the construction of the tree through the sample size restriction.

Despite being similar in that we both use geometric objects that partition the space of covariates, there are three fundamental differences between our approach and CRFs. The first difference is geometric. CRFs use regression trees, whereas we use Hasse diagrams. Regression trees are appealing in many settings because of their flexibility in representing complex, nonlinear, relationships between variables. Regression trees, however, require imposing a hierarchy between variables that is not supported by the data. This hierarchy is “baked in” to the structure of the trees and is evident from how we describe constructing trees in the previous paragraph. The data, however, are not fully hierarchical and are instead partially ordered.

This mismatch creates an identification issue. Within education and within income, there are clear orderings. There is, however, no hierarchy between education and income. One tree may, therefore, split first based on income and then split on education conditional on income while another tree does the opposite. In both cases, we can trace the trees to end up with the same estimated treatment effects for any group of covariates (as shown in [Wager and Athey \(2018\)](#)). The trees themselves, however, arise from this arbitrary ordering and are, thus, not interpretable. Work such as [Bénard and Josse \(2023\)](#) describe measures of variable importance in CRFs, but the problem of an arbitrarily imposed hierarchy is still present. Hasse diagrams, in contrast, are the natural geometry for partially ordered sets, alleviating this issue and allowing the researcher to interpret the pooling structure on the domain of the covariates directly.

The second difference is computational but has conceptual implications. In both our approach and CRFs, we do not take the structure of the partition as known. Both approaches must, therefore, account for additional uncertainty in treatment effect estimates that arises from not knowing the partition. In CRFs, bootstrap samples over the data propagate this uncertainty. CRFs then aggregate over trees using Monte Carlo averaging over $b = 1, \dots, B$ bootstrap samples of the covariates and outcomes, $\{Z_1, \dots, Z_n\}$,

$$RF(\pi; Z_1, \dots, Z_n) \approx \frac{1}{B} \sum_{b=1}^B T(\pi; \xi_b; Z_{b1}^*, \dots, Z_{bn}^*),$$

where π represents a pool or leaf specifying a combination of features and levels. The ξ_b term is an additional stochastic component. The trees sampled as part of this process create a “forest” are, by definition, random draws given the data. That is, given a different set of data, the distribution of likely trees would change. They are also not guaranteed to be optimal or nearly optimal. If the goal is to estimate average treatment effects, this approach represents a principled way to explore the space of trees. If the goal, however, is to identify potential models of heterogeneity, then sampling randomly is very unlikely to produce high quality trees. With Rashomon partitions, by definition, we guarantee that all models in our set are of high posterior.

To this point, we have not discussed inference in CRFs. A key contribution of [Wager and Athey \(2018\)](#) is forming so-called “honest” trees that account for issues that arise when using the same data to learn trees and then to make inference conditional on the group of trees. In our work, we use a Bayesian framework to address this issue, which also has the advantage of being able to estimate functions of treatment effects (see 1). Future work, however, could consider Rashomon sets for honest regression trees. This work would build upon our own work as well as [Xin et al. \(2022\)](#) that introduces Rashomon sets for classification trees. The algorithm for inference would begin with splitting as proposed by [Wager and Athey \(2018\)](#) to preserve honest inference, then construct Rashomon sets using the algorithm from [Xin et al. \(2022\)](#). Since the space of trees is enormous, finding the “best” tree is impossible, which creates issues for finding the Rashomon set since it is used to define the reference partition. Fortunately, a recent paper by [Hu et al. \(2019\)](#) provides an algorithm. While this approach would allow the CRF framework to find optimal trees, it does not address the identifiability issue that arises when using trees for data that are only partially ordered. Similar work was explored in [Hahn et al. \(2020\)](#), who estimate heterogeneous treatment effects using a sum of Bayesian regression trees, which they refer to as the Bayesian causal forest. They decompose the outcome into a mean outcome and a treatment effect. Since they are only interested in the treatment effect, the mean outcome becomes a nuisance parameter. They impose

a vague prior on the mean and a strong prior on the treatment effect. Otherwise, the tree estimation procedure is identical to Bayesian Additive Regression Trees (Chipman et al., 2010).

Third, both our approach and CRFs impose regularization but do so in philosophically very different ways. We take the perspective that we do not know and cannot fully enumerate correlation structure in a high dimensional space. So we use the ℓ_0 prior, which we show is the least informative prior in Theorem 2. In other words, we regularize, and impose a prior, on the size of the partition. In doing so, we are trading off information on full distribution to robustly identify partitions. On the other hand, causal forests regularize on the number of observations in each leaf of the tree. Specifically, they require at least k samples in each leaf. This choice is sensible because with insufficient data there is no information. At the same time, this is odd as the regularization depends directly on the data. Elaborating on this, we can write the posterior for some tree T given data \mathbf{y}, \mathbf{X} as

$$\mathbb{P}(T \mid \mathbf{y}, \mathbf{X}) \propto \mathbb{P}(\mathbf{y} \mid T, \mathbf{X})\mathbb{P}(T \mid \mathbf{X}) \text{ where } \mathbb{P}(T \mid \mathbf{X}) \propto \exp \left\{ -\frac{\lambda}{\min_{\pi \in \Pi(T)} n_{\pi}(\mathbf{X})} \right\},$$

where $\Pi(T)$ is the set of pools (leaves) in T and $n_{\pi}(\mathbf{X})$ is the number of observations in \mathbf{X} that belong to pool π . This prior down-weights and discards partitions where for *some* π the observations are low. In that sense, the prior effectively assumes that in the background there is a kind of stratification – that observations are sampled from some process such that all pools have enough observations, though of course *the true partition is unknown*. This feels awkward as there is a relationship between the data collection process and the actual true partitioning wherein the user of the causal forest is assuming that they have effectively stratified data collection against the unknown partitions.

Together, these differences mean that the scope of our method is wider than CRFs. While both methods can estimate heterogeneity in treatment effects and control for multiple testing, we also produce interpretable explanations of heterogeneity. For the reasons outlined above, namely identification and sampling, it is not possible to extract information on the relationship between covariates from elements of the random forest. We can, of course, test for any hypothesis about potential heterogeneity between arbitrary combinations of features, but CRFs require that we specify the hypothesis *a priori*. In our setting, however, finding the set of high posterior probability partitions gives a policymaker or researcher as set of potential models of heterogeneity and interaction between the covariates that can be used to design future policies or generate new research hypotheses. On the other hand, our method assumes that the posterior has separated modes. If the posterior distribution is very flat or has many (many) very similar modes, then the Rashomon set will be very large and our benefits in terms of interpretability will diminish.

E.4. Treatment heterogeneity via Machine Learning Proxies. Chernozhukov et al. (2018) propose a general framework for using machine learning proxies to explore treatment effect heterogeneity. They allow for estimation of multiple outcomes, including conditional average treatment effects and treatment effect heterogeneity between the most and least impacted groups. Rather than search the space of covariates directly, Chernozhukov et al. (2018) uses a machine learning method to create a “proxy” for the heterogeneous effects. This approach has the advantage that it can be applied in high dimensional settings. A downside, however, is that the machine learning proxies are often uninterpretable in terms of the original covariates, making it necessary to post-process the treatment effect distributions to gain insights about particular covariates.

We now give a brief overview to unify notation but do not exhaustively cover all the estimators presented in Chernozhukov et al. (2018). Say that $s_0(Z)$ is the true conditional average treatment effect, $\mathbb{E}[Y(1)|Z] - \mathbb{E}[Y(0)|Z]$. Ascertaining the functional form of the relationship between the non-intervention covariates X and the outcome Y , though, is complicated when X is high dimensional. In response, Chernozhukov et al. (2018) use a machine learning method (e.g. neural networks, random forests, etc) to construct a proxy for $s_0(Z)$ using an auxiliary dataset. In a heuristic sense, this proxy serves the role of a partition π , in that it aggregates across covariates to separate the data based on the treatment effect. This analogy is most direct when the machine learning model is a decision tree (which it need not be) since in that case leaves of the tree would correspond to partitions of the covariate space based on treatment effect. After computing the machine learning proxy, Chernozhukov et al. (2018) then project it back to the space of the observed outcomes. It is then also possible to construct clusterings based on the proxies and related those clusterings back to the outcomes. Chernozhukov et al. (2018) differs from our approach in many of the same ways as the comparison with Wager and Athey (2018), namely that we focus on identifying multiple explanations for heterogeneity and that we utilize the Hasse diagram as a geometric representation of partial ordering. We also find that this structure is sufficient to explore models for heterogeneity on the space of the covariates without the need to use proxies.

APPENDIX F. LAPLACE APPROXIMATION AND GENERALIZED BAYESIAN INFERENCE

F.1. Laplace approximation. Here, we briefly outline how to approximate the full posterior using the Rashomon set and Laplace’s method. Our goal is to estimate

$$p(\boldsymbol{\beta} | \mathbf{Z}) = \sum_{\Pi \in \mathcal{P}_\theta} p(\boldsymbol{\beta} | \mathbf{Z}, \Pi) \mathbb{P}(\Pi | \mathbf{Z})$$

We will do this by constructing a specific data-generating process. Consider the following data-generating process after fixing a partition Π . For each pool $\pi_j \in \Pi$, draw $\gamma_j \stackrel{i.i.d.}{\sim} \mathcal{N}(\mu_0, \tau^2)$ i.e., draw $\gamma \sim \mathcal{N}(\boldsymbol{\mu}_0, \boldsymbol{\Lambda}_0)$.²¹ Here, $\gamma \in \mathbb{R}^{|\Pi|}$ and $\boldsymbol{\Lambda}_0 = \tau^2 \mathcal{I}_{|\Pi|}$ where \mathcal{I}_m is an identity matrix of size m .

Then, we can define a transformation matrix $\mathbf{P} \in \{0, 1\}^{K \times |\Pi|}$, where K is the number of possible feature combinations, that assigns each γ of each pool to the feature combinations in that pool,

$$P_{ij} = \begin{cases} 1, & \text{feature combination } i \in \pi_j \\ 0, & \text{else} \end{cases}.$$

The mean vector for the feature combinations is given by $\boldsymbol{\beta} = \mathbf{P}\boldsymbol{\gamma}$. By properties of the multivariate normal, we have $\boldsymbol{\beta} \mid \Pi \sim \mathcal{N}(\boldsymbol{\mu}_\Pi, \boldsymbol{\Lambda}_\Pi)$, where $\boldsymbol{\mu}_\Pi = \mathbf{P}\boldsymbol{\mu}_0$ and $\boldsymbol{\Lambda}_\Pi = \mathbf{P}\boldsymbol{\Lambda}_0\mathbf{P}^\top$. Specifically, note that the means of all feature combinations in a given pool don't just share the same mean, but are effectively equivalent to each other.

Then, given some feature combinations \mathbf{D} , we draw the outcomes as

$$\mathbf{y} \mid \mathbf{D}, \boldsymbol{\beta}, \Pi \sim \mathcal{N}(\mathbf{D}\boldsymbol{\beta}, \boldsymbol{\Sigma}) \implies \mathbf{y} \mid \mathbf{D}, \boldsymbol{\gamma}, \Pi \sim \mathcal{N}(\mathbf{D}\mathbf{P}\boldsymbol{\gamma}, \boldsymbol{\Sigma}).$$

Therefore, $\boldsymbol{\gamma} \mid \mathbf{Z}, \Pi \sim \mathcal{N}(\boldsymbol{\mu}_n, \boldsymbol{\Lambda}_n^{-1})$ where

$$\begin{aligned} \boldsymbol{\mu}_n &= \boldsymbol{\Lambda}_n \left((\mathbf{D}\mathbf{P})^\top (\mathbf{D}\mathbf{P}) \hat{\boldsymbol{\gamma}} + \boldsymbol{\Lambda}_0 \boldsymbol{\mu}_0 \right) \\ \boldsymbol{\Lambda}_n^{-1} &= (\mathbf{D}\mathbf{P})^\top (\mathbf{D}\mathbf{P}) + \boldsymbol{\Lambda}_0 \\ \hat{\boldsymbol{\gamma}} &= ((\mathbf{D}\mathbf{P})^\top (\mathbf{D}\mathbf{P}))^{-1} (\mathbf{D}\mathbf{P})^\top \mathbf{y} \end{aligned}$$

Next, $\mathbb{P}(\Pi \mid \mathbf{Z}) = \mathbb{P}(\Pi) \int_{\boldsymbol{\gamma}'} p(\mathbf{Z} \mid \boldsymbol{\gamma}', \Pi) p(\boldsymbol{\gamma}' \mid \Pi) d\boldsymbol{\gamma}'$. We know that $\mathbb{P}(\Pi) = C \exp\{-\lambda |\Pi|\}$ where C is the normalization constant (or the partition function). Therefore, we have

$$\begin{aligned} \mathbb{P}(\Pi \mid \mathbf{Z}) &= C A_{1,\Pi} A_{2,\Pi} e^{-\lambda |\Pi|} \int_{\boldsymbol{\gamma}'} \exp\{-g(\boldsymbol{\gamma}')\} d\boldsymbol{\gamma}', \\ g(\boldsymbol{\gamma}') &= \frac{1}{2} (\boldsymbol{\gamma}' - \boldsymbol{\mu}_0)^\top \boldsymbol{\Lambda}_0 (\boldsymbol{\gamma}' - \boldsymbol{\mu}_0) + \frac{1}{2} (\mathbf{y} - \mathbf{D}\mathbf{P}\boldsymbol{\gamma}')^\top \boldsymbol{\Sigma}^{-1} (\mathbf{y} - \mathbf{D}\mathbf{P}\boldsymbol{\gamma}') \end{aligned}$$

where $A_{1,\Pi}, A_{2,\Pi}$ are known constants from the normal distributions. It is easy to verify that

$$\begin{aligned} \nabla g(\boldsymbol{\gamma}') &= \boldsymbol{\Lambda}_0 \boldsymbol{\gamma}' + (\mathbf{D}\mathbf{P})^\top \boldsymbol{\Sigma}^{-1} \mathbf{D}\mathbf{P}\boldsymbol{\gamma}' - \boldsymbol{\Lambda}_0 \boldsymbol{\mu}_0 - (\mathbf{D}\mathbf{P})^\top \boldsymbol{\Sigma}^{-1} \mathbf{y} \\ \nabla^2 g(\boldsymbol{\gamma}') &= \boldsymbol{\Lambda}_0 + (\mathbf{D}\mathbf{P})^\top \boldsymbol{\Sigma}^{-1} \mathbf{D}\mathbf{P} \end{aligned}$$

²¹In this case, these draws need not be independent of identical. The computations just become a little more tedious.

Since $\nabla^2 g(\gamma')$ is positive semi-definite for all γ' , g is convex. Therefore, solving for $\nabla g(\gamma') = 0$ allows us to find the minimum, $\gamma^* = (\mathbf{\Lambda}_0 + (\mathbf{D}\mathbf{P})^\top \mathbf{\Sigma}^{-1}(\mathbf{D}\mathbf{P}))^{-1}(\mathbf{\Lambda}_0 \boldsymbol{\mu}_0 + (\mathbf{D}\mathbf{P})^\top \mathbf{\Sigma}^{-1} \mathbf{y})$.

Using Laplace approximation, we get

$$\mathbb{P}(\Pi \mid \mathbf{Z}) \approx C A_{1,\Pi} A_{2,\Pi} e^{-\lambda|\Pi| - g(\gamma^*)} (2\pi)^{|\Pi|/2} \det(\mathbf{\Lambda}_0 + (\mathbf{D}\mathbf{P})^\top \mathbf{\Sigma}^{-1}(\mathbf{D}\mathbf{P}))^{1/2}.$$

This allows us to approximate the original quantity of interest, $p(\boldsymbol{\beta} \mid \mathbf{Z})$ through a variable transformation of $\boldsymbol{\gamma}$ where all the constants are known except for C . Exactly computing C is NP-Hard and is reminiscent of partition functions used in graphical models (not to be confused with the ‘‘partition’’ that we are using in this work). See [Agrawal et al. \(2021\)](#) for a survey of methods used to estimate or approximate the constant C .

F.2. Generalized Bayesian inference. We have our mean squared error for a given partition Π ,

$$\begin{aligned} \mathcal{L}(\Pi; \mathbf{Z}) &= \frac{1}{n} (\mathbf{y} - \hat{\mathbf{y}})^\top (\mathbf{y} - \mathbf{y}), \\ \hat{y}_i &= \frac{\sum_{\pi \in \Pi} \mathbb{1}\{k(i) \in \pi\} \sum_j \mathbb{1}\{k(j) \in \pi\} y_j}{\sum_{\pi \in \Pi} \mathbb{1}\{k(i) \in \pi\} \sum_j \mathbb{1}\{k(j) \in \pi\}} \end{aligned} \tag{F.1}$$

where \hat{y}_i is the mean outcome in the pool $\pi \in \Pi$ containing the feature combination of unit i , $k(i)$.

Our goal is to show that minimizing $\mathcal{L}(\Pi; \mathbf{Z})$ corresponds to maximizing the likelihood $\mathbb{P}(\mathbf{y} \mid \mathbf{D}, \Pi)$. Consider the same data-generating process in [Appendix F.1](#). Specifically, we require independence over γ_i and we will assume that the prior over $\boldsymbol{\gamma}$ is diffuse i.e., $\tau^2 \gg 1$. As before, given some feature combinations \mathbf{D} , we draw the outcomes as

$$\mathbf{y} \mid \mathbf{D}, \boldsymbol{\beta}, \Pi \sim \mathcal{N}(\mathbf{D}\boldsymbol{\beta}, \mathbf{\Sigma}) \implies \mathbf{y} \mid \mathbf{D}, \boldsymbol{\gamma}, \Pi \sim \mathcal{N}(\mathbf{D}\mathbf{P}\boldsymbol{\gamma}, \mathbf{\Sigma}).$$

This allows us to find the likelihood,

$$\begin{aligned} \mathbb{P}(\mathbf{y} \mid \mathbf{D}, \Pi) &= \int_{\boldsymbol{\beta}} \mathbb{P}(\mathbf{y} \mid \mathbf{D}, \Pi, \boldsymbol{\beta}) \mathbb{P}(\boldsymbol{\beta} \mid \Pi) d\boldsymbol{\beta} = \int_{\boldsymbol{\gamma}} \mathbb{P}(\mathbf{y} \mid \mathbf{D}, \Pi, \boldsymbol{\gamma}) \mathbb{P}(\boldsymbol{\gamma} \mid \Pi) d\boldsymbol{\gamma} \\ &= \int_{\boldsymbol{\gamma}} \mathbb{P}(\mathbf{y} \mid \mathbf{D}, \mathbf{P}, \boldsymbol{\gamma}) \mathbb{P}(\boldsymbol{\gamma} \mid \Pi) d\boldsymbol{\gamma} \\ &\propto \int_{\boldsymbol{\gamma}} \exp \left\{ -\frac{1}{2} (\mathbf{y} - \mathbf{D}\mathbf{P}\boldsymbol{\gamma})^\top \mathbf{\Sigma}^{-1} (\mathbf{y} - \mathbf{D}\mathbf{P}\boldsymbol{\gamma}) \right\} \exp \left\{ -\frac{1}{2} (\boldsymbol{\gamma} - \boldsymbol{\mu}_0)^\top \boldsymbol{\Lambda}_0^{-1} (\boldsymbol{\gamma} - \boldsymbol{\mu}_0) \right\} d\boldsymbol{\gamma} \end{aligned}$$

After re-arranging the terms in the exponent, we have

$$-\frac{1}{2} \left((\boldsymbol{\gamma} - \mathbf{M}^{-1} \mathbf{u})^\top \mathbf{M} (\boldsymbol{\gamma} - \mathbf{M}^{-1} \mathbf{u}) + \mathbf{y}^\top \mathbf{\Sigma}^{-1} \mathbf{y} + \boldsymbol{\mu}_0^\top \boldsymbol{\Lambda}_0^{-1} \boldsymbol{\mu}_0 - \mathbf{u}^\top \mathbf{M}^{-1} \mathbf{u} \right),$$

where $\mathbf{M} = \mathbf{P}^\top \mathbf{D}^\top \boldsymbol{\Sigma}^{-1} \mathbf{P} \mathbf{D} + \boldsymbol{\Lambda}_0^{-1}$ and $\mathbf{u} = \mathbf{P}^\top \mathbf{D}^\top \boldsymbol{\Sigma}^{-1} \mathbf{y} + \boldsymbol{\Lambda}_0^{-1} \boldsymbol{\mu}_0$. Notice that when integrating with respect to $\boldsymbol{\gamma}$, the first quadratic term becomes a constant in \mathbf{y} . Therefore,

$$\mathbb{P}(\mathbf{y} \mid \mathbf{D}, \Pi) \propto \exp \left\{ -\frac{1}{2} (\mathbf{y}^\top \boldsymbol{\Sigma}^{-1} \mathbf{y} + \boldsymbol{\mu}_0^\top \boldsymbol{\Lambda}_0^{-1} \boldsymbol{\mu}_0 - \mathbf{u}^\top \mathbf{M}^{-1} \mathbf{u}) \right\}.$$

Now, as the prior over $\boldsymbol{\gamma}$ becomes more diffuse i.e., as $\tau^2 \rightarrow \infty$, we have that $\boldsymbol{\Lambda}_0^{-1} \rightarrow \mathbf{0}$. Therefore, $\boldsymbol{\mu}_0^\top \boldsymbol{\Lambda}_0^{-1} \boldsymbol{\mu}_0 \rightarrow \mathbf{0}$, $\mathbf{M} \rightarrow \mathbf{P}^\top \mathbf{D}^\top \boldsymbol{\Sigma}^{-1} \mathbf{P} \mathbf{D}$, and $\mathbf{u} \rightarrow \mathbf{P}^\top \mathbf{D}^\top \boldsymbol{\Sigma}^{-1} \mathbf{y}$. This allows us to simplify,

$$\begin{aligned} \mathbb{P}(\mathbf{y} \mid \mathbf{D}, \Pi) &\propto \exp \left\{ -\frac{1}{2} (\mathbf{y}^\top \boldsymbol{\Sigma}^{-1} \mathbf{y} - (\mathbf{P}^\top \mathbf{D}^\top \boldsymbol{\Sigma}^{-1} \mathbf{y})^\top (\mathbf{P}^\top \mathbf{D}^\top \boldsymbol{\Sigma}^{-1} \mathbf{D} \mathbf{P})^{-1} (\mathbf{P}^\top \mathbf{D}^\top \boldsymbol{\Sigma}^{-1} \mathbf{y})) \right\} \\ &\propto \exp \left\{ -\frac{1}{2} \mathbf{y}^\top (\boldsymbol{\Sigma}^{-1} - \boldsymbol{\Sigma}^{-1} \mathbf{D} \mathbf{P} (\mathbf{P}^\top \mathbf{D}^\top \boldsymbol{\Sigma}^{-1} \mathbf{D} \mathbf{P})^{-1} \mathbf{P}^\top \mathbf{D}^\top \boldsymbol{\Sigma}^{-1}) \mathbf{y} \right\} \end{aligned}$$

The likelihood is maximized when the log-likelihood is maximized,

$$\begin{aligned} \log \mathbb{P}(\mathbf{y} \mid \mathbf{D}, \Pi) &= -\frac{1}{2} \mathbf{y}^\top (\boldsymbol{\Sigma}^{-1} - \boldsymbol{\Sigma}^{-1} \mathbf{D} \mathbf{P} (\mathbf{P}^\top \mathbf{D}^\top \boldsymbol{\Sigma}^{-1} \mathbf{D} \mathbf{P})^{-1} \mathbf{P}^\top \mathbf{D}^\top \boldsymbol{\Sigma}^{-1}) \mathbf{y} + c \\ \frac{\partial \log \mathbb{P}(\mathbf{y} \mid \mathbf{D}, \Pi)}{\partial \mathbf{y}} &\stackrel{\text{set}}{=} 0 \\ \implies \mathbf{y} &= \mathbf{D} \mathbf{P} (\mathbf{P}^\top \mathbf{D}^\top \boldsymbol{\Sigma}^{-1} \mathbf{D} \mathbf{P})^{-1} \mathbf{P}^\top \mathbf{D}^\top \boldsymbol{\Sigma}^{-1} \mathbf{y} \\ &= \mathbf{D} \mathbf{P} \hat{\boldsymbol{\gamma}} = \mathbf{D} \hat{\boldsymbol{\beta}}, \end{aligned}$$

where $\hat{\boldsymbol{\beta}} = \mathbf{P} \hat{\boldsymbol{\gamma}}$ and $\hat{\boldsymbol{\gamma}} = (\mathbf{P}^\top \mathbf{D}^\top \boldsymbol{\Sigma}^{-1} \mathbf{D} \mathbf{P})^{-1} \mathbf{P}^\top \mathbf{D}^\top \boldsymbol{\Sigma}^{-1} \mathbf{y}$. This is exactly the solution to is the solution to the following ordinary least-squares problem,

$$\min_{\boldsymbol{\gamma}} \|\mathbf{y} - \mathbf{D} \mathbf{P} \boldsymbol{\gamma}\|_2^2.$$

Next, we will show that this ordinary least squares problem is identical to $\mathcal{L}(\Pi; \mathbf{Z})$. In order to make this argument cleaner, we will assume that $\boldsymbol{\Sigma} = \sigma^2 \mathcal{I}_n$. Now, observe the structure of \mathbf{D} . In any row i , $D_{ik} = 1$ if observation i is assigned to feature combination k , and $D_{ik} = 0$ otherwise. So, $\mathbf{D}^\top \mathbf{D}$ is a diagonal matrix of size $K \times K$ where $(\mathbf{D}^\top \mathbf{D})_{kk}$ is the number of observations assigned to feature combination k , n_k . And $\mathbf{D}^\top \mathbf{y}$ sums all outcomes y_i corresponding to each feature combination k .

Similar to how \mathbf{D} collects all observations into their respective feature combinations, \mathbf{P} collects all feature combinations into their respective pools. Therefore $(\mathbf{P}^\top \mathbf{D}^\top \mathbf{D} \mathbf{P})^{-1} \mathbf{P}^\top \mathbf{D}^\top \mathbf{y}$ is the average outcome in each pool. This is exactly our estimated $\hat{\mathbf{y}}$ in Equation F.1. In other words, $\mathcal{L}(\Pi; \mathbf{Z})$ is exactly the minimized squared error (up to some scaling constant).

Therefore, maximizing the posterior $\mathbb{P}(\mathbf{y} \mid \mathbf{D}, \Pi) \mathbb{P}(\Pi)$ corresponds to minimizing the mean-squared error with the ℓ_0 penalty. This has connections to loss-based generalized Bayesian inference (Bissiri et al., 2016). Here, we have described one possible prior on $\boldsymbol{\beta}$ to recover the mean-squared

error. However, other such priors exist that describe such analytic loss functions. We refer the reader to Section 4 of [Chipman et al. \(2010\)](#) for examples of such priors used for BARTs.

APPENDIX G. APPENDIX TO SIMULATIONS

G.1. Performance metrics for Simulation 1. We used the following performance metrics to evaluate Lasso and models in the RPS in Figure 4 in Section 6:

- (1) Overall mean-squared error (MSE): Suppose \hat{y}_i and y_i are the estimated and true outcomes for unit i , then the overall MSE is defined as

$$\text{MSE} = \frac{1}{n} \sum_{i=1}^n (\hat{y}_i - y_i)^2.$$

- (2) Best policy MSE: Let y_{\max} be the true best policy effect and \hat{y}_{\max} be the estimated best policy effect. Then the best policy MSE is

$$\text{MSE}_{\text{best}} = (\hat{y}_{\max} - y_{\max})^2.$$

- (3) Best policy coverage: Let π^* and $\hat{\pi}^*$ be the true and estimated set of policies with the highest effect. Then, we define the best policy coverage as the intersection-over-union of these two sets

$$\text{IOU} = \frac{|\pi^* \cap \hat{\pi}^*|}{|\pi^* \cup \hat{\pi}^*|}.$$

These metrics are easily understood for a single model. For the RPS, we reported the performance metric averaged across all partitions in the RPS.

We visualize the RPS through a heat map. An example heatmap with instructions on how to read it is shown in Figure G.1. We also use these heatmaps in our empirical data examples in Appendix H.

For Simulation 1, we visualize the RPS in a heatmap in Figure G.2. As the size of the dataset increases, the Rashomon set becomes smaller as we become more confident in our estimates.

G.2. Simulation with linear outcomes. Here, we discuss the setup for the simulation described in Section 8 and Figure 9. As described previously, there are three features, age, drug A, and drug B. Age takes on two values, young and old, denoted by 1 and 2 respectively. Drug A takes on three non-control dosages $\{1, 2, 3\}$ and drug B takes on five non-control dosages $\{1, 2, 3, 4, 5\}$. We assume that there is no treatment effect unless drug A and drug B are taken together. The partition matrix

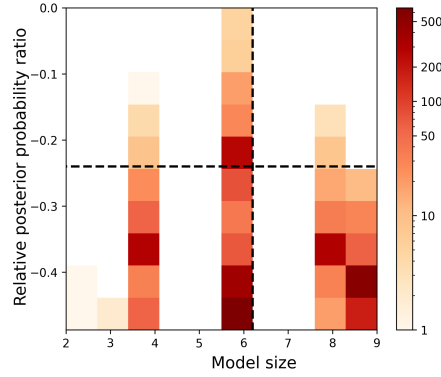


FIGURE G.1. Visualizing the Rashomon set through a heat map. This heatmap actually reflects a 2D histogram binned by the model size (number of pools in a partition) and the relative posterior probability ratio i.e., $(\mathbb{P}(\Pi | \mathbf{Z}) - \max \mathbb{P}(\Pi | \mathbf{Z})) / \max \mathbb{P}(\Pi | \mathbf{Z})$. The color of the bin reflects the number of times, averaged per simulation, a model at that sparsity and probability (distinct models may be in the same bin) appear in some Rashomon set. One might refine the set of partitions further by the probability and the sparsity. For example, if we want models with a relative probability of at least -0.25, then we look only at models that are above the dashed black horizontal line. If we want models with fewer than 6 pools, then we look only at models to the left of the dashed black vertical line. If we want both criteria to be satisfied, we look at the top left box.

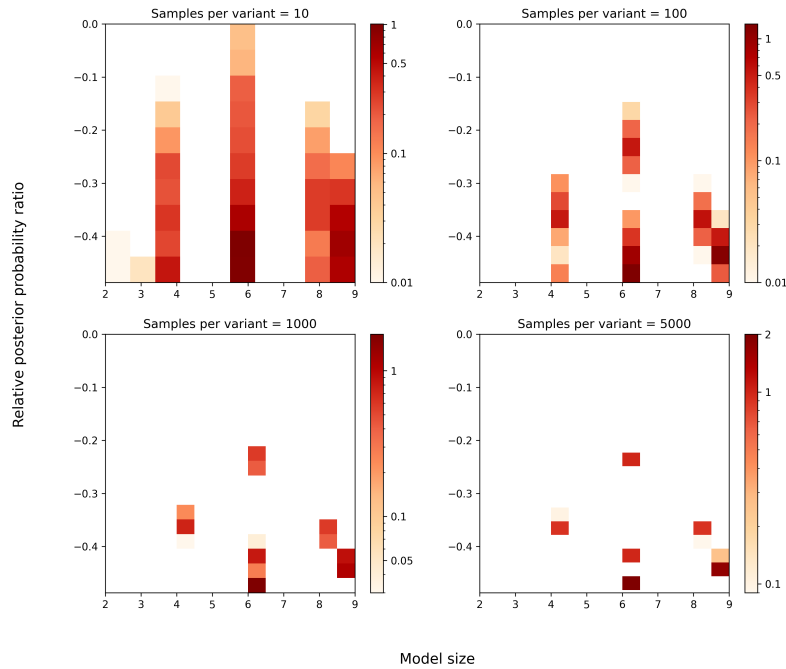


FIGURE G.2. Visualizing the Rashomon set in Simulation 1. Notice how as the size of the data set grows, the Rashomon set concentrates around a few very good models, one of which corresponds to the data generating process.

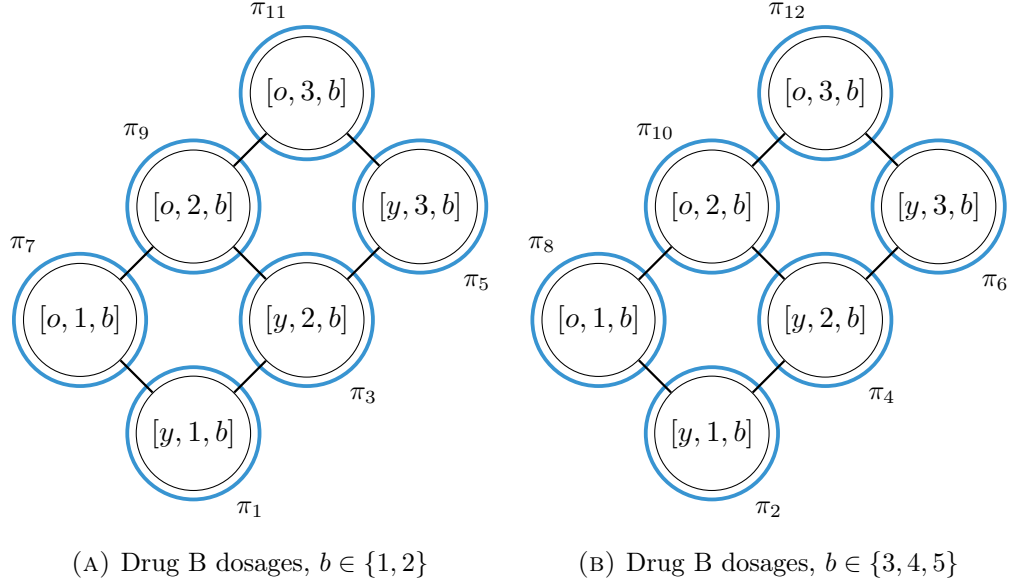


FIGURE G.3. Hasse diagram for simulation with linear outcomes. y is young and o is old.

is

$$\Sigma = \begin{bmatrix} 0 & - & - & - \\ 0 & 0 & - & - \\ 1 & 0 & 1 & 1 \end{bmatrix}.$$

We visualize the twelve pools in Figure G.3 indicating heterogeneity in age and the dosages of drugs A and B. And the linear coefficients for the outcomes in each pool are given by

$$\beta_1 = [0, -1, 0, 1]$$

$$\beta_2 = [1.5, -4, 0, 1.5]$$

$$\beta_3 = [0, -1, -0, 1]$$

$$\beta_4 = [4.5, -4, 0, 0.5]$$

$$\beta_5 = [4, -2, -1, 1]$$

$$\beta_6 = [1, 1, 1, -1]$$

$$\beta_7 = [-3, 2, -3, 1]$$

$$\beta_8 = [0, 0, 0, 0]$$

$$\beta_9 = [4, 2, -3, -1]$$

$$\beta_{10} = [0, 0, 0, 0]$$

$$\beta_{11} = [5, 2, -3, 0]$$

$$\beta_{12} = [5, -1, 0, -1],$$

where the first coefficient is the intercept and the remaining elements are slopes on each feature. For feature profiles with zero treatment effect, we set the effect to be 0, a constant. For the feature profile where drugs A and B are administered together, a random error is drawn independently and identically from $\mathcal{N}(0, 1)$. We draw 10 measurements for each feature combination. We set $\lambda = 4 \times 10^{-3}$.

APPENDIX H. APPENDIX TO EMPIRICAL DATA EXAMPLES

H.1. Charitable giving and telomere lengths. Figures H.1 and H.2 visualize the Rashomon sets for the charitable giving datasets of [Karlan and List \(2007\)](#) and the NHANES telomere lengths using the 2D histogram that is described in Figure G.1 in Appendix G.

H.2. Heterogeneity in the impact of microcredit access. For the microcredit data from [Banerjee et al. \(2015\)](#), we present the results for all profiles in Figure H.3. This includes the robust profiles we discussed in Figure 8 as well as the non-robust ones.

Additionally, we look at the treatment effect heterogeneity across genders,

$$\text{HTE}(\mathbf{x}) = \mathbb{E} [\{Y_i(1, F, \mathbf{x}) - Y_i(0, F, \mathbf{x})\} - \{Y_i(1, M, \mathbf{x}) - Y_i(0, M, \mathbf{x})\}],$$

where $Y_i(\cdot, F, \cdot)$ is interpreted as the potential outcome of household i were it headed by a woman, and $Y_i(\cdot, M, \cdot)$ is the potential outcome of household i were it headed by a man. As before, we use the sample means $\hat{y}(\cdot)$ to find $\widehat{\text{HTE}}(\mathbf{x})$ and $\text{sign}\{\widehat{\text{HTE}}(\mathbf{x})\}$. Again, we sort \mathbf{x} into profiles and repeat the same counting and averaging exercise. We visualize the results as before in Figure H.4. For most profiles, we see essentially no robust conclusions about gender heterogeneity in treatment effects. We highlight a few robust items below.

We see an increase in loans procured by households headed by women with past business experience when compared to households headed by men. When these households are already in debt with no previous experience, they tend to borrow less. We see no heterogeneity by gender in the amount of informal loans procured.

Households headed by women tend to consistently spend more. However, they spend more money on durable goods than households headed by men. We also see that, in the absence of past experience, there is a decline in expenditure on tempting goods compared to households headed by men. We also see a higher tendency for women to invest in business assets more than men.

We find that households headed by women with no past experience have a lower revenue than men. But this effect is reversed when the households do have previous business experience. However, there is no heterogeneity by gender in the profit or the number of employees. We also find that households headed by women tend to spend fewer hours working when they are in debt or when there is regional competition. But this makes a negligible difference in the profits.

We find that in households headed by women, there is less participation in the business by women if the household is in debt and there is competition from neighbors. We also find that fewer girls attend school in households headed by women with no previous experience than in households headed by men.

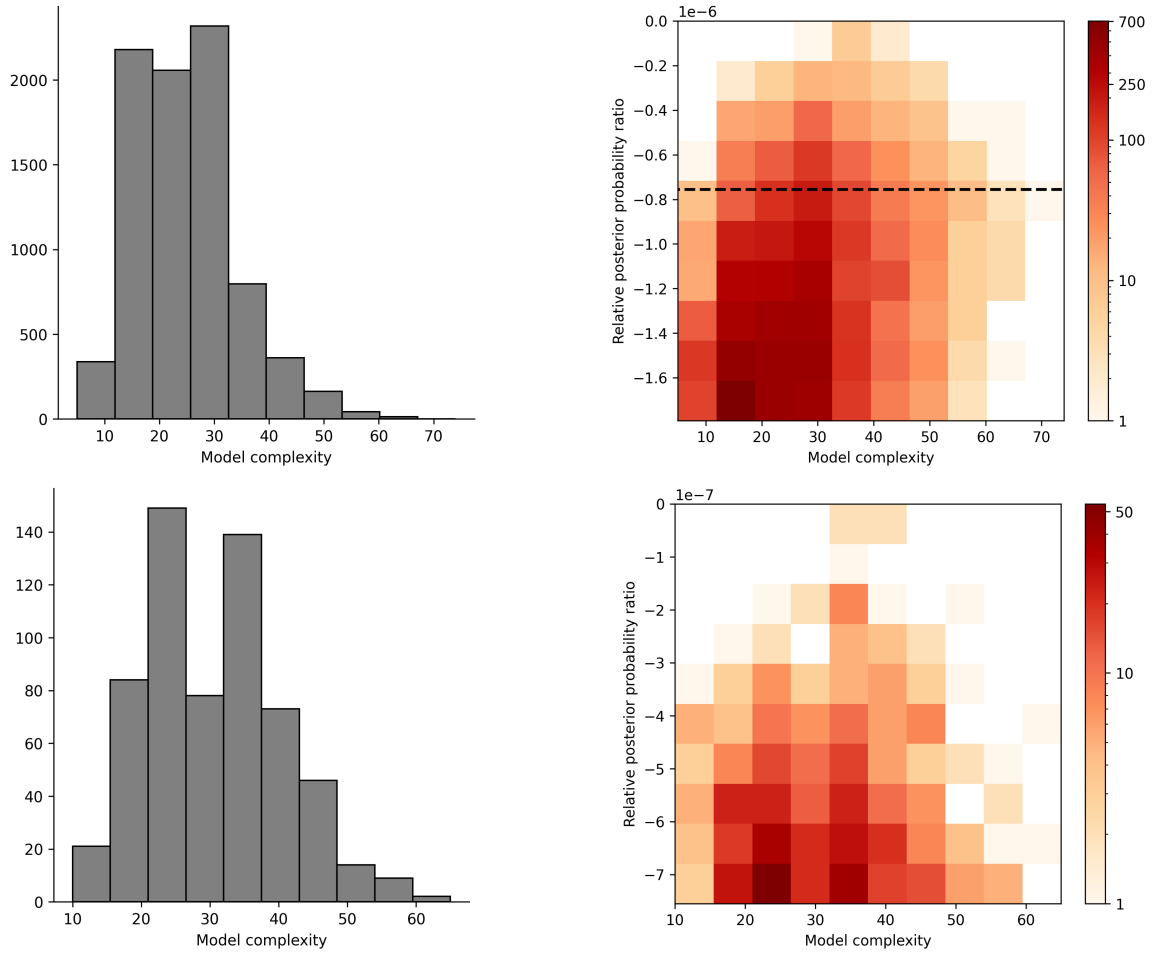


FIGURE H.1. Visualizing the Rashomon set for [Karlan and List \(2007\)](#) charitable donations dataset. The top two panels show the distribution of partition sizes and a 2D histogram of how partition sizes and relative posterior probabilities vary. The black dotted line in the 2D histogram shows our chosen Rashomon threshold. The bottom two panels show the same after pruning low-posterior models.

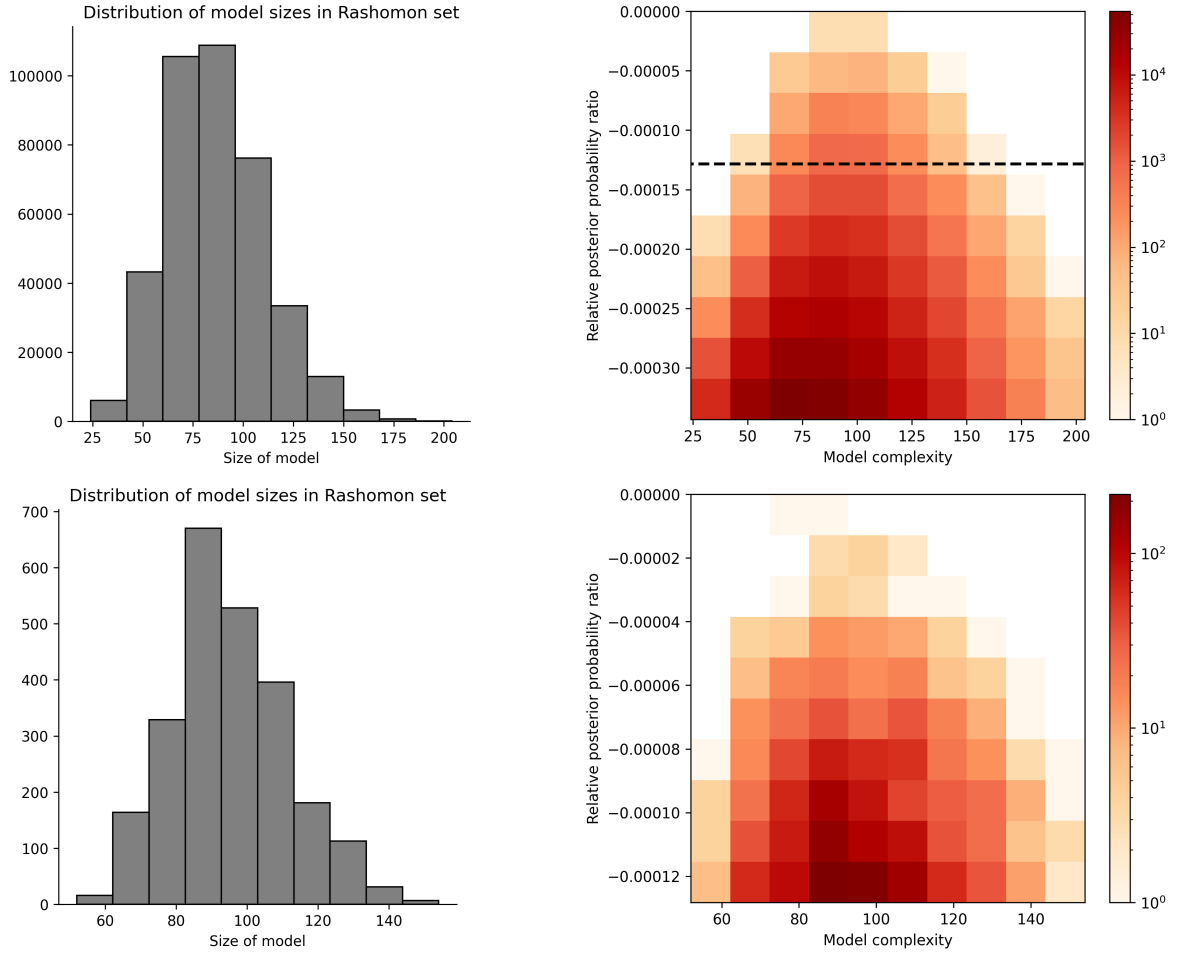


FIGURE H.2. Visualizing the Rashomon set for NHANES telomeres dataset. The top two panels show the distribution of size of models and their relative posterior probability relative. The black dashed vertical and horizontal lines show the sparsity cutoff and Rashomon cutoff respectively. The bottom two panels show the same after pruning low-posterior models.

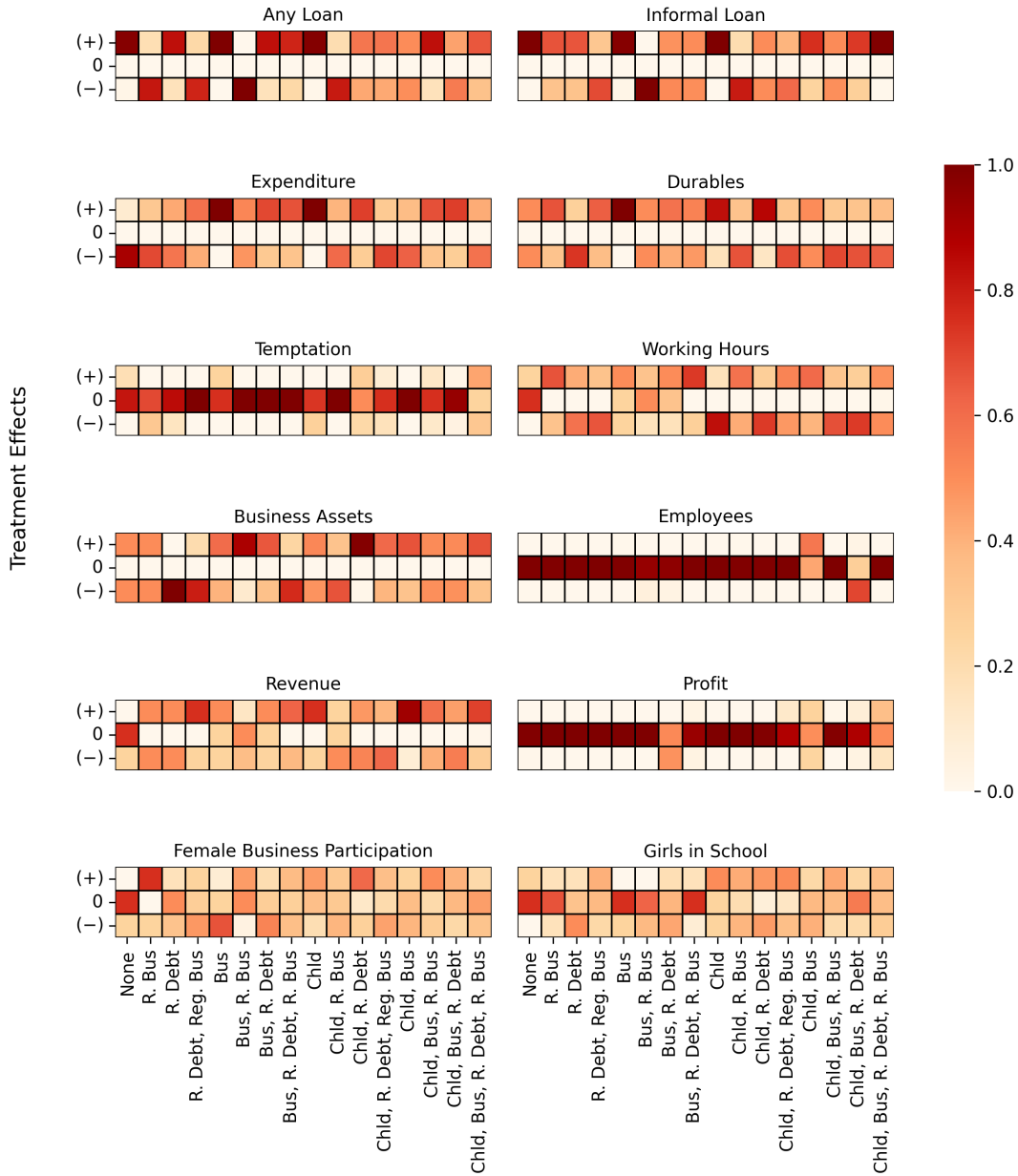


FIGURE H.3. Here, we visualize the average number of models in the Rashomon set indicating a positive, zero, or negative effect. Each column corresponds to a different feature profile where the label denotes which features are active (i.e., do not take the lowest level). “None” means that all features are taking these lowest values. We also allow the gender of the household head and education status of the household head to take on any value in all of the sixteen feature profiles.

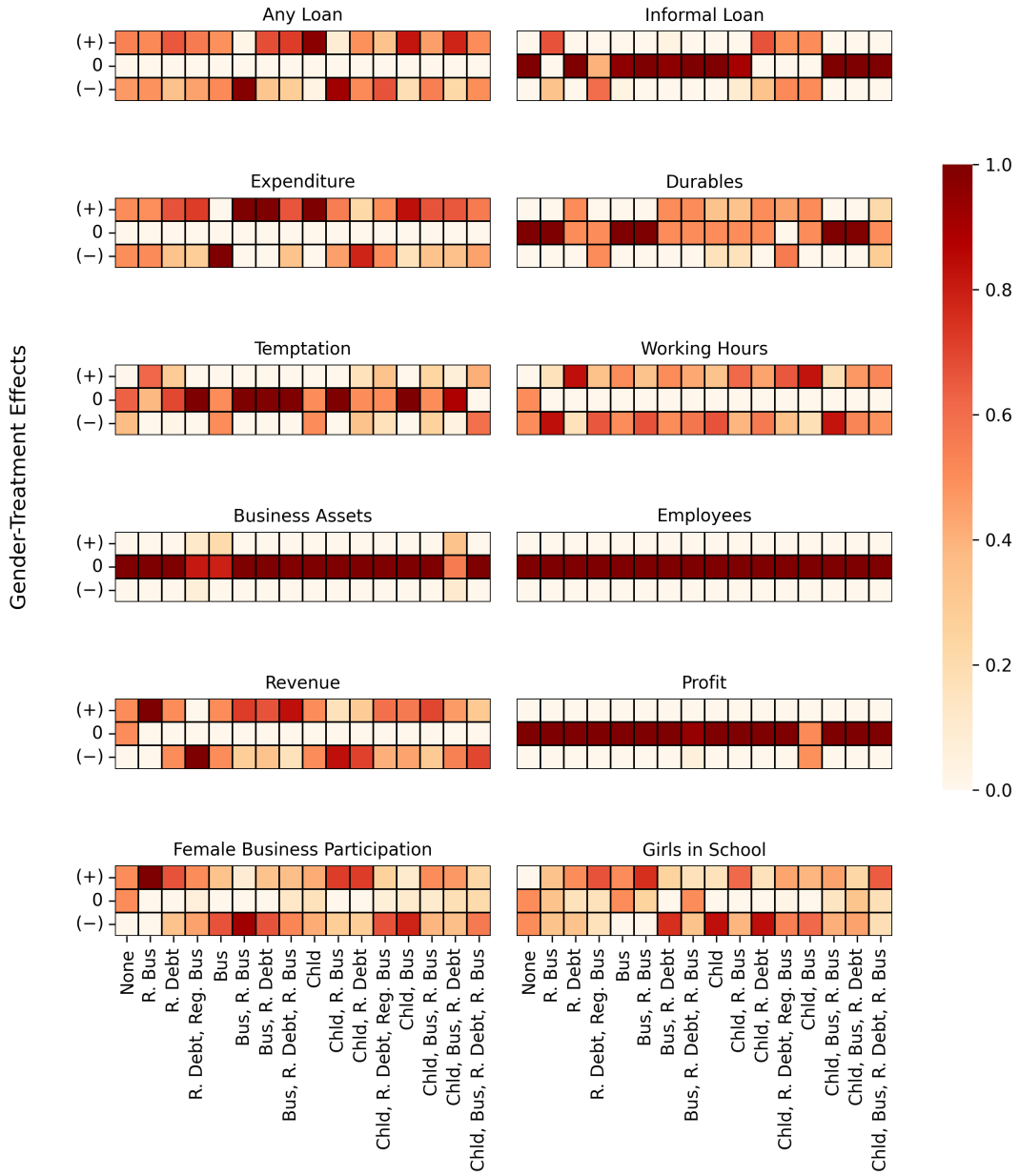


FIGURE H.4. Here, we visualize the average number of models in the Rashomon set indicating a positive, zero, or negative effect. The axis labels should be read as in Figure H.3.